

**PARAMETRIC STUDY OF LOAD TRANSFER IN
TWO-BOLTED SINGLE LAP HYBRID (BONDED/BOLTED) SHEAR JOINTS**

A Thesis by

Nagesh Ganji

B.E., Chaithanya Bharathi Institute of Technology

Hyderabad, India, 2001

A thesis submitted to the Department of Mechanical Engineering
and the faculty of the graduate school of
Wichita State University
in partial fulfillment of
the requirements for the degree of
Master of Science

May 2007

© Copyright 2007 by Nagesh Ganji
All Rights Reserved

**PARAMETRIC STUDY OF LOAD TRANSFER IN
TWO-BOLTED SINGLE LAP HYBRID (BONDED/BOLTED) SHEAR JOINTS**

This thesis has been read by each member of the committee and recommends that it be accepted in partial fulfillment of the requirements for the degree of Master of Science, with a major in Mechanical Engineering.

Dr. Hamid M Lankarani, Committee Chair

Dr. Ramazan Asmatulu, Committee Member

Dr. Bayram Yildirim, Committee Member

To my loving parents

ACKNOWLEDGEMENTS

I like to thank my advisor Dr. H.M. Lankarani for his endless support, suggestions and guidance throughout my course at Wichita State University. I owe him the deepest gratitude for his constant encouragement, patience and motivation which helped in completion of my thesis successfully. My special thanks to Dr. Ramazan Asmatulu and Dr. Bayram Yildirim for being in committee and proving me with their valuable suggestions.

My thesis would remain incomplete without acknowledging the support of my managers, colleagues, and complete Department of Mechanical Engineering who have provided lively atmosphere during my course at Wichita State.

Finally I like to thank my family and all my friends who where a great encouragement and endless support throughout my life.

ABSTRACT

A composite material can be defined as two or more materials combined to form another material with enhanced properties. A Composite material shows high strength to weight ratio, light weight, tailored properties, high stiffness, high corrosion resistance and high fatigue life. In the recent past, the usage of composite materials in the aviation industry has been increasing, and most of the lap joints are being used in aircraft fuselage.

In this study we mainly focus on the load transfer in hybrid (bonded/bolted) joints when they are subjected to tensile load. It is difficult to calculate the load transfer in hybrid (bonded/bolted) joints because of the difference in stiffness of the varied loads. A three dimensional finite element model has been developed to compute the load transfer in hybrid composite single lap joint.

The main aim of this study is to predict the load transfer in the hybrid single lap joint and also investigate the effects of various parameters such as material properties, tensile load, adherend thickness, bolt diameter and overlap length on the load transfer by bolt. And we have observed that hybrid joining (the combination of mechanical fastening and adhesive bonding) can provide enhanced structural performance, when we compare it with adhesive bonding. In this study we also discussed about the modeling of contact between bolt and hole and nonlinear material behavior of the model.

The model has been validated by comparing the results of FE model with experimental results for single bolted hybrid lap joint. The experimental bolt load values were compared to results of the finite element model and both were found to be in good agreement.

TABLE OF CONTENTS

Chapter	Page
1. INTRODUCTION	1
1.1 Introduction.....	1
1.1.1 Mechanical Joints.....	2
1.1.2 Design Methods	4
A) Bolted Joints.....	4
B) Bonded Joints.....	5
1.1.3 Pre-Tension	6
1.1.4 Defining of Model.....	7
1.2 Objective and Methodology.....	8
2. LITERATURE REVIEW	10
2.1 Review	10
2.2 Outline.....	15
3. FINITE ELEMENT ANALYSIS OF HYBRID LAP JOINT	16
3.1 FEM	16
3.2 Development and Modeling Contact Surfaces	16
3.3 Boundary and Loading Conditions	20
3.4 Pretension.....	21
3.5 Formulation.....	23
3.6 Validation.....	26
4. RESULTS	29
4.1 Load Distribution.....	29
4.2 Influence of Material Properties	33
4.3 Influence of Tensile Load	37
4.4 Influence of Adherend thickness	42
4.5 Influence of Bolt diameter	47
4.6 Influence of Overlap length	52
4.7 Results and Discussions.....	56
5. CONCLUSIONS AND RECOMMENDATIONS	59
5.1 Conclusions.....	59
5.2 Future Work.....	60
REFERENCES	61

TABLE OF CONTENTS (continued)

Chapter	Page
Appendix A	63
Appendix B	78

LIST OF TABLES

Table		Page
3.1	Dimensions of Fastener Component.....	19
3.2	Material Types and their Properties.....	25
4.1	Model Matrix	32

LIST OF FIGURES

Figure	Page
1.1 Bonded Lap Joints	5
1.2 Basic Process flow	6
1.3 Pre-Tension Section	7
3.1 Flat Panel with Adhesive	17
3.2 Protruding head bolt.....	17
3.3 Layout of Single Lap Joint.....	18
3.4 Layout of Fastener	19
3.5 Boundary and Loading Conditions	21
3.6 Surface Pre-tension	22
3.7 Pre-tension Node.....	22
3.8 Meshed model of Plates with Holes.....	23
3.9 Mesh near the Hole	24
3.10 Biased Mesh at plates Far End.....	24
3.11 Meshed Model	25
3.12 Bolt load versus total applied load.....	27
4.1 Deformation under tensile load.....	30
4.2 Von-mises Stress Distribution in the adherends	30
4.3 Principal Stress Distribution	31
4.4 Von-mises stress distribution.....	31
4.5 Load transfer by bolt 1 for MODEL A	33
4.6 Load transfer by bolt 1 for MODEL B	33

LIST OF FIGURES (continued)

Figure		Page
4.7	Load transfer by bolt 1 for MODEL C	34
4.8	Load transfer by bolt 2 for MODEL A	34
4.9	Load transfer by bolt 2 for MODEL B	35
4.10	Load transfer by bolt 2 for MODEL C	35
4.11	Load transfer by bolt 1 for different material models.....	36
4.12	Load transfer by bolt 2 for different material models.....	36
4.13	Load transfer by bolt 1 for MODEL G	38
4.14	Load transfer by bolt 1 for MODEL H	38
4.15	Load transfer by bolt 1 for MODEL I.....	39
4.16	Load transfer by bolt 2 for MODEL G	39
4.17	Load transfer by bolt 2 for MODEL H	40
4.18	Load transfer by bolt 2 for MODEL I.....	40
4.19	Load transfer by bolt 1 for different tensile loads.....	41
4.20	Load transfer by bolt 2 for different tensile loads.....	41
4.21	Load transfer by bolt 1 for MODEL D	43
4.22	Load transfer by bolt 1 for MODEL E.....	43
4.23	Load transfer by bolt 1 for MODEL F.....	44
4.24	Load transfer by bolt 2 for MODEL D	44
4.25	Load transfer by bolt 2 for MODEL E.....	45
4.26	Load transfer by bolt 2 for MODEL F.....	45
4.27	Load transfer by bolt 1 for different Adherend thicknesses	46

LIST OF FIGURES (continued)

Figure		Page
4.28	Load transfer by bolt 2 for different Adherend thicknesses	46
4.29	Load transfer by bolt 1 for MODEL J	48
4.30	Load transfer by bolt 1 for MODEL K	48
4.31	Load transfer by bolt 1 for MODEL L	49
4.32	Load transfer by bolt 2 for MODEL J	49
4.33	Load transfer by bolt 2 for MODEL K	50
4.34	Load transfer by bolt 2 for MODEL L	50
4.35	Load transfer by bolt 1 for different Bolt diameters	51
4.36	Load transfer by bolt 2 for different Bolt diameters	51
4.37	Load transfer by bolt 1 for MODEL M	52
4.38	Load transfer by bolt 1 for MODEL N	53
4.39	Load transfer by bolt 1 for MODEL O	53
4.40	Load transfer by bolt 2 for MODEL M	54
4.41	Load transfer by bolt 2 for MODEL N	54
4.42	Load transfer by bolt 2 for MODEL O	55
4.43	Load transfer by bolt 1 for different Overlap lengths	55
4.44	Load transfer by bolt 2 for different Overlap lengths	56

CHAPTER ONE

INTRODUCTION

1.1 Introduction

Structural joints play an important role in load transfer throughout the assembly, so they are given importance in a structural assembly. Continuous improvements are necessary in these structural joints which help in improving the capacity of load it can withstand and structural integrity, with a reduction of structural weight and number of parts. Bolted joints are of two types, first is the tensile joint which comes into play when the forces on the bolt joint act parallel to the bolt axis and the second is the shear joint, where the forces on the joint act normal to the top of the bolt axis. In these two categories, regularly tensile joint is used in the assemblies.

A composite material consists of two or more materials combined together to give a material with enhanced properties. As the composite materials can be designed to most of the shapes, it can help in reduction of parts in any structural assembly.

As the recent decades have shown, the use of advanced composites in primary and secondary aircraft industries is steadily growing. The increased application of composites in the aircraft industries is growing as these materials offer a number of advantages compared to conventional engineering materials such as steel and aluminum. A good combination of low density with high stiffness and strength can be achieved. Through this the structural weight can be reduced, and as a result the aircraft can fly farther and faster with greater payload and reduced fuel cost. Advanced composites are recognized as uniquely flexible in design capabilities and ease in manufacturing. By using advanced manufacturing techniques it is possible to reduce large identical composite structures

with complex shapes, thus providing a high degree of parts integration and lowering manufacturing and assembling cost [10].

1.1.1 Mechanical joints

Mechanically fastened joints are one of the most important elements in aircraft structures. Regardless of material combination in the parts joined, the joint is a critical element whose design is vital for overall structural performance. As has already been mentioned, the use of bolted joints allows connected structural components to be further disassembled, thus increasing the degree of component integration. Typical examples of mechanically fastened joints in composite aircraft structures are skin-to-spar/rib connections in awing structure, wing-to –fuselage connection and attachment of fittings, etc [10].

Mechanically fastened joints can be classified into two general types by the amount of load being transferred as lightly loaded and highly loaded joints. Examples of lightly loaded joints are the connections between substructure and skin. Root joint of a wing is an example of a highly loaded joint [10].

The functioning principle of bolted joints is based on the micro and macroscopic mechanical interface, such as friction between the jointed parts, shear or tensile shear forces in fasteners, and contact forces between the jointed components. Dissimilar materials can be fastened by means of mechanical joints. This feature is used intensively in the aircraft industry to join aluminum components with composite structures. Most of the mechanical joints encountered in aircraft structures have multiple fasteners. The

number and type of fasteners needed to transfer the given loads are usually established by airframe designers relative to available space, productivity and assembly [10].

Joining of polymer matrix composite materials has traditionally been achieved by mechanical fastening or adhesive bonding. Combining these techniques has been considered unnecessary in terms of structural performance as the adhesive provides a stiffer load path and thus transfers the majority of the load. However, these assumptions are often related to high performance aerospace joints where long overlap lengths (defined here as overlap length/ adherend thickness P40) and high modulus epoxy adhesives are used [9].

In non-aerospace applications, joining polymer matrix Composites using alternative methods such as hybrid joints combining mechanical fastening and adhesive bonding could be motivated. Hybrid joining techniques have previously been considered in relation to repair and improvement of Damage tolerance. Hart-Smith conducted a theoretical investigation of combined bonded/bolted Stepped lap joints between titanium and carbon fiber reinforced plastic (CFRP). While no significant strength benefits were found in comparison to perfectly bonded Joints, the combined bonded/bolted joint was found to be beneficial for repairing damaged bonded joints and limiting damage propagation. Under room temperature and ambient humidity conditions, 98% of the applied load was predicted to be transferred by the adhesive [9].

The adhesive used in this thesis is a two component polyurethane material (Pliogrip 7400/7410, Ashland Speciality Chemicals GmbH). The low modulus polyurethane adhesive contributes to a more flexible joint with larger relative displacement between the adherends. This displacement allows for a significant transfer

of the load to the bolt. The main part of the load is transferred at the ends of the overlap leaving the centre of the joint relatively unloaded. Throughout the thesis adhesive thickness taken as 0.6 mm and $E=0.6$ Gpa. The benefit of adding bolts to a bonded joint is greater if the joint is flexible either as a result of the adhesive material or joint design. However, the method could also provide performance improvements for a wide range of joints in adverse environments with both elevated temperature and moisture reducing the performance of the adhesive [9].

1.1.2 Design methods

A) Bolted Joints:

Bolted joints when not properly designed may result in structural failure during their life cycle and also due to fatigue loading. In addition, a badly designed bolted joint may be overweight leading to structural instability. Main ways in which a bolt can be loaded are: tension, shear and combined shear and tension. A bolt is primarily designed to withstand tensile forces. While designing a bolted joint in which a bolt takes significant amount of tensile and shear loading, proper analysis or calculation must be done to withstand combined stress. Various analysis programs have been studied by Synder et al, and discussed their pros and cons [18].

It is also important that in a structural joint, bolt preload or torque applied to secure the components be properly determined. A bolt goes into a state of tension when torque is applied on the joint. Some of the factors that affect the bolt tension with the amount of torque applied are nominal bolt diameter, friction coefficient and bolt strength [19]. A rough estimate of the required torque to be applied is given by:

$$T = K \times D \times P \quad (1.1)$$

Where T is the required torque, K is friction coefficients, D is bolt diameter and P is total load.

B) Bonded Joints:

In bonded joints, load transfer between the structural members is done by adhesion, as shown in Figure 1.1. Main advantage of bonded joint is that it holds the members together trying to resist the stress to pull apart. Tensile stresses are equally distributed over the entire joint area and shear stress is across the adhesive bond. Even distribution of stresses eliminates high stress concentrations. Moreover, bonded joints are lighter in weight compared to bolted or welded joints and offer a pleasing look. Other advantages of bonded joints include that they provide maximum fatigue resistance, effectively bond dissimilar materials together and simplify production [13].

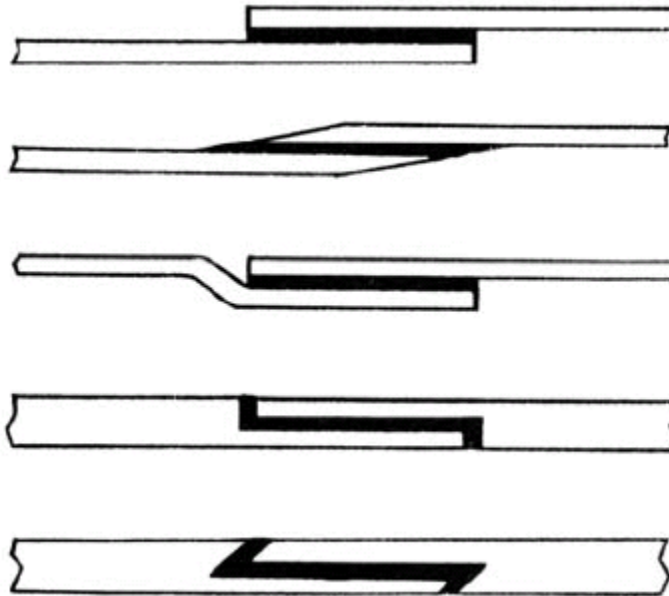


Figure 1.1 Bonded Lap Joints [13]

Some issues to be considered while selecting a bonded joint is that the joint disassembly is not possible. Bonded joint requires additional surface preparation that is not required in a bolted joint. Adhesively bonded joints also require an NDI and are also sensitive to environmental changes.

1.1.3 Pre-tension

In a joint connected using a fastener, it is necessary that the joint is fastened with a particular tension. If the fastener pretension is too tight, it may cause damage to the structure or the fastener itself might break. On the other hand, if the applied pretension is too less, it might result in excessive vibration of the structure or unnecessary leaks. So, it is necessary that the fastener is tightened with appropriate tension [17].

In ABAQUS, the *PRE-TENSION SECTION option is used to define the tension force or torque in the bolt. In this process it is necessary to define a pretension surface in the finite element model for applying tension force. The surface is chosen approximately at the center of the fastener shank. Once, the assembly load is prescribed, it is then applied to the pretension surface of the element to simulate the tension of the assembly.

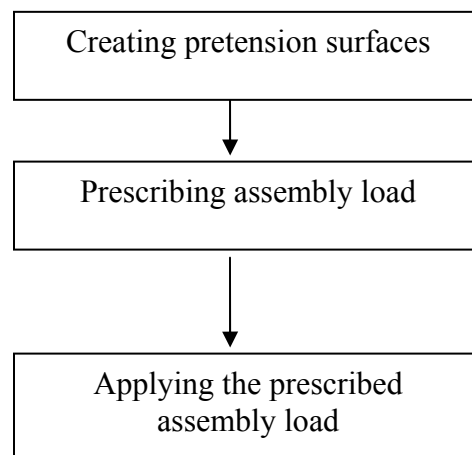


Figure 1.2 Basic process flow

A pretension node which controls the pretension section should be defined. The pretension node is mainly used to apply load preload across the pretension section and maintain the tightening adjustment so that the load across the fastener may increase or decrease upon loading of the structure. This node has only one degree of freedom. A point load is applied to the pretension node representing the torque applied to the fastener. This load acts in the direction of normal on the part of the fastener underlying the pretension section. The total force transmitted across pretension is the combination of reaction force at pretension node and any concentrated load at the node [17].



Figure 1.3 Normal to pretension away from underlying elements

1.1.4 Defining of Model

When analyzing the load transfer in a lap joint which is connected using a fastener, it is required to define contact between two plates being fastened and also between the plate holes and the fastener. ABAQUS/Standard defines contact between two

bodies in terms of two surfaces that may interact; these surfaces are called a “contact pair.”

ABAQUS /Standard enforce contact by forming equations of involving groups of nearby nodes. One of the important features after selecting contact pair surfaces in ABAQUS is assignment of “master” and “slave” surfaces [1]. Generally, smaller surface should be the slave surface and the larger surface which is in contact should be the master surface. If the distinction cannot be made, it is better that the master surface should be the one with higher stiffness. In terms of mesh, the body with coarser mesh should be defined as master surface [1].

In the present study contact should be defined between lower surface of upper plate in lap joint and upper surface of lower plate, upper plate hole and fastener, lower plate hole and fastener. Considering the master-slave algorithm described earlier, fastener has been defined as master surface and plates are defined as master surfaces.

1.2 Objective & Methodology

The main aim of this thesis is to predict the load transfer by a bolt in a single lap hybrid joint (composite material) and studies the effects of various design parameters such as bolt diameter, overlap length, adherend thickness, elastic properties of the materials and tensile load on load transfer by bolt for single lap hybrid joint.

A 3D model created for single lap hybrid joint included with two fasteners. In three dimensional modeling developing the surface contact between the hole and the bolt plays an important role.

The model is validated by comparing the results with an experimental solution for determining the load transfer by a one fastener in a single lap hybrid joint. A parametric study has been conducted to determine the effects of various parameters such as bolt diameter, overlap length, adherend thickness, elastic properties of the materials and tensile load on load transfer by bolt.

This study aims to see how a design and fabrication parameters influence on the transfer of load by bolt in hybrid joints. In the chapter 2, we talk about literature review and it gives the information regarding how various methods of finite element methods as they are used to model and understand the load transfer by a bolt in a single lap hybrid joint. Chapter 3 gives a brief description of the finite element analysis of hybrid lap joint. Chapter 4 deals with the results of load distribution by bolt in single lap hybrid joint. Chapter 5 explains the conclusions and recommendations.

CHAPTER TWO

LITERATURE REVIEW

2.1 Review

Research on structural joints is being carried out from last few years. Current literature review explains the research done on bonded and bolted joints, where it helps in understanding of different types of experimental and analytical methods used to find how these bonded and bolted joints work efficiently.

Lehnhoff conducted a FEA which helps in understanding and revealing phenomena related to axisymmetric bolted joints and mainly focused to see how external loads effects stress distribution and deformation of bolted joints. Finite element modeling was performed and gap elements were used at contacting surfaces. Out radius was given zero slope boundary conditions to show the integration of other bolts in the simulation. For leak prevention there is a need of providing proper bolt spacing in the flange. So when the desired compression pressure is known then bolt spacing can be determined and finally a desired pressure for parameters can be produced. Separation radius helps in maintaining a sealed joint and it is depended on the bolt size, external load magnitude and location and finally on connected material thickness ration. Separation radii increase with the bolt size. It was observed that at maximum external load and maximum radial position of external load, stress was decreased at faster rate with radial distance which resulted in decreased separation radius [6].

Evaluation of stress intensity factor (SIF) for cracks in metallic joints is an issue in sound damage tolerance analysis due to design complexity with variations in load transfer and fasteners interference. A methodology was developed by Cope using finite elements for representing the

fasteners in lap joints and empirical force-displacement relation was used to determine the material properties to represent spring elements of fasteners. Loads, stress and SIF of lap joint cracks were determined by combining two fastener types. Investigation was done using Fracture analysis Code 2D/layered (FRANC 2D/L). As joint displacement is a major part of fasteners displacement, proper spring force-displacement is necessary to obtain proper displacement compatibility. In case of linear elastic material behavior, the fastener displacement δ is calculated using elastic modulus of sheet (E) and its thicknesses t_1 & t_2 , applied load (F), which is represented by following empirical relation:

$$\delta = \left(\frac{F}{E.d} \right) + \left[B + C \cdot \left(\frac{d}{t_1} + \frac{d}{t_2} \right) \right] \quad (2.1)$$

Where, d is fastener diameter and B and C are empirical constants. Cope research suggested to develop computationally efficient lap joint models using combination of explicit and spring element representation of fasteners. Also mentioned there is a need of further investigation geometric nonlinearity influence on calculated results and need of fully develop of fastener modeling approach [2].

Simulation using FEM modelling of bolted joints became a common practice, but this resulting in inaccurate analytical results. So, Rodriguez compared both analytical and experimental results from FEM and sinusoidal vibration, respectively. Finally it was concluded that accuracy of modelling techniques of bolted joints with stress concentration should be compared with real vibration testing to be confident about the results [14].

In another research of Lehnhoff, bolt threads effect on bolt and member stiffness was determined using axisymmetric FEA on bolted joints. The study was conducted on four different material members and all the members showed decrease in stiffness as magnitude of external

load increases. There was a significant difference even when there is no external load applied, with 65% decrease when changing from steel to aluminum members, 53% from steel to cast iron and 63% from steel to aluminum/cast iron. These members showed a significant difference when compared when threaded geometry was included. For all the models it is observed that the bolt stiffness decreased and member stiffness increased. Decrease in bolt stiffness might be due to increased flexibility of bolt and decrease in cross sectional area when threads are included. Increase in member stiffness may be explained as cause of decrease of initial member deflection. Member materials have impact on the stiffness of the member; bolt material change shows no change in bolt stiffness. So, member material should be given importance to increase overall joint stiffness [11].

Aluminum based structures took an important part in daily based usage structures and so it's connecting links. Plates are used as connecting elements for these aluminum alloys. In Menzemer's investigation of shear failure, commercially available aluminum magnesium silicon alloy in T6 condition was selected and a total number of twenty rectangular plates were fabricated and tension test was conducted on them. Various parameters which influence mechanically fastened joints were included in this study such as specimen geometric dimensions and orientation and fastener and fasteners lines (gage) spacing. Specimens were divided into four configurations on the basis of joint lengths and gage spacing and all samples were evaluated using high strength steel bolts. Results plotted on deflection-load graphs show an initial progressively increasing slope, which indicated slack removal from the load train coupled with a gradual slip into bearings. Plastic domain was reached after linear load-displacement region when initial load was removed. Decrease in load was observed when load was reached ultimate in most test specimens and finally load carrying capability was continually dropping until test

was terminated. All the specimens showed similar ultimate strengths and there were no sharp yield points and curve was similar to stress-strain curve in uniaxial tension test. Deformation varied with the overall joint length of the specimen, as the length is short the deformation is small and as length increases so do the deformation. Observation was made that deformation increases with the larger gage spacing. Stress strain distribution was also calculated for finite element model and the results were compared with the experimental results, which showed a reasonable agreement between both [7].

Failure damage analysis was conducted on deformed and failed surfaces of test specimens by examining samples using JEOL scanning electronic microscope (SEM). This examination shows the presence of local shearing and elongated dimples on the specimen surface. The growth of voids is observed to be directly proportional to the applied load. Effective stress σ_{eff} is calculated using ultimate strength (σ_u) and yield strength (σ_y) as shown below:

$$\sigma_{eff} = 0.6 \times \sigma_y + 0.6 \times CI \times (\sigma_u - \sigma_y) \quad (2.2)$$

Where, CI is connection length factor. For some joint lengths CI becomes equal to zero and/or σ_{eff} equal the σ_y and for joints longer than critical length shear stress will be below σ_y [7].

Detail investigation of load shearing between bolt and abutment was done by Gerbert. This investigation was carried on both theoretically that is finite element analysis FEA and experimentally. The load factor in terms of stiffness is calculated by using

$$\Phi = \frac{C_s}{C_s + C_u} \quad (2.3)$$

Where, C_s is the mounting stiffness of bolt and C_u is the mounting stiffness of abutment. Validity when the external load applied directly on the bolt head. In the rest of the cases fraction

of load factors is effective and is determined $\Phi_n = n\Phi$, where n is the load location factor and Φ is mounting load factor. It is also found that the load location factor is independent of external load location when external load is not applied close to the bolt head and abutment contact [20].

Riccio carried an experimental investigation to study the influence of geometrical and material properties on increase of damage when tensile load applied. This study was conducted using single lap bolted composite joints, where protruding and countersunk joints with varied bolt diameters and different member combinations such as composite to aluminum and composite to composite. Static tensile test was performed using INSTRON 4504 testing machine together with INSTRON extensometer and then followed by non-destructive ultrasonic test to see internal damage of fibers and matrix in the joints. The results showed that protruding bolts have more resistant and are capable to handle more load before damage than countersunk bolts, but there is no significant difference in terms of failure load. Maximum displacement at failure was larger for countersunk joints and protruding joints show damage area all around the hole which might be due to contact area of bolt head and plate [8].

Eric studied mechanical behavior of the hybrid joints which are single lap bonded/bolted joints and the material is assumed to have elastic behavior. 2D model was created using special finite BB element to simulate bonded element. As there is need of accurate local stiffness and fastener simulation shows complex behavior, two approaches were suggested. One is experimental tests and beam theory and the other is numerical 3D FE model which is validated by experimental results. To find adhesive shear stress T and peel stress S using analytical approach the following equations were used:

$$T = \frac{G_s}{e_s} (u_2 - u_1 - \frac{1}{2} e_r (\theta_1 + \theta_2)) \quad (2.4)$$

$$S = \frac{E_s}{e_s} (w_1 - w_2) \quad (2.5)$$

Where, G_s is coulomb's modulus of adhesive in MPa, e_s is adhesive thickness in mm, E_s is adhesive young's modulus in MPa, e_r is adherent thickness in mm, u is x-direction displacement in mm, w is y-direction displacement in mm, θ is angular displacement around z-direction in rad. There was a good agreement between the results of three approaches that is, between numerical, analytical and experimental [12].

Fukuoka investigated the static and fatigue strength of hybrid (adhesive/bolted) joints in structural reaction injection moulded (SRIM) composite materials. The authors performed an experimental investigation on a single-lap joint geometry considering the effect of different washer designs. It was concluded that the performance of the hybrid joints was dependent upon the Washer design which affected the distribution of the bolt clamping force. The hybrid joints were shown to have higher static strength and longer fatigue life than adhesive bonded joints for the studied material system [4].

2.2 Outline

Bearing failure, shear failure and tension failure and their combinations are most commonly observed failures in fastener joints. Joints strength is affected by different parameters, but it is mostly failed due to joints overlap length, fastener and hole clearance, bolt head and laminate contact friction and last but the least the laminate thickness. So, for a better design of a hybrid lap joint all the parameters should be given consideration and should be studied carefully.

CHAPTER THREE

FINITE ELEMENT ANALYSIS OF HYBRID LAP JOINT

Three dimensional finite element models were developed to investigate the transfer of load through bolt in a single lap hybrid joint with two rows of fasteners. The FE model results are validated by comparing with experimental solution for single lap hybrid joint connected with single fastener.

3.1 Finite Element Modeling (FEM)

ABAQUS package was used in creating and analyzing the Finite element models. Since ABAQUS is a powerful engineering simulation program it is capable of solving most challenging non-linear simulations .We can also find extensive libraries of element types and extensive list of material models in ABAQUS, which helps us to simulate any kind of engineering material. For non-linear simulations, the necessary parameters are the geometry, boundary conditions, material characteristics and loads. Increments of load and relating tolerances in non-linear analysis are automatically given by the software itself.

3.2 Development and Modeling Contact surfaces

Model has three major components on which analysis has to be performed they are, Panels with adhesive and 2 protruding bolts (shown in Figure 3.1 & 3.2)

- Flat Panels
- Adhesive
- Two protruding head bolts.

Figures 3.3 and 3.4 show pictorial view of single lap hybrid joint and its geometric parameters of panels, adhesive and bolts.

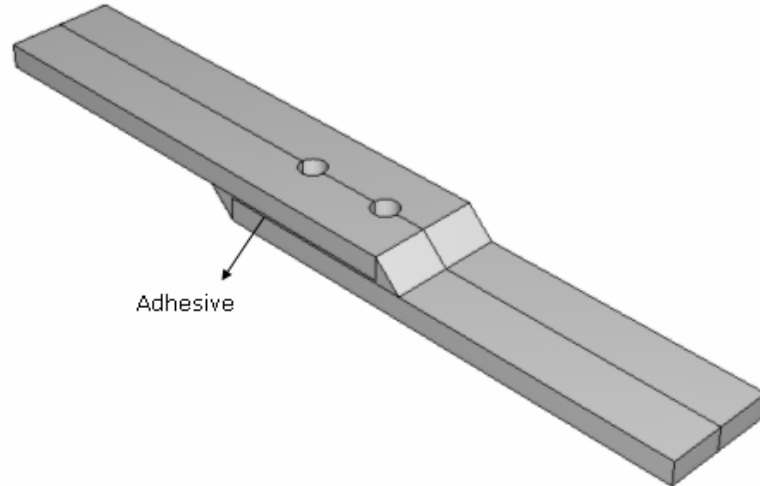


Figure 3.1 Flat panels with adhesive

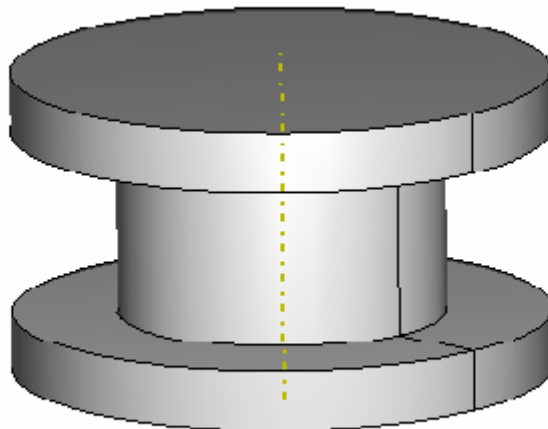


Figure 3.2 Protruding head bolt

Figure 3.3 shows the dimensions of all the parts in a single hybrid lap joint. Assumption was made that the joints are prismatic plates made of composite materials fastened with two rows of fasteners and adhesive. The right side of the bolt is considered as bolt 1 and the left side

of the bolt is assumed as bolt2. The aim of this model was to study the effect of different parameters on load transfer by bolt. The contact area between the bolt and the hole is defined and 8-node brick elements were used to mesh the components.

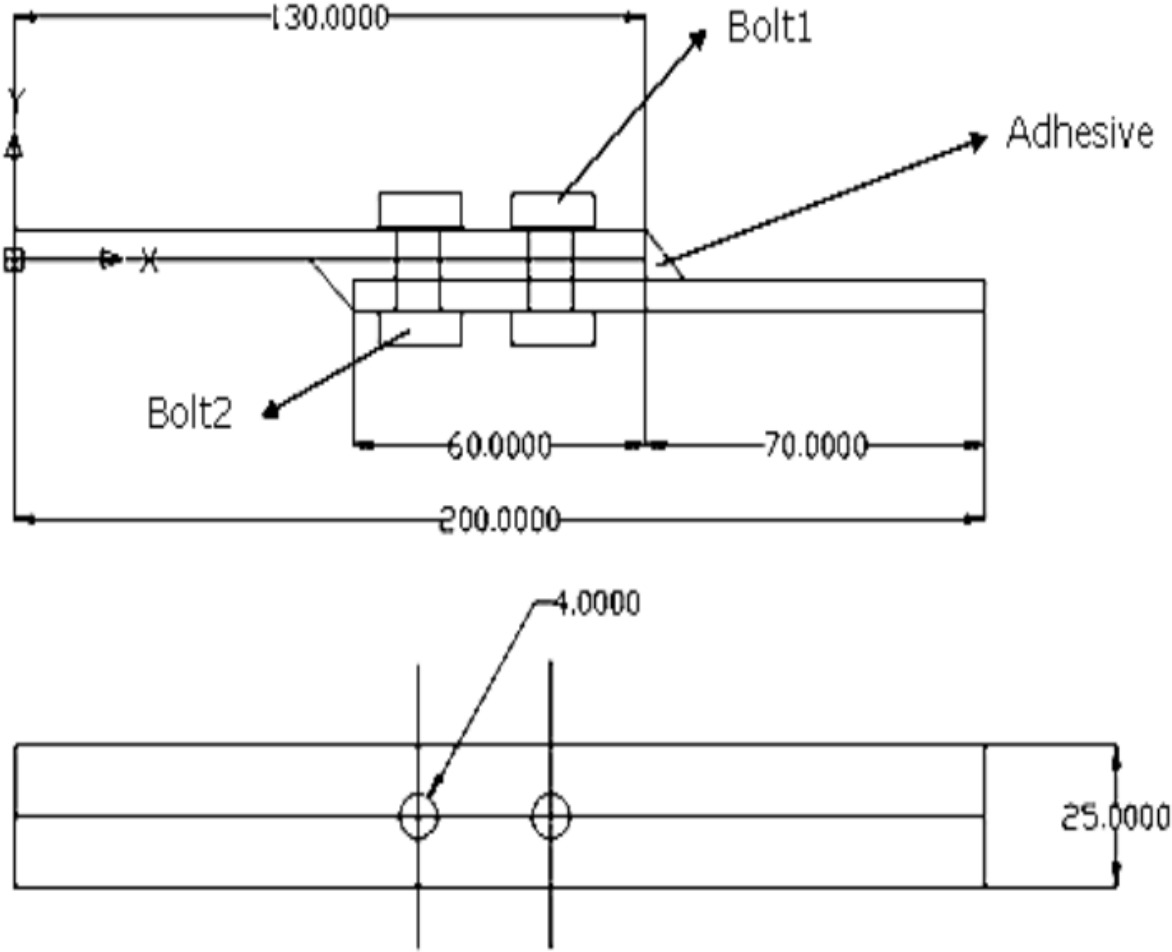


Figure 3.3 Layout of single lap hybrid joint

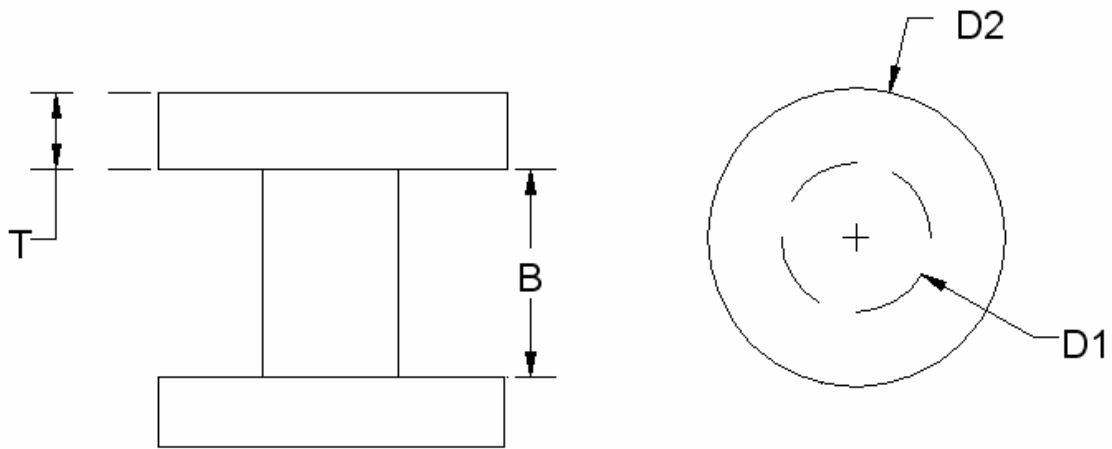


Figure 3.4 Layout of fastener

TABLE 3.1 Dimensions of the Fastener Component

parameter	T	B	D1	D2
Single hybrid lap joint	2	11.4	6	10

Modeling of contact surface between hole and the bolt is done using sliding interface with a coefficient of friction. A neat fit was considered always between the hole and bolt. Providing contact surface helps in prevention of elements to penetrate into each other, which also resist relative surface sliding. The coefficient of friction (μ) is empirical property of contact materials and contact pressure is (P). Product of these two gives the limiting friction shear stress value i.e. ' μP '.

Where, for most common materials μ can be given as, $0.1 \leq \mu \leq 0.3$. A friction coefficient of 0.2 was taken between the hole and bolt. In this thesis, master-slave algorithm has been used to define contact pairs, in this approach master is a hole and slave is a bolt. The bolt shear load was determined by adding the nodal forces on the mid-surface of the bolt.

3.3 Boundary and Loading Conditions

As shown in Figure 3.5. In single lap hybrid joint the left edge surface of the upper panel was constrained in X, Y and Z directions and the right edge surface of the lower panel is left free to move in X-direction only. Uniform tensile load was applied at the right end of the plate. The effects of both non-linear material properties and non-linear geometry were included in the analyses.

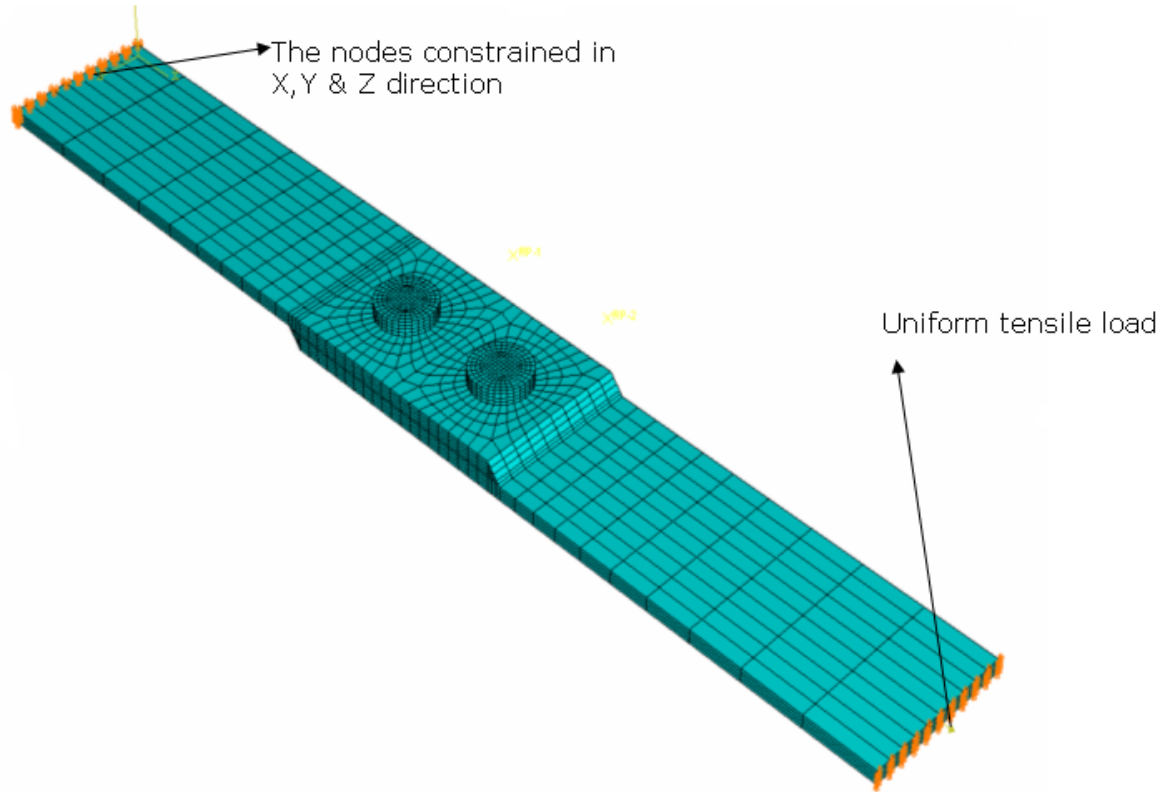


Figure 3.5 Boundary and loading conditions

3.4 Pre-tension

Circular cross section was defined as pre-tension section which is located at fastener center which divides it symmetrically as shown in the Figure 3.6. The assembly load across the pretension section is transmitted by the pre-tension node. The pre-tension node should not be attached to any of the elements in the model and the coordinates at this point are not significant. A load concentration of 5 KN is applied in Z-direction at pre-tension node (Figure 3.7.).

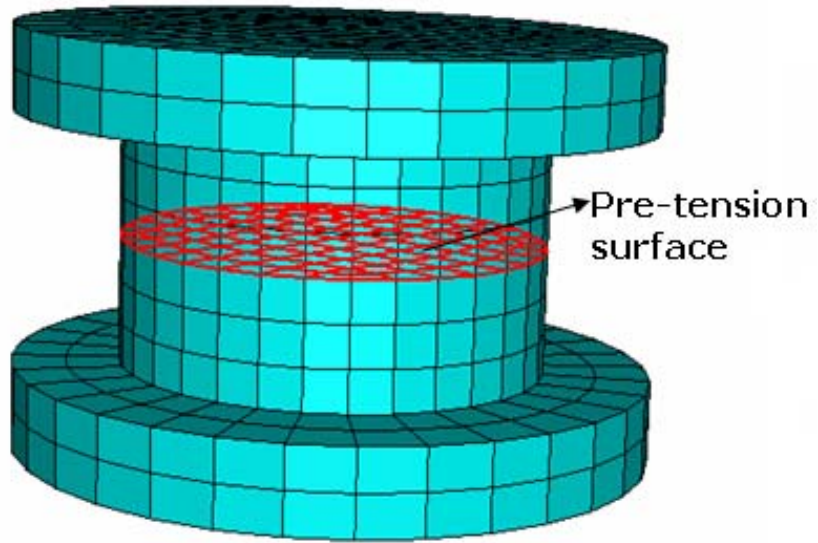


Figure 3.6 Surface Pre-tension

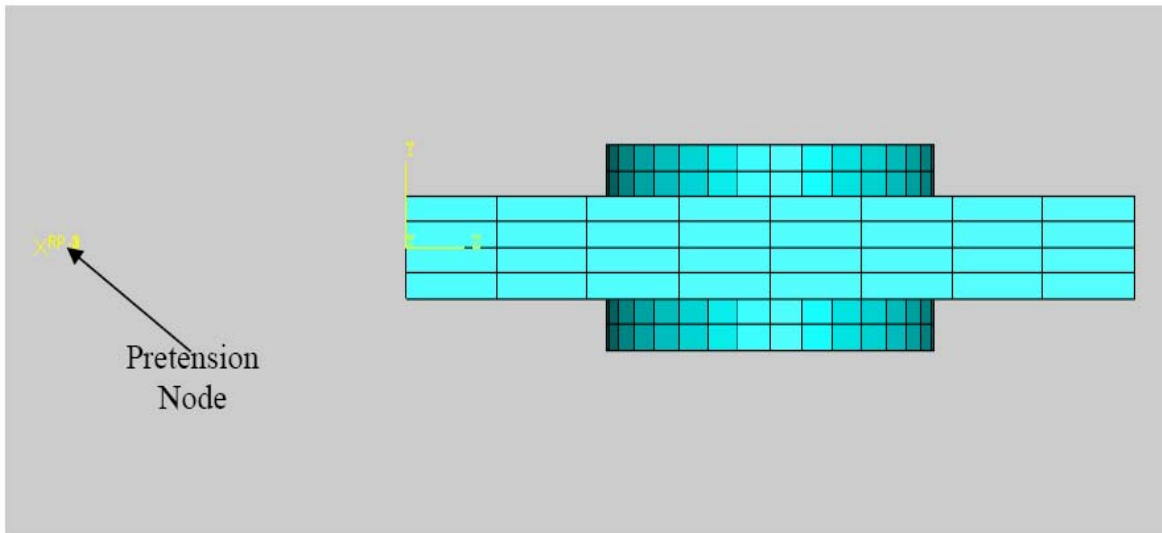


Figure 3.7 Pre-tension node

3.5 Formulation

Components of single lap hybrid joints were meshed in ABAQUS using different methods in this analysis. The Figure 3.8 shows the typical Finite element meshed model of plates with out bolts of the lap joints.

The flat panels are meshed in square shape and at the overlapped region and region around the hole are meshed in circular shape. Fine mesh is used to model the interface between the hole and the fastener and biased mesh was used at the far ends where, the flat panels don't overlap as shown in the Figure 3.10 and Figure 3.9 depicts mesh field around the hole. All the components (namely, flat panels, adhesive and bolt) of the single lap hybrid joint are meshed using 3-dimenssional 8- node solid brick elements. Figure 3.11 shows finite element meshed model of a fastener. Table 3.2 discusses about material properties.

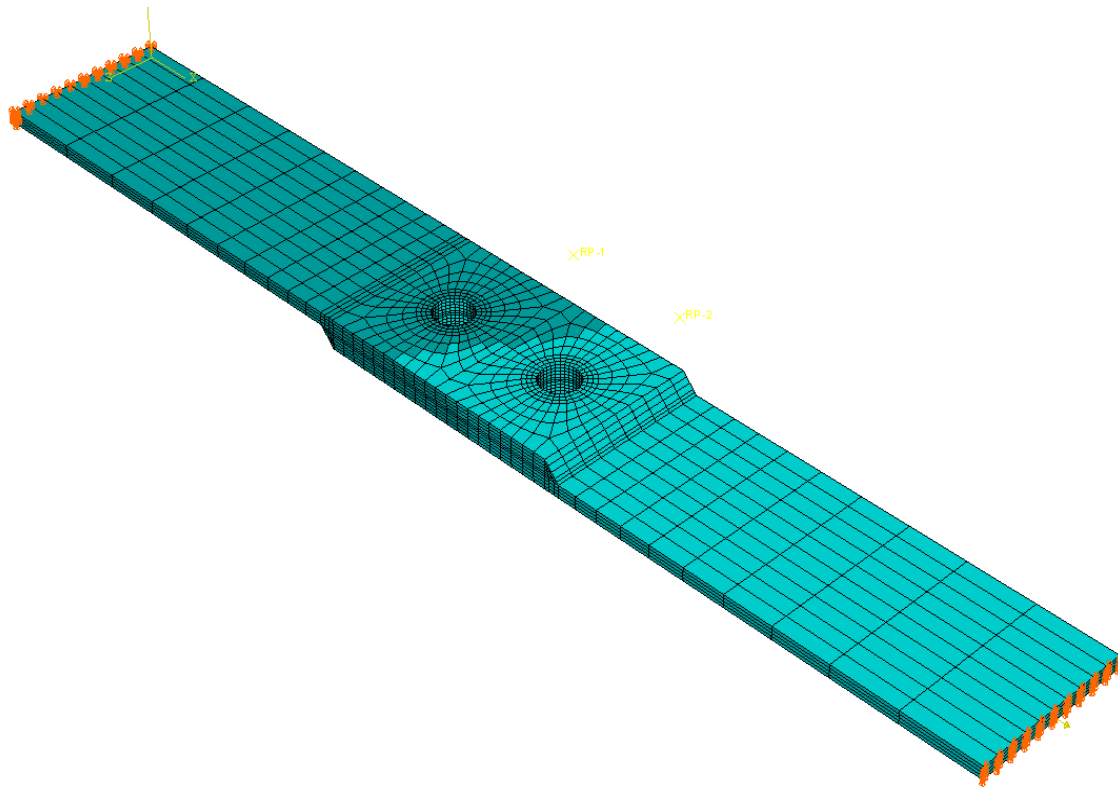


Figure 3.8 Meshed model of plates with holes

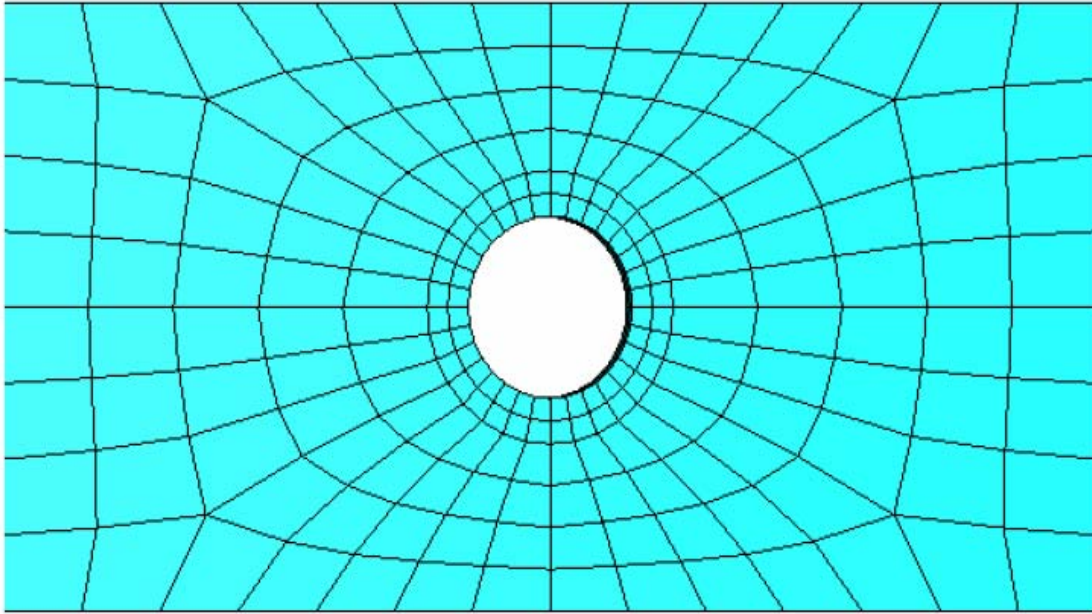


Figure 3.9 Mesh near the hole

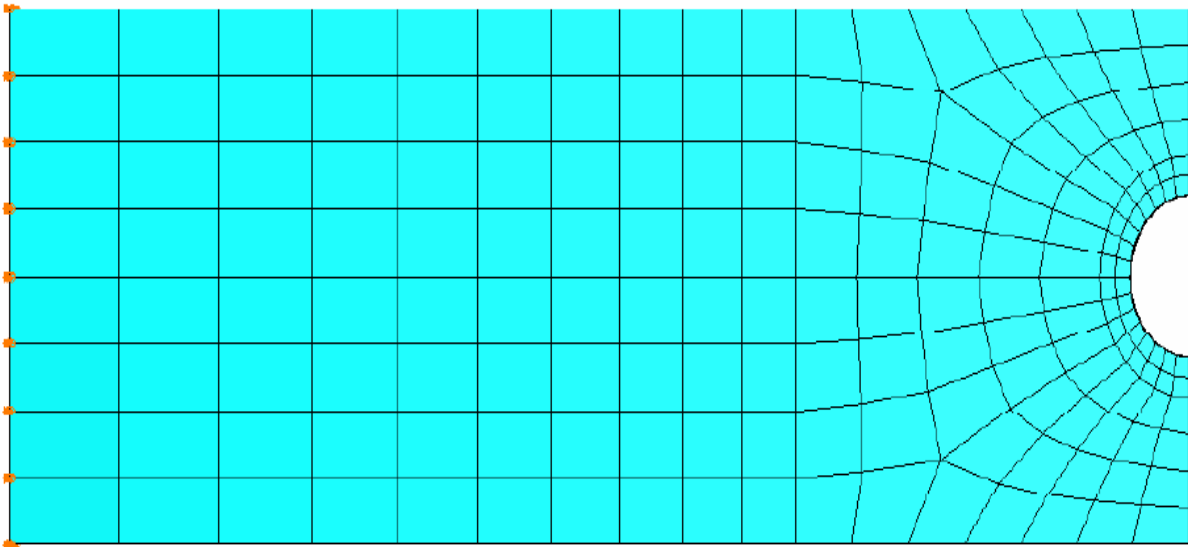


Figure 3.10 Biased mesh at plates far end

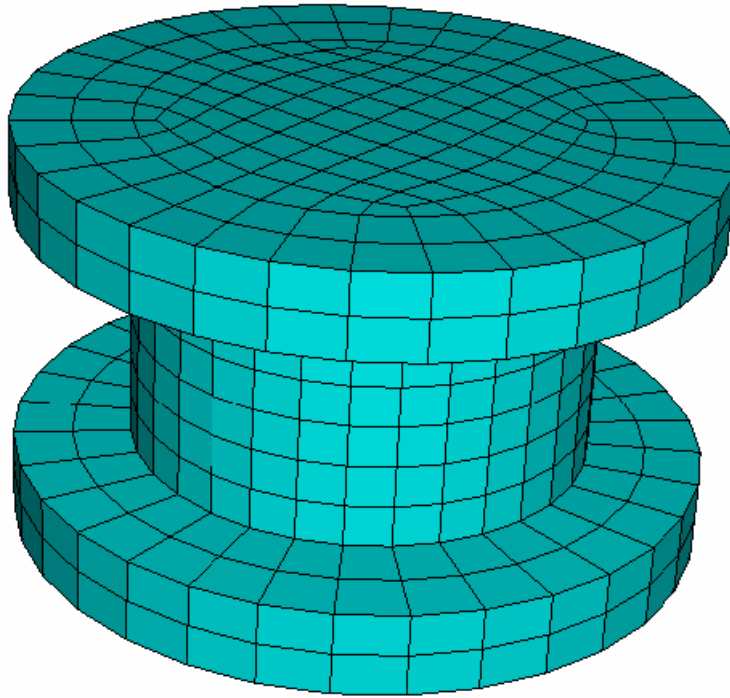


Figure 3.11 Meshed model

TABLE 3.2 Material Types and their Properties

Material	E11 (Gpa)	E22 (Gpa)	E33 (Gpa)	G12 (Gpa)	G13 (Gpa)	G23 (Gpa)	ν_{12}	ν_{13}	ν_{23}
<i>Carbon fiber/ epoxy</i>	98	7.8	7.8	4.7	4.7	3.2	0.34	0.34	0.44
<i>HTA/6376</i>	140	10	11	5.2	5.2	3.9	0.3	0.3	0.5
<i>Laminate</i> <i>(Hexcel composites)</i>	54.25	54.25	10	20.72	4.55	4.55	0.31	0.33	0.33

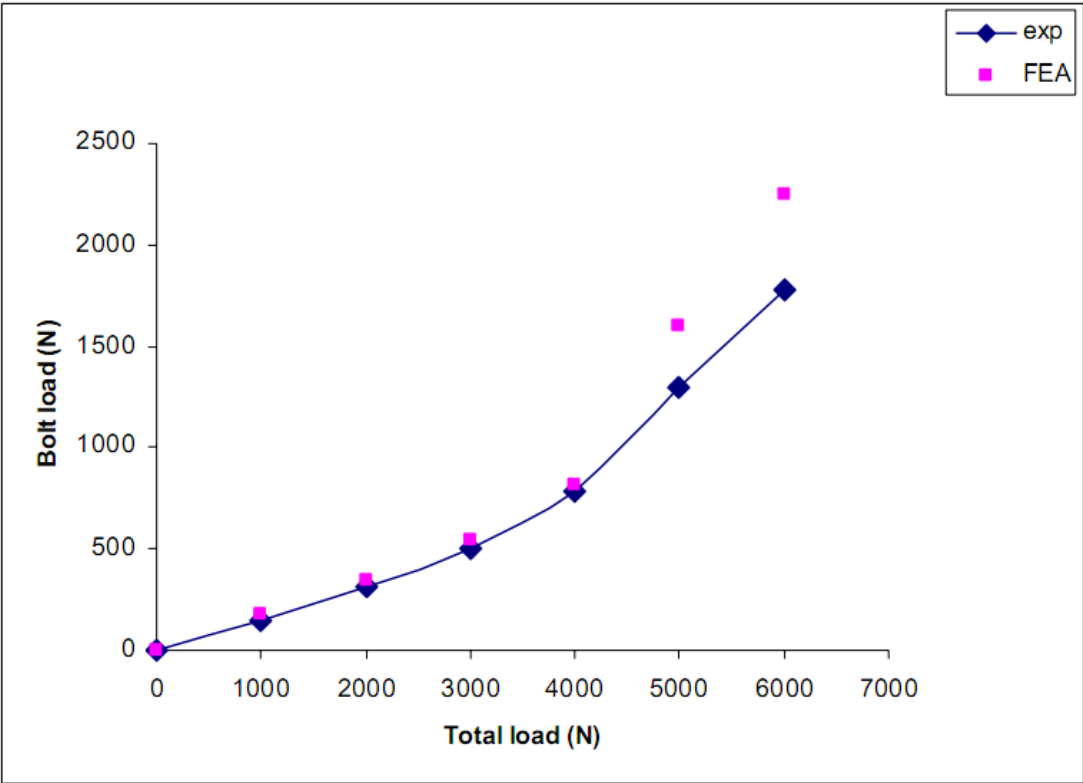
3.6 Validation

The finite element model developed in this study has been validated by comparing the FE model results for single bolted single lap hybrid joint with experimental results for single bolted single lap hybrid lap joint. The aim of the experimental program was to measure the load distribution in the hybrid joint and validate the results obtained from the finite element model [9].

The joint was fitted with an instrumented bolt which was used to measure the shear load. The dimensions of the joint were restricted by the design of the instrumented bolt. The mid-length of the bolt shank must lie in the shear plane of the joint to ensure correct measurement of the bolt shear load. This placed a restriction on the thickness of the adherends used in the joint. The laminate adherends were fabricated from the carbon fiber /epoxy unidirectional pre-preg system HTA/6376 (Hexcel Composites). The bonding surfaces were grit-blasted and degreased prior to bonding and the joints were cured according to the manufacturer's specification. A hole of diameter of 6 mm was machined in the joint using a dagger drill with a backing plate used to prevent back face delamination. The joint was subject to quasi-static tensile testing which was conducted using a universal testing machine (Instron 4505) with a 100 KN load cell. The system was fully computer controlled and allowed for acquisition of load, displacement and strain data. The tests were run in displacement control at a rate of 0.5 mm/min. Loading was stopped at sub-critical load levels in order to prevent damage to the instrumented bolt. The load transferred by the bolt in the hybrid joint was measured using a specially instrumented bolt. The technique was previously used to measure the bolt load transfer in multi-row lap shear joints. The bolt was a titanium hi-torque lock bolt which was adapted to include load measurement instrumentation. The bolt was instrumented with two strain gauge rosettes on each side of the

bolt. The strain gauges were located equidistant from the shear plane of the joint. Connection of the strain gauges in a full Wheatstone bridge eliminated the effect of the axial bolt strains on the shear strain measurement [9].

The signal from the measurement bolt was calibrated by testing a single-lap bolted joint manufactured from the same adherend material. The measurement bolt was inserted in the hole and finger tightened to limit the effects of lateral clamping. Tensile load was applied to the bolted joint and the signal from the measurement bolt and testing machine load cell recorded. The procedure was repeated three times in order to obtain an average signal characteristic. The measurement signal from the bolt was correlated to the load cell reading providing a calibration curve for the bolt. The curve of bolt load versus total applied load (Figure 3.12) is shown to be non-linear with the bolt load increasing at a greater rate as the joint is loaded [9].



3.12 Bolt load versus Total applied load

The load transfer by bolt increases by 18% when the tensile load is increased from 1000N to 2000N as shown in the Figure 3.12. The difference in load transfer by bolt is 20% when the tensile load of 3000N is used. There is an increase of 27% when the tensile load is increased from 3000N to 4000N and the increase is 68% for the tensile load of 5000N. There is an increase of 74% when the tensile load is increased from 5000N to 6000N.

It can be observed from the plot that there is an increase in tensile load values along X-direction there is change of load transfer values by bolt on the Y axis followed very closely up to 4000N and after that there is significant difference between experimental and FEA values of load transfer by bolt as seen in the Figure 3.12.

CHAPTER FOUR

RESULTS

The following chapter gives a detailed overview of the load transfer computed using finite element model for a single lap bolted/hybrid joint. A parametric study has been carried out to find the effect of various parameters namely Adherend thickness, Material properties, Bolt diameter, tensile load and the overlap length, on the load transfer by bolt.

4.1 Load Distribution

In a single lap Hybrid/Bolted joint, the applied tensile load on the joints transfers from one component to another through either interface friction or through transverse shear force and it is observed that the eccentricity loading leads to bending in joints (Fig 4.1). For the current condition failure mode prediction is difficult, due to the bending effects. Load transfer outputs are computed by the bolt in the lower plate which is near to the tensile load applied edge.

Von-mises stress near holes is shown in Figure 4.2. As the compressive stress between the bolt and the hole is less, this is a signal that there is a transfer of load at the joints due to interface friction.

Principal stress distribution in X-direction and Von-mises stress near the hole are shown in Figures 4.3 and 4.4.

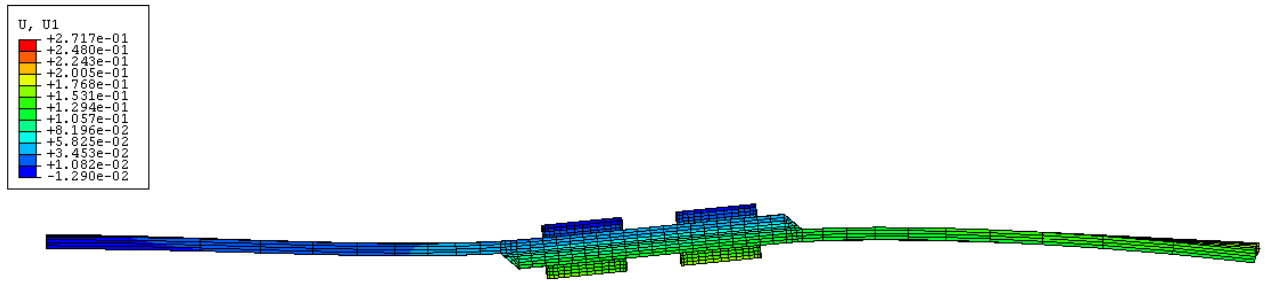


Figure 4.1 Deformation under tensile load

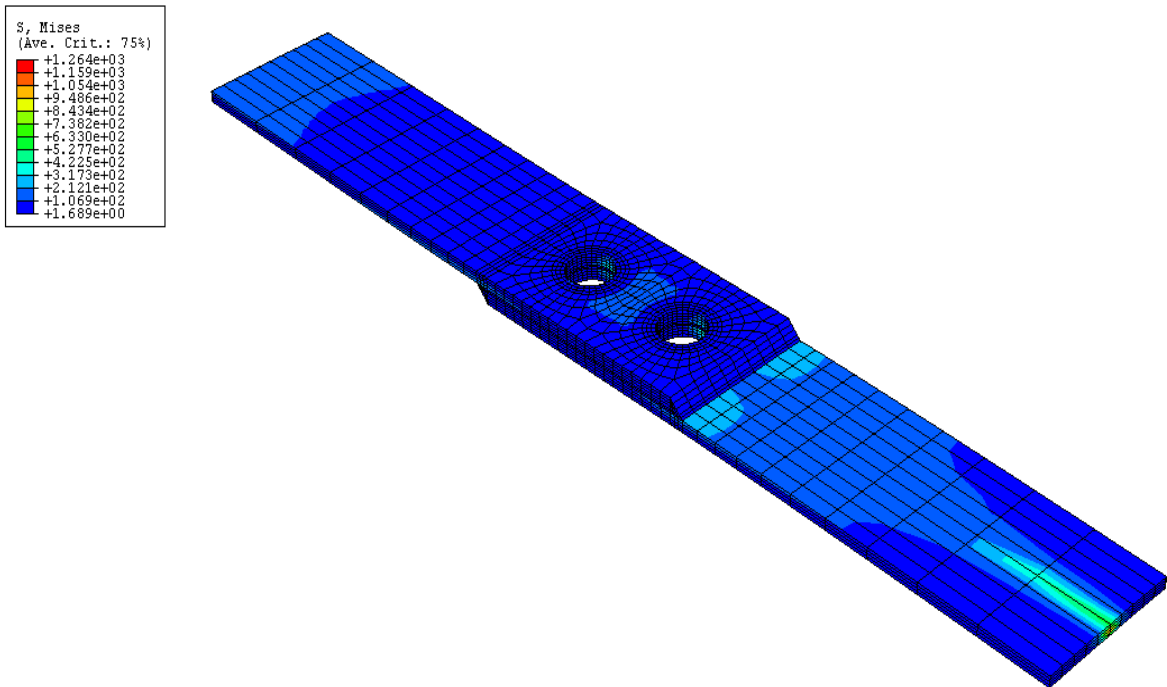


Figure 4.2 Von-mises stress distribution in the adherends

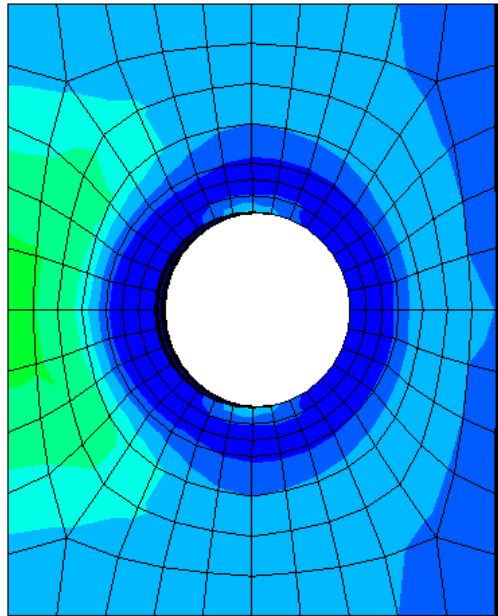
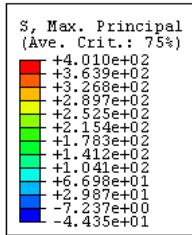


Figure 4.3 Principle stress distribution

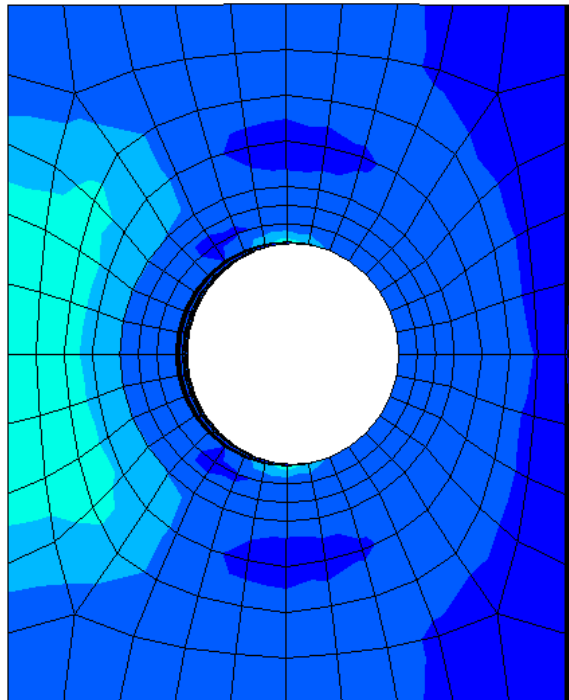
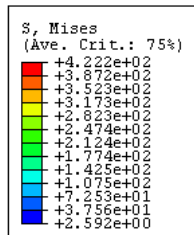


Figure 4.4 Von-mises stress distribution

Model matrix with different parameter sets shown in Table 4.1. Model matrix shows different set of models such as MODEL A, MODEL B, MODEL C, MODEL D, MODEL E, MODEL F, MODEL G, MODEL H, MODEL I, MODEL J, MODEL K, MODEL M, MODEL N and MODEL O. Parameters include adherend thicknesses of 1.8mm, 3.6mm, 5.4mm; bolt diameters of 6mm, 7mm, 8mm; overlap lengths of 40mm, 50mm, 60mm; tensile loads of 1000N, 3000N, 4000N and materials carbon/fiber epoxy, HTA/6376 composites laminate (Hexcel composites) have been used. These above mentioned models are discussed in detail with simulations in Appendix A.

Table: 4.1 Model Matrix

Model	Material	Adherend thickness(mm)	Bolt diameter(mm)	Overlap length(mm)	Tensile load(N)
Model A	Carbon/fiber epoxy	1.8	6.0	40.0	1000
Model B	HTA/6376	1.8	7.0	40.0	1000
Model C	Laminate	1.8	8.0	40.0	1000
Model D	Carbon/fiber epoxy	1.8	6.0	40.0	4000
Model E	Carbon/fiber epoxy	3.6	7.0	40.0	4000
Model F	Carbon/fiber epoxy	5.4	8.0	40.0	4000
Model G	Carbon/fiber epoxy	5.4	6.0	40.0	1000
Model H	Carbon/fiber epoxy	5.4	7.0	40.0	3000
Model I	Carbon/fiber epoxy	5.4	8.0	40.0	4000
Model J	Carbon/fiber epoxy	1.8	6.0	50.0	1000
Model K	Carbon/fiber epoxy	1.8	7.0	50.0	3000
Model L	Carbon/fiber epoxy	1.8	8.0	50.0	4000
Model M	Carbon/fiber epoxy	1.8	6.0	40.0	4000
Model N	Carbon/fiber epoxy	1.8	7.0	50.0	4000
Model O	Carbon/fiber epoxy	1.8	8.0	60.0	4000

4.2 Influence of Material Properties

Effects of material properties on load transfer were studied by changing elastic properties and study was done on three different materials. The detailed material properties of these materials have been shown in the Table 3.2.

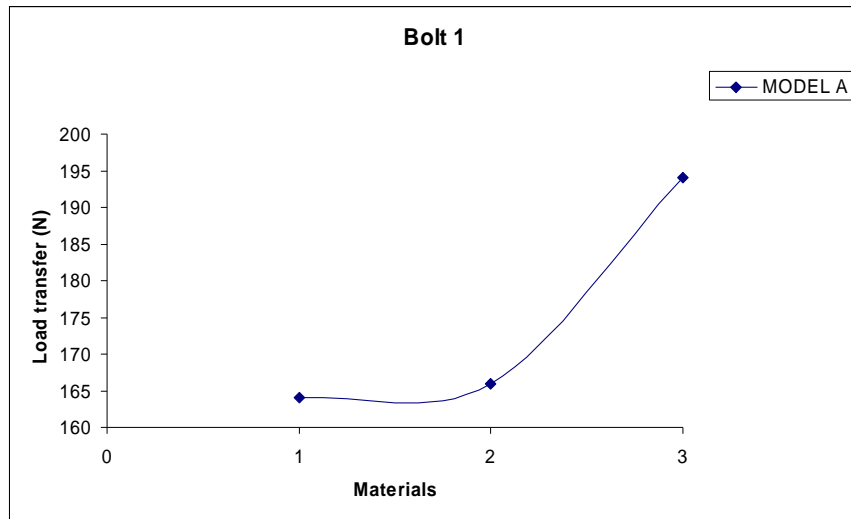


Figure 4.5 Load transfer by bolt 1 for MODEL A

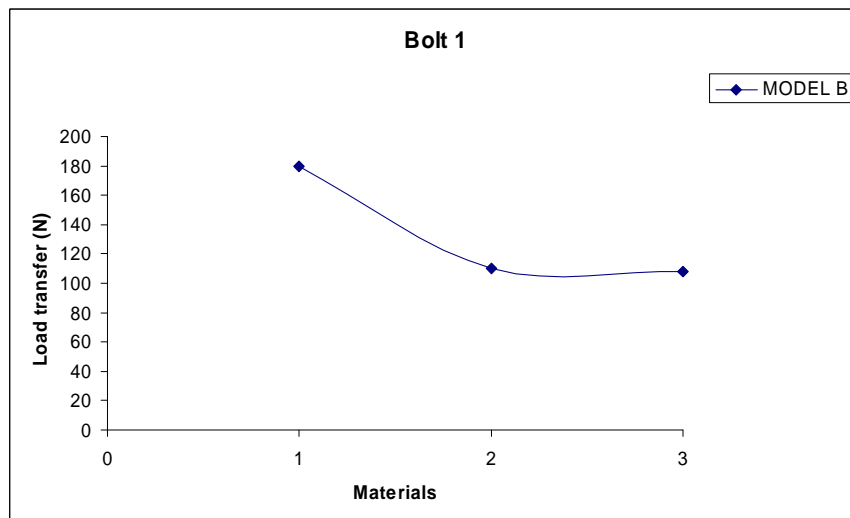


Figure 4.6 Load transfer by bolt 1 for MODEL B

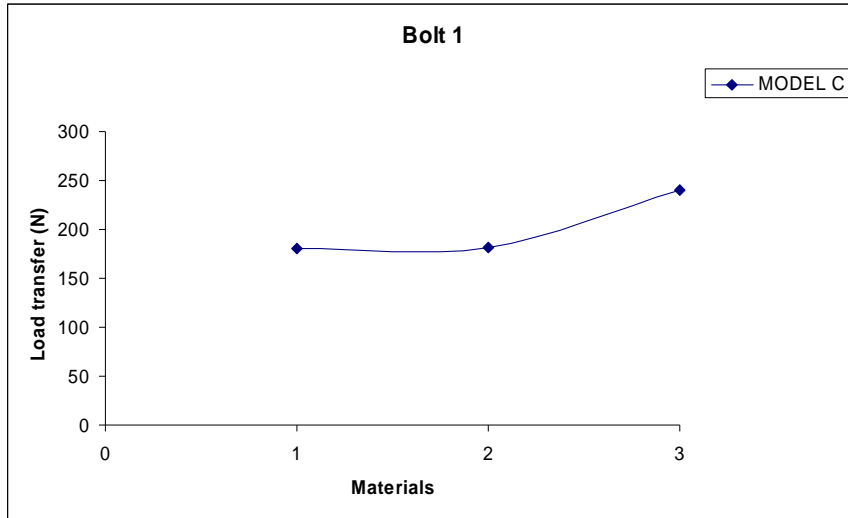


Figure 4.7 Load transfer by bolt 1 for MODEL C

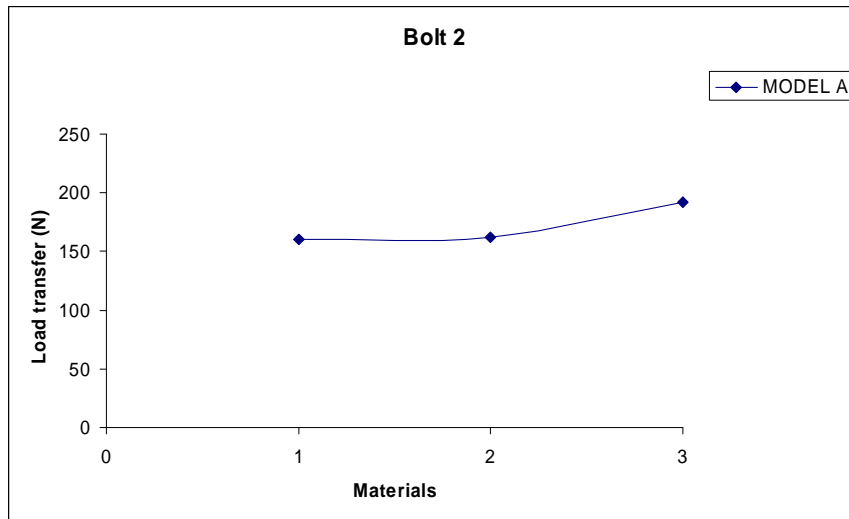


Figure 4.8 Load transfer by bolt 2 for MODEL A

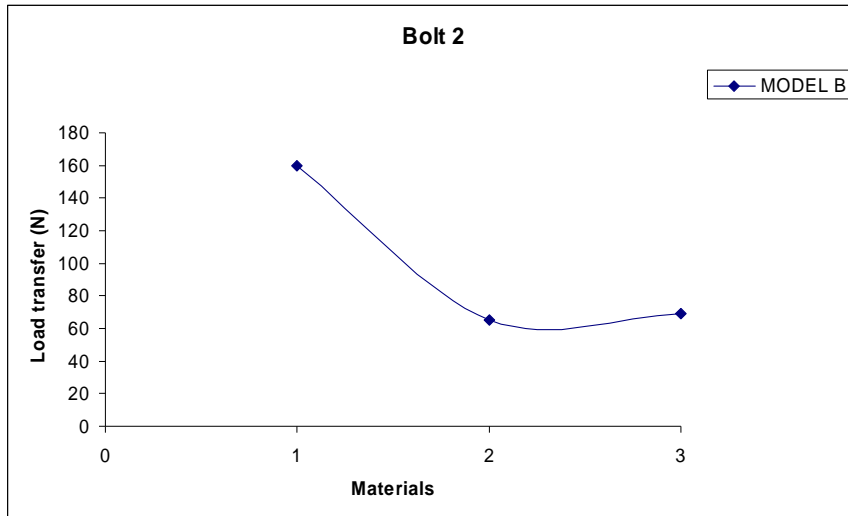


Figure 4.9 Load transfer by bolt 2 for MODEL B

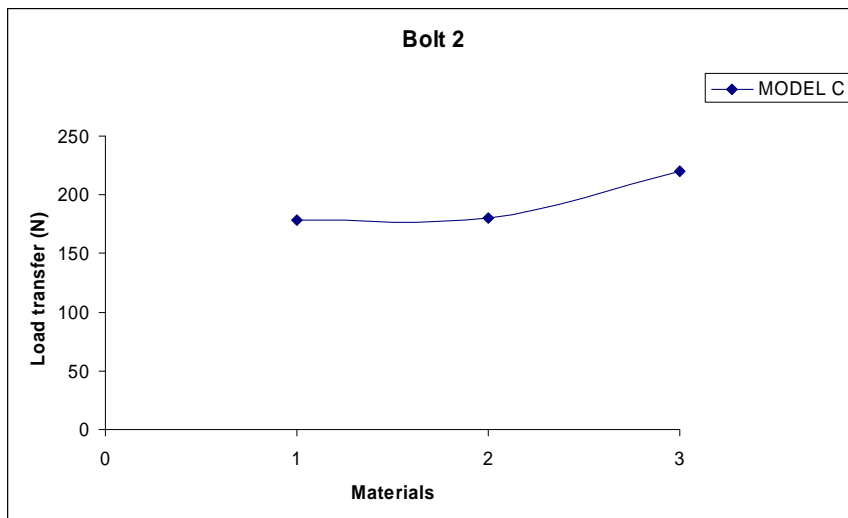


Figure 4.10 Load transfer by bolt 2 for MODEL C

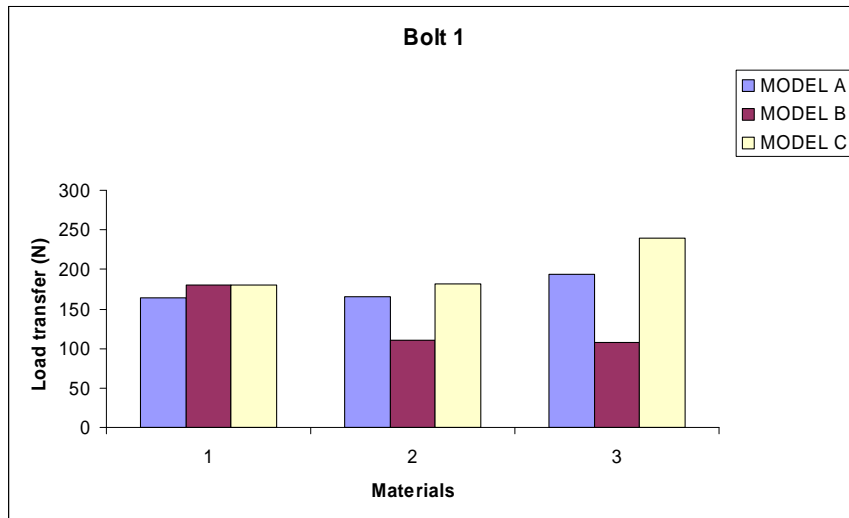


Figure 4.11 Load transfer by bolt 1 for different material models

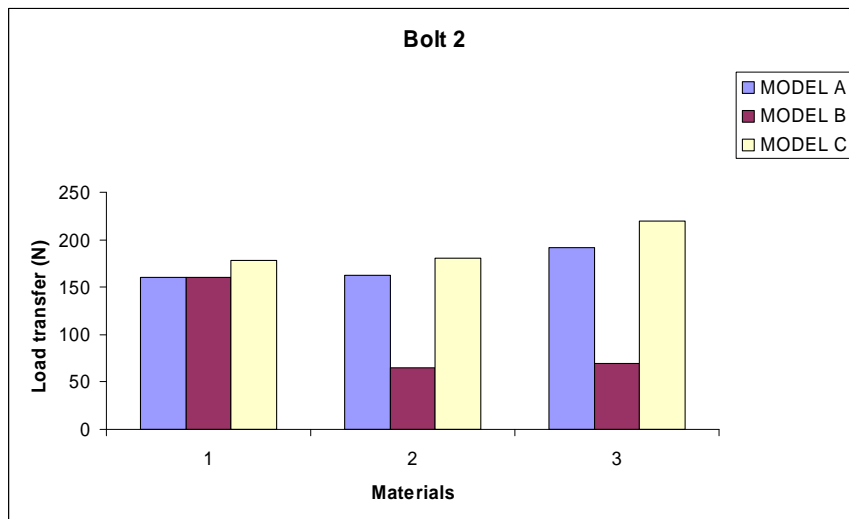


Figure 4.12 Load transfer by bolt 1 for different material models.

There is a difference of 7% load transfer by Bolt 1 when carbon/fiber epoxy is used over HTA/6376. The difference is 16% when Laminate (Hexcel composites) is used as shown in the Figure 4.11.

There is a difference of 6% load transfer by Bolt 2 when carbon/fiber epoxy is used over HTA/6376. The difference is 12% when Laminate (Hexcel composites) is used as shown in the Figure 4.12.

However, significant change was observed from the graphs (Figures 4.11 and 4.12) in transfer of load by bolt along Y direction when the elastic properties of the plates on the X axis were changed.

4.3 Influence of Tensile Load

The effect of tensile load on the load transfer by bolt is studied by running the finite element analysis for three values of tensile load.

Loads of 1000N, 3000N and 4000N are being studied. The Figure 4.19 and 4.20 illustrates the distribution of the load transfer developed by the bolt for different tensile loads applied to the joint.

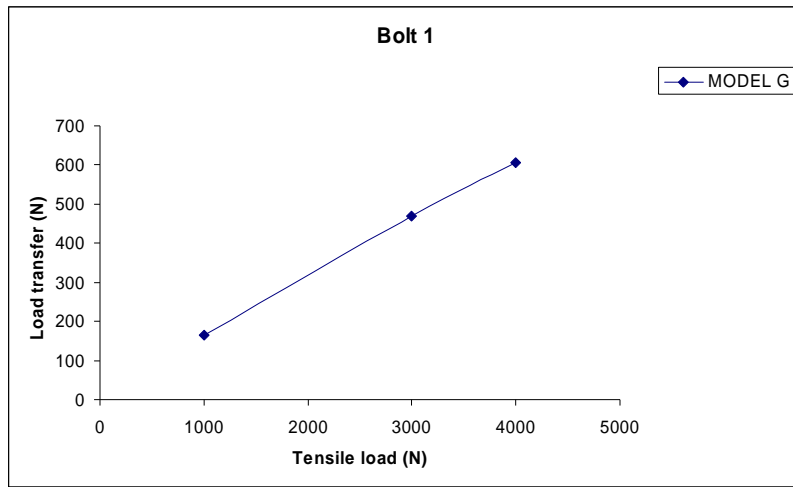


Figure 4.13 Load transfer by bolt 1 for MODEL G

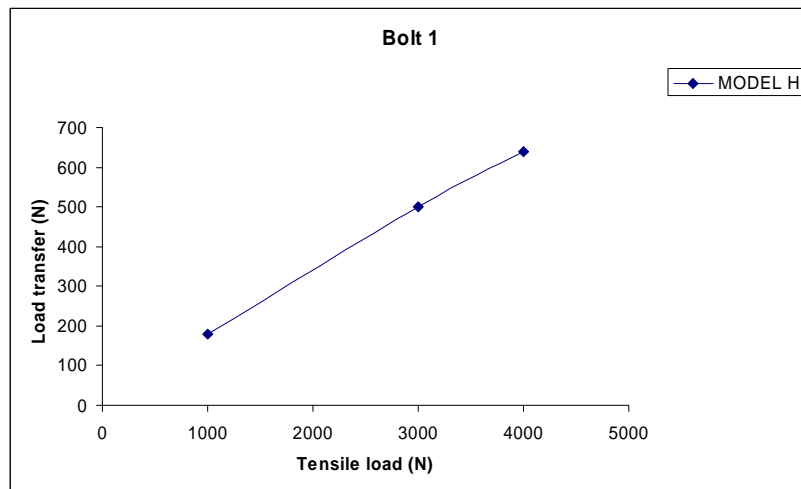


Figure 4.14 Load transfer by bolt 1 for MODEL H

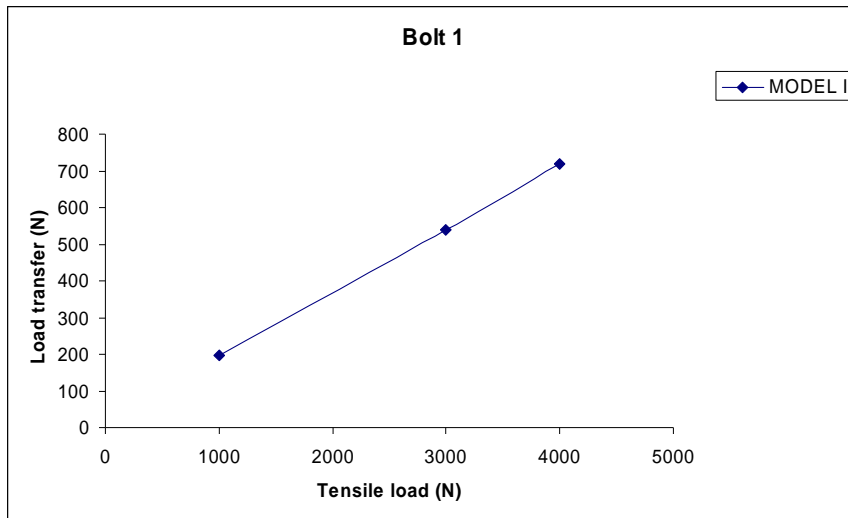


Figure 4.15 Load transfer by bolt 1 for MODEL I

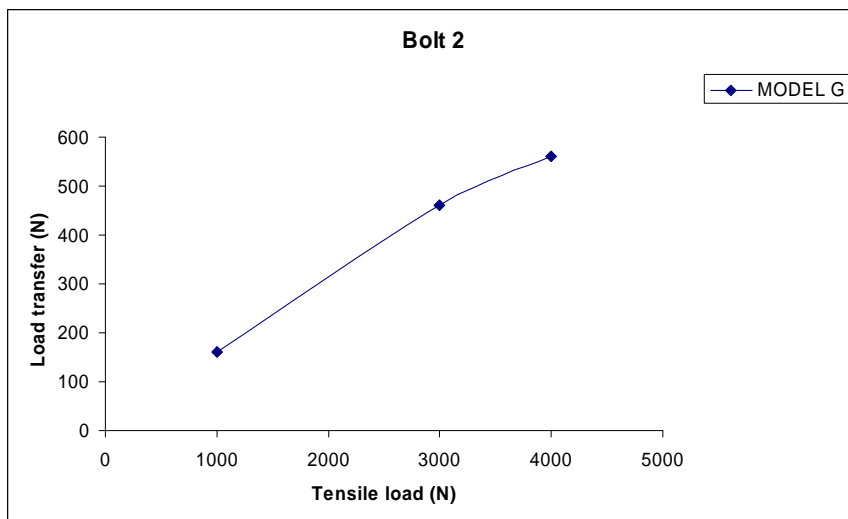


Figure 4.16 Load transfer by bolt 2 for MODEL G

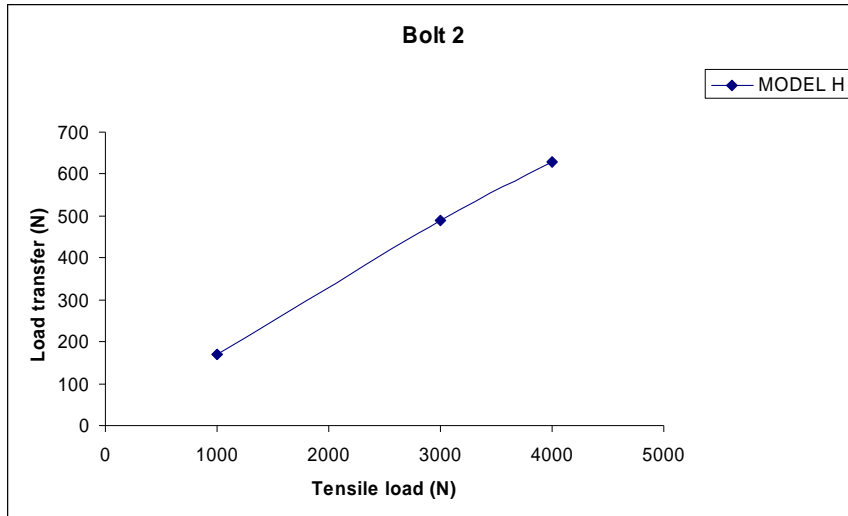


Figure 4.17 Load transfer by bolt 2 for MODEL H

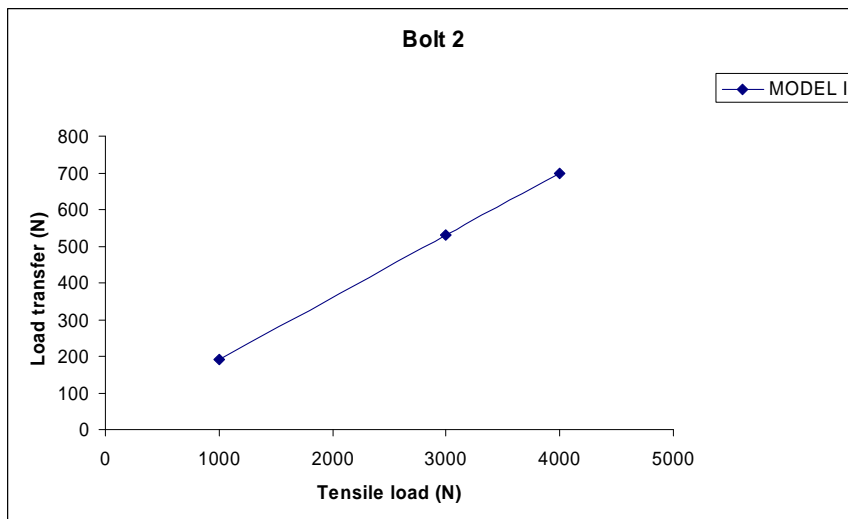


Figure 4.18 Load transfer by bolt 2 for MODEL I

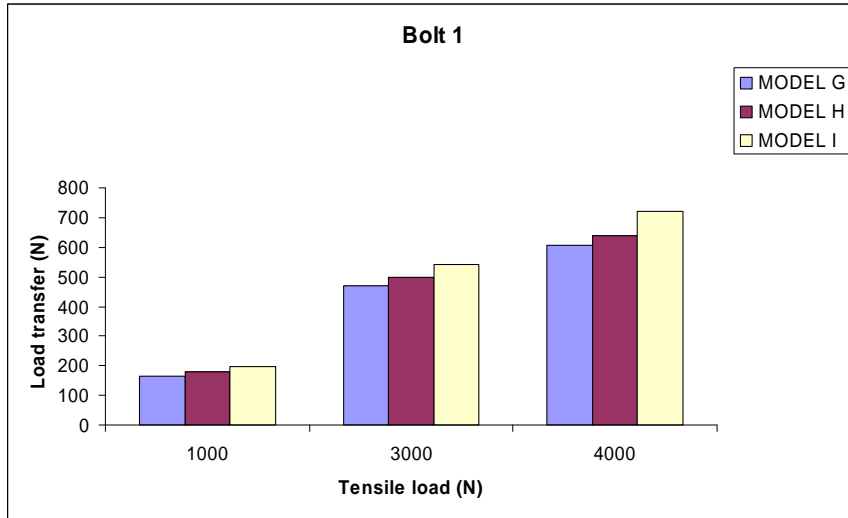


Figure 4.19 Load transfer by bolt 1 for different tensile loads.

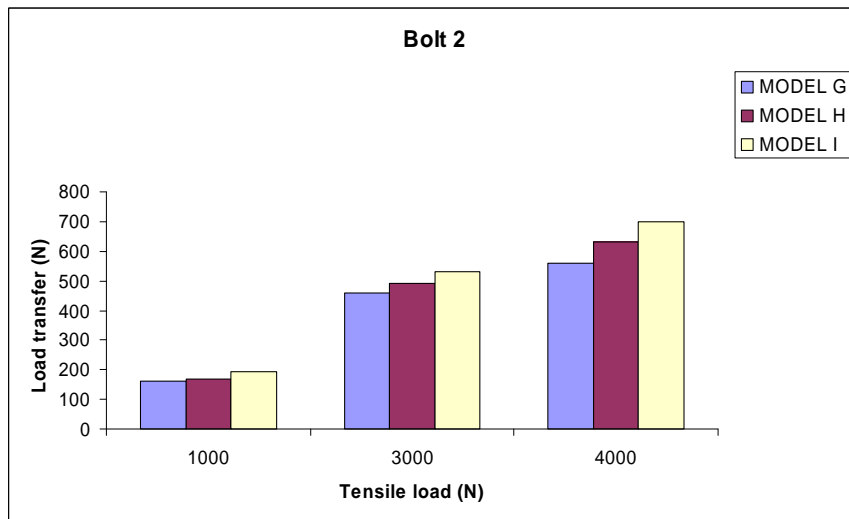


Figure 4.20 Load transfer by bolt 2 for different tensile loads

The load transfer by Bolt 1 increases by 65% when the tensile load is increased from 1000N to 3000N as shown in the Figure 4.19. The difference in load transfer by bolt is 25% when the tensile load of 4000N is used.

The load transfer by bolt 2 also increases with the increase of the tensile load as shown in the Figure 4.20. There is an increase of 60% when the tensile load is increased from 1000N to 3000N and the increase is 20% for the tensile load of 4000N.

It can be observed from the plots that there is increase in tensile load values along X direction there is change of load transfer values by bolt on the Y axis as seen in the Figures 4.19 and 4.20.

4.4 Influence of Adherend thickness

The effect of Adherend thickness is studied by running the finite element analysis for different values of Adherend thicknesses.

Adherend thicknesses of 1.8mm, 3.6mm and 5.4mm are used keeping all the other parameters constant.

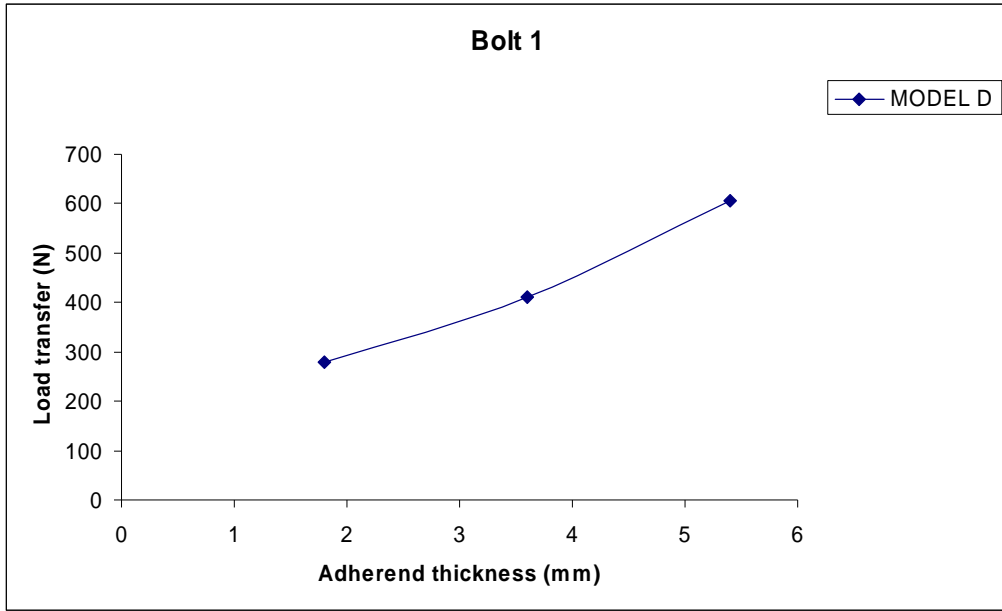


Figure 4.21 Load transfer by bolt 1 for MODEL D

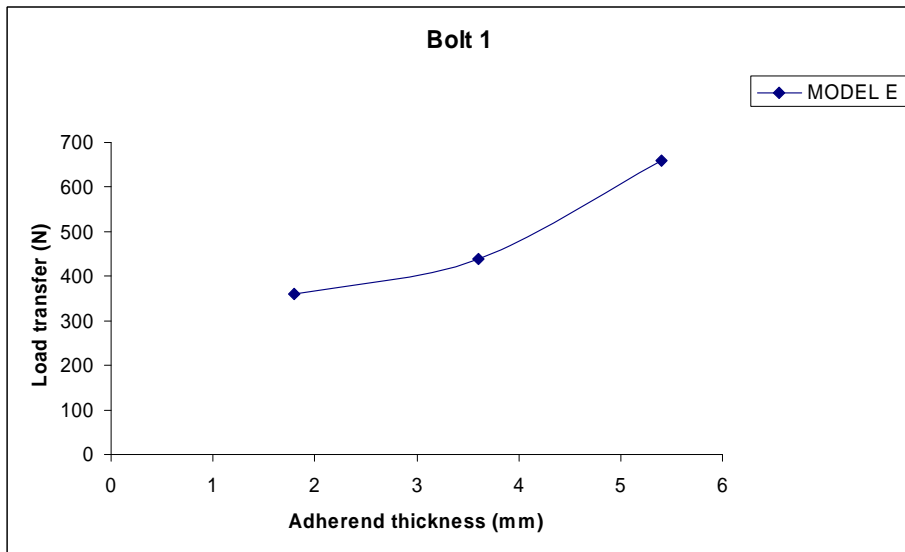


Figure 4.22 Load transfer by bolt 1 for MODEL E

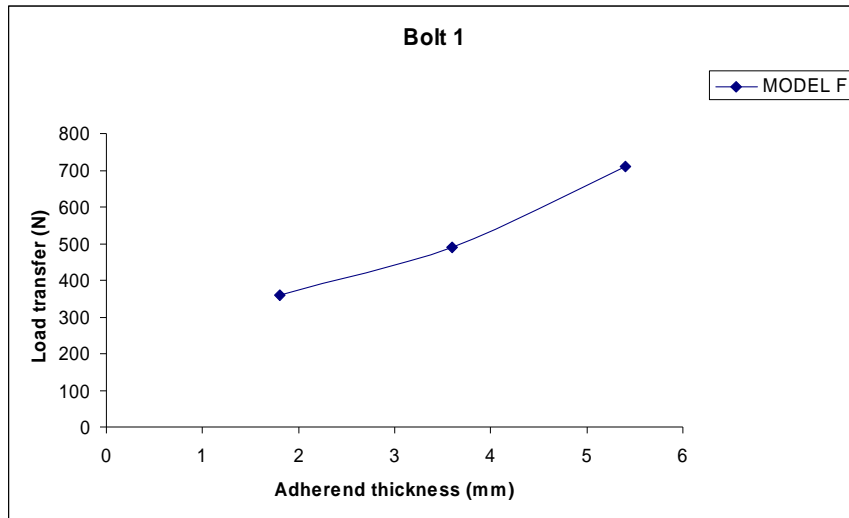


Figure 4.23 Load transfer by bolt 1 for MODEL F

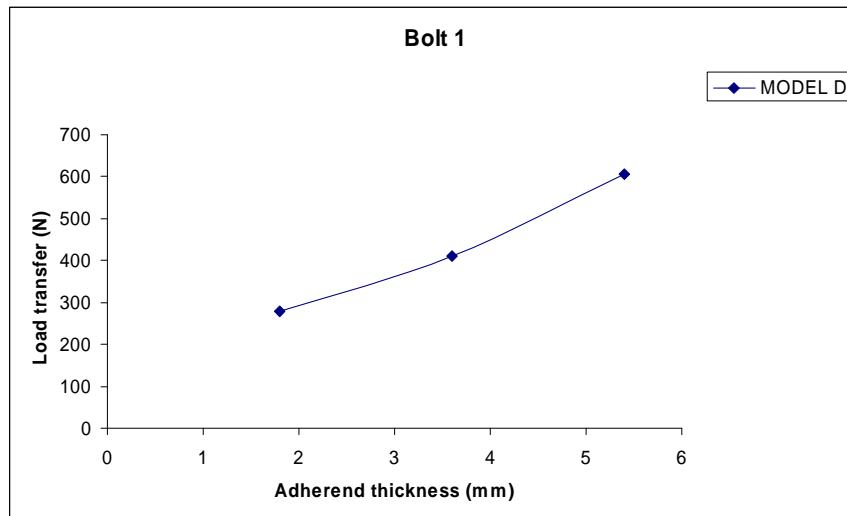


Figure 4.24 Load transfer by bolt 2 for MODEL D

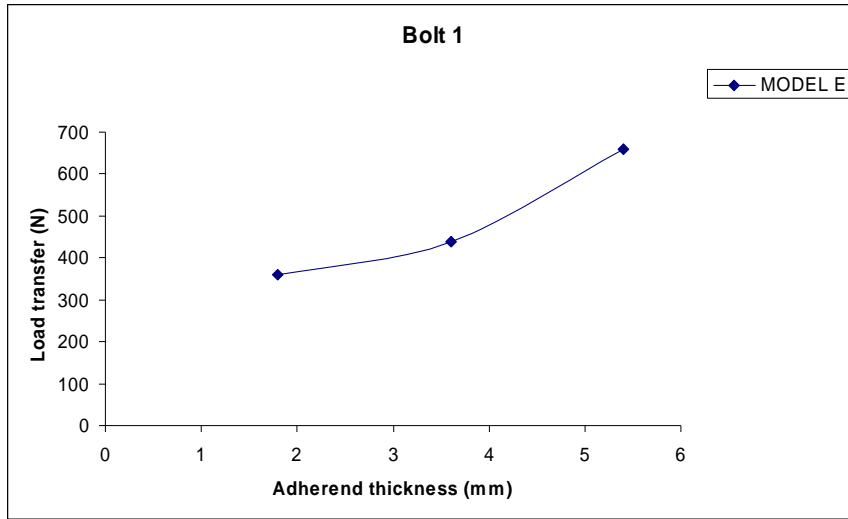


Figure 4.25 Load transfer by bolt 2 for MODEL E

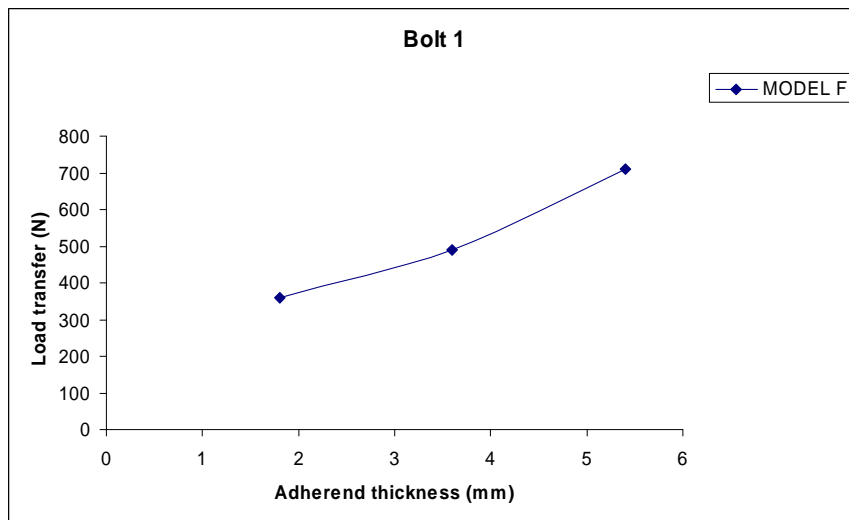


Figure 4.26 Load transfer by bolt 2 for MODEL F

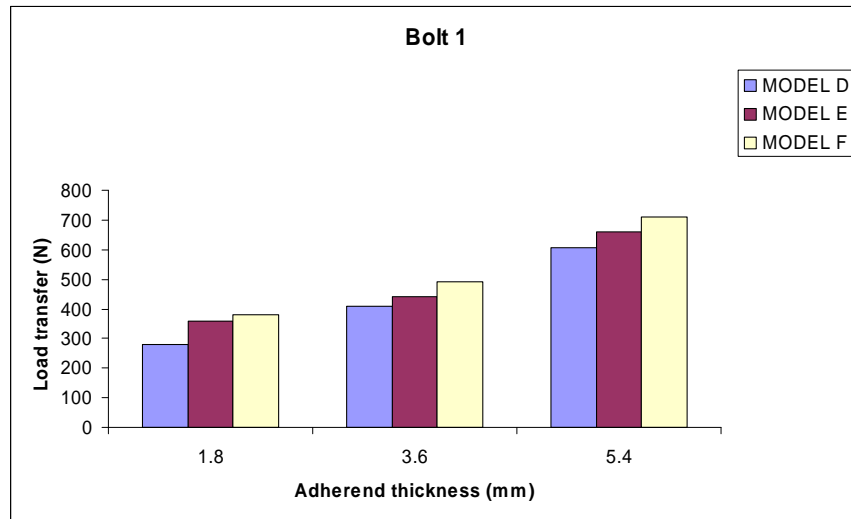


Figure 4.27 Load transfer by bolt 1 for different Adherend thicknesses.

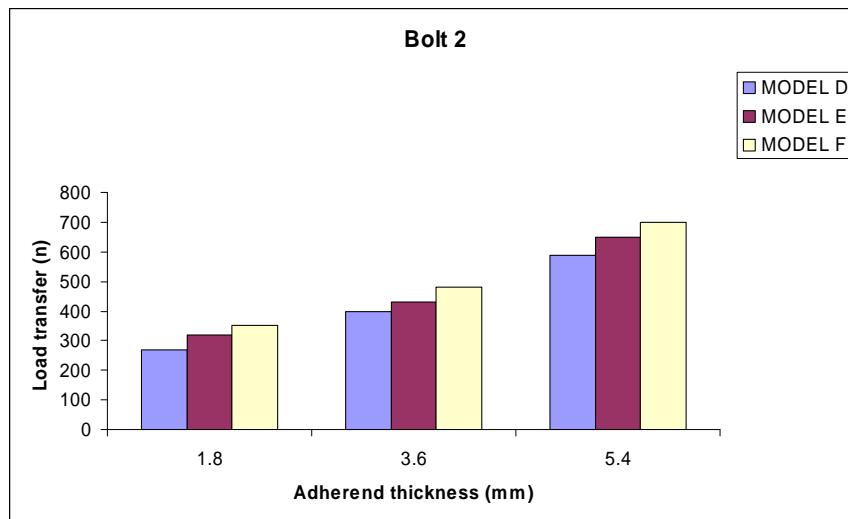


Figure 4.28 Load transfer by bolt 2 for different Adherend thicknesses

The load transfer by Bolt 1 increases by 48% when the Adherend thickness is increased from 1.8mm to 3.6mm as shown in the Figure 4.27. The difference in load transfer by bolt is 54% when the Adherend thickness of 5.4mm is used.

The load transfer by bolt 2 also increases with the increase of the Adherend thickness as shown in the Figure 4.28. There is an increase of 43% when the Adherend thickness is increased from 1.8mm to 3.6 mm and the increase is 47% for the Adherend thickness of 5.4mm.

As observed in the graphs, it can be concluded that the adherend thickness is directly proportional to the load transfer.

4.5 Influence of Bolt Diameter

To study the bolt diameter effect on transfer of load by bolt, the hole diameters were modified as mentioned below in the FEM when the analysis was performed.

Bolt diameters of 6mm, 7mm and 8mm were being used to study the effect of the bolt diameter.

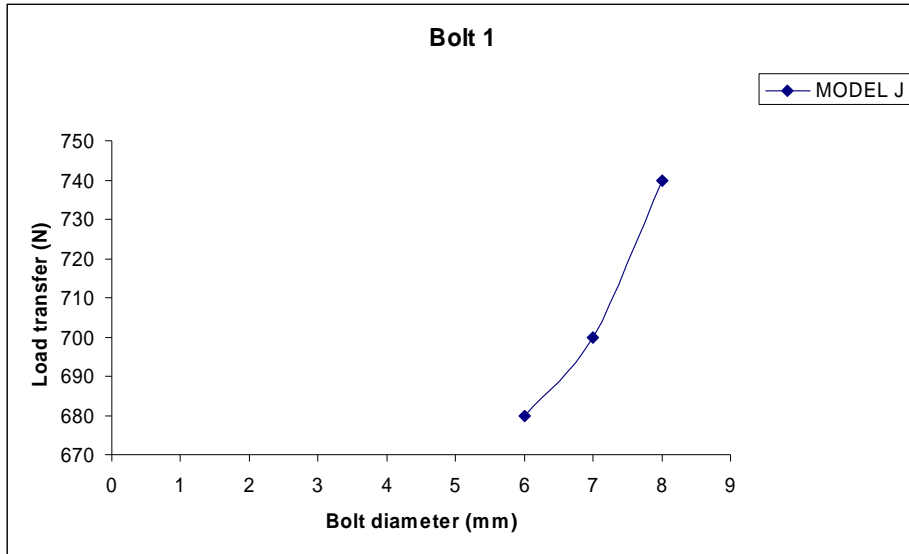


Figure 4.29 Load transfer by bolt 1 for MODEL J

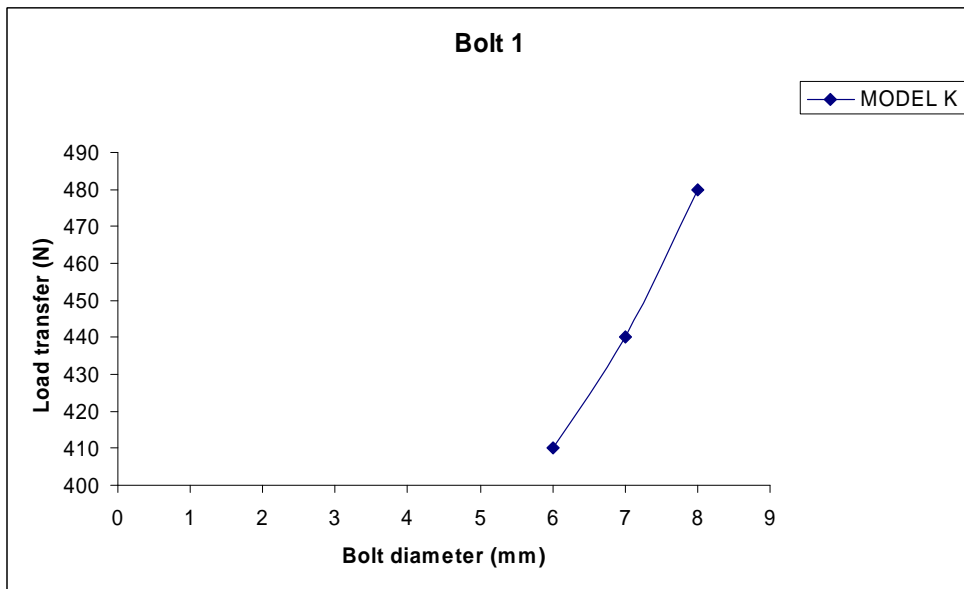


Figure 4.30 Load transfer by bolt 1 for MODEL K

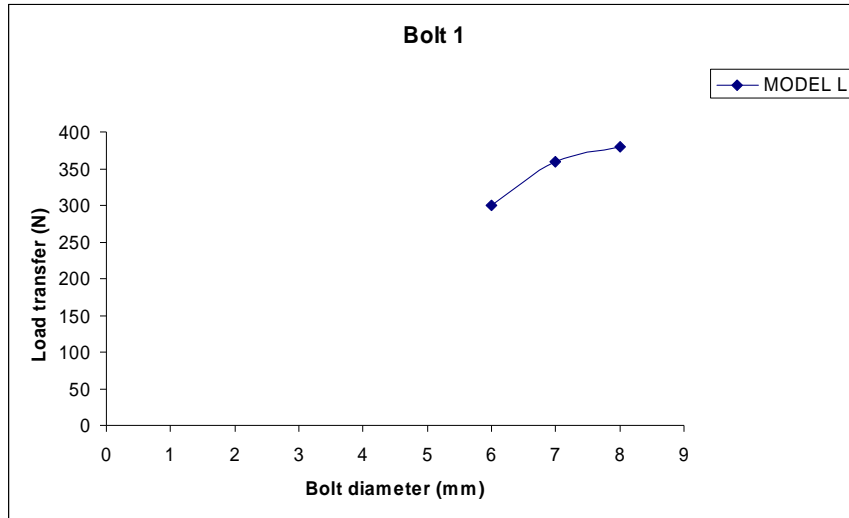


Figure 4.31 Load transfer by bolt 1 for MODEL L

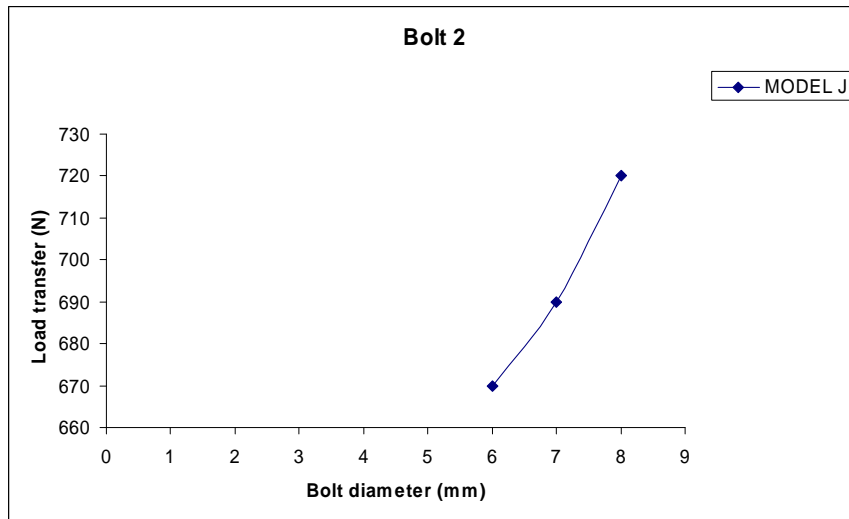


Figure 4.32 Load transfer by bolt2 for MODEL J

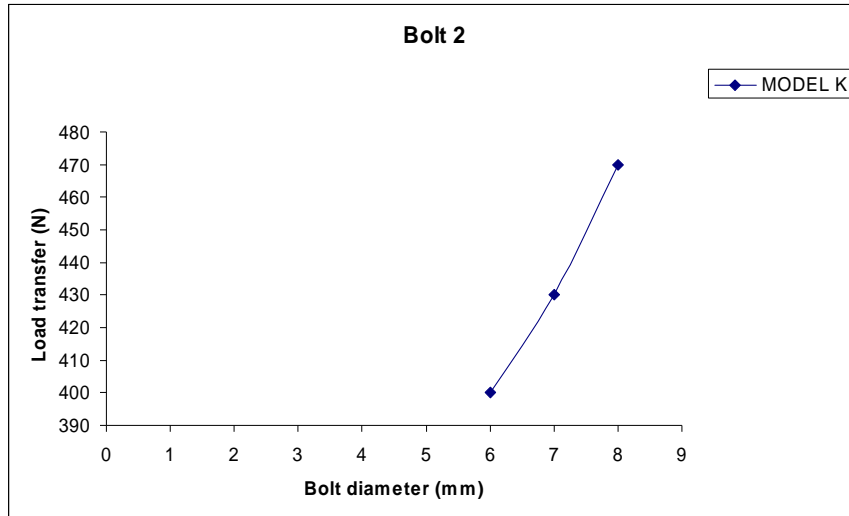


Figure 4.33 Load transfer by bolt 2 for MODEL K

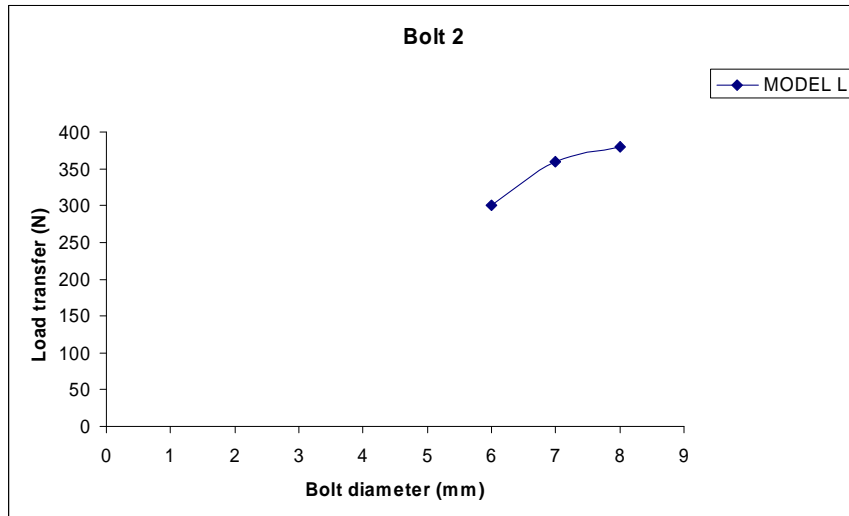


Figure 4.34 Load transfer by bolt 2 for MODEL L

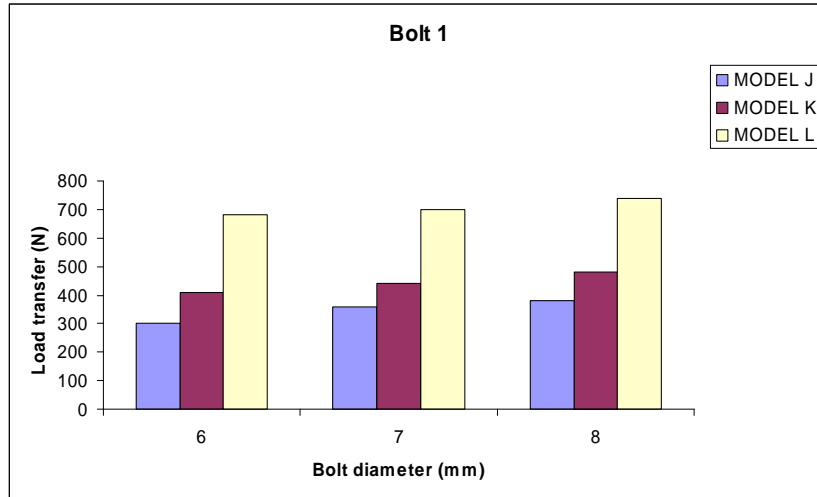


Figure 4.35 Load transfer by bolt 1 for different Bolt diameters.

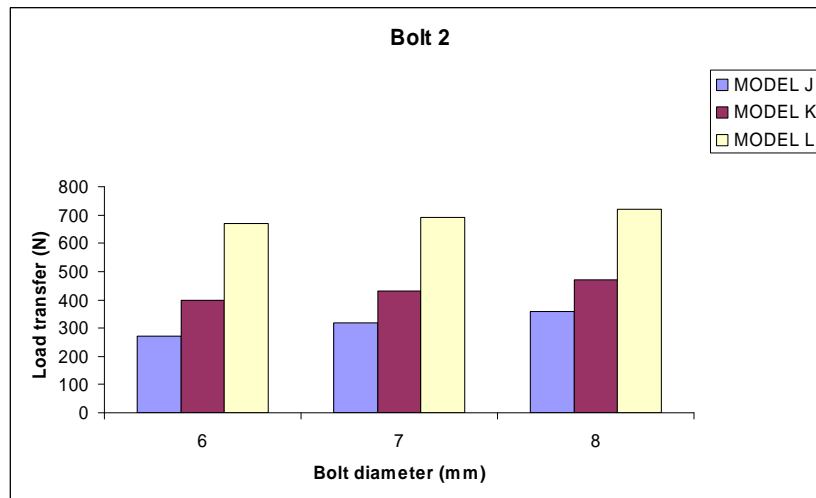


Figure 4.36 Load transfer by bolt 2 for different Bolt diameters

Increase in bolt diameter (Bolt 1) from 6mm to 7mm shows an increment of 24% in the load transfer which is shown in Figure 4.35. The difference in load transfer by bolt is 13% when the bolt diameter of 8mm is used.

The load transfer by bolt 2 also increases with the increase of the bolt diameter as shown in the Figure 4.36. Bolt 2 shows a 22% increment in load transfer when its diameter changed from 6mm to 7mm and an increment to 11% for 8mm diameter.

It can be observed from the plots that there is increase in bolt diameter values along X direction there is change of load transfer values by bolt on the Y axis as seen in the Figures 4.35 and 4.36.

4.6 Influence of Overlap length

By changing the overlap length, its effect on the load transfer by the bolt is determined. Three overlap lengths 40mm, 50mm and 60mm are used to determine the effect on the load transfer.

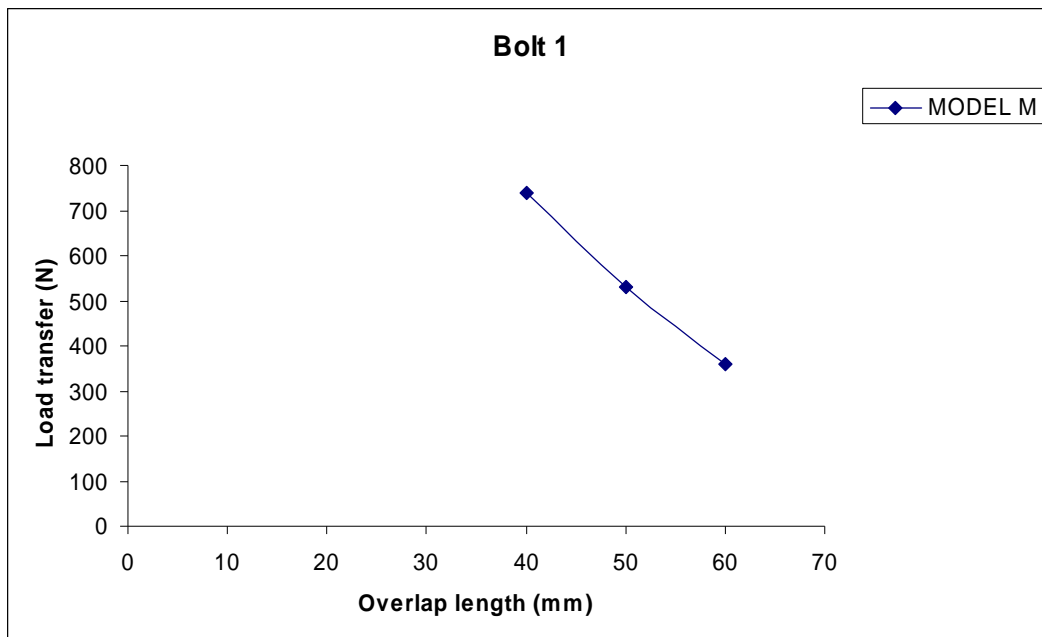


Figure 4.37 Load transfer by bolt 1 for MODEL M

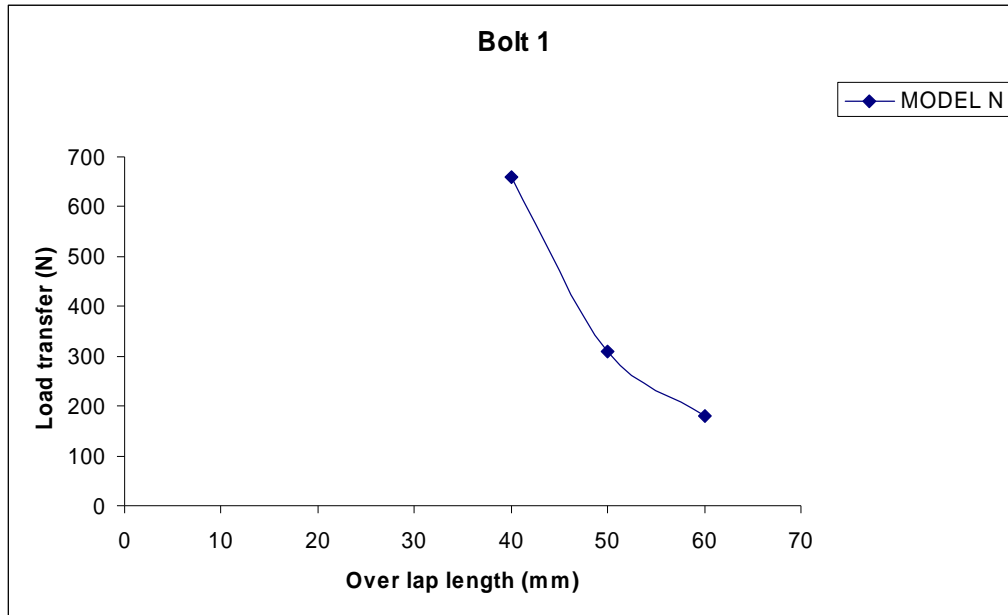


Figure 4.38 Load transfer by bolt 1 for MODEL N

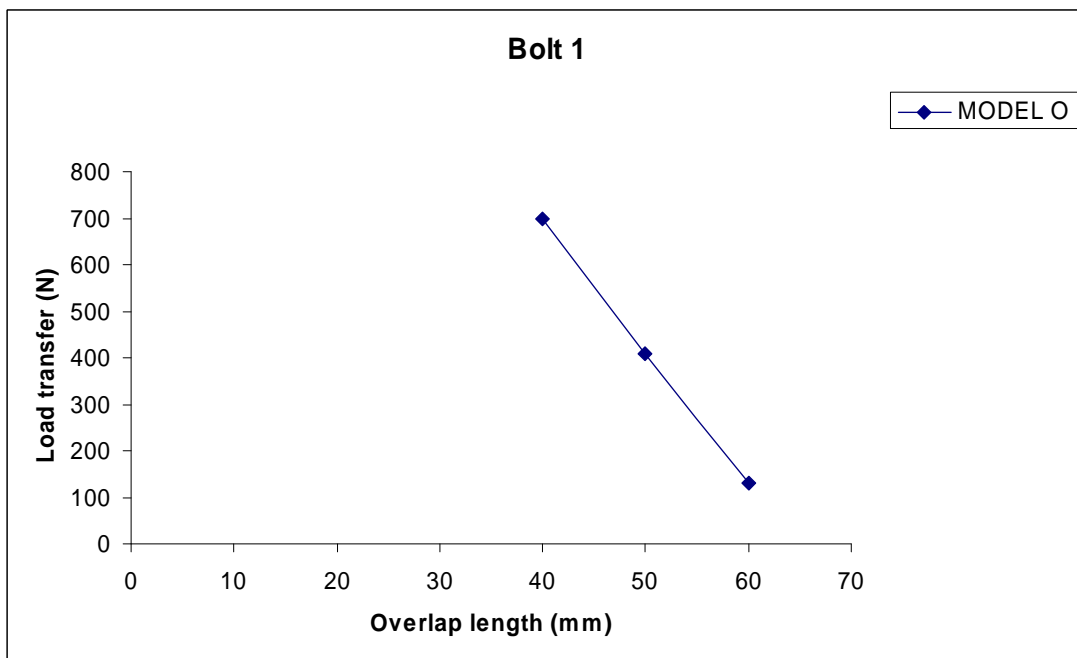


Figure 4.39 Load transfer by bolt 1 for MODEL O

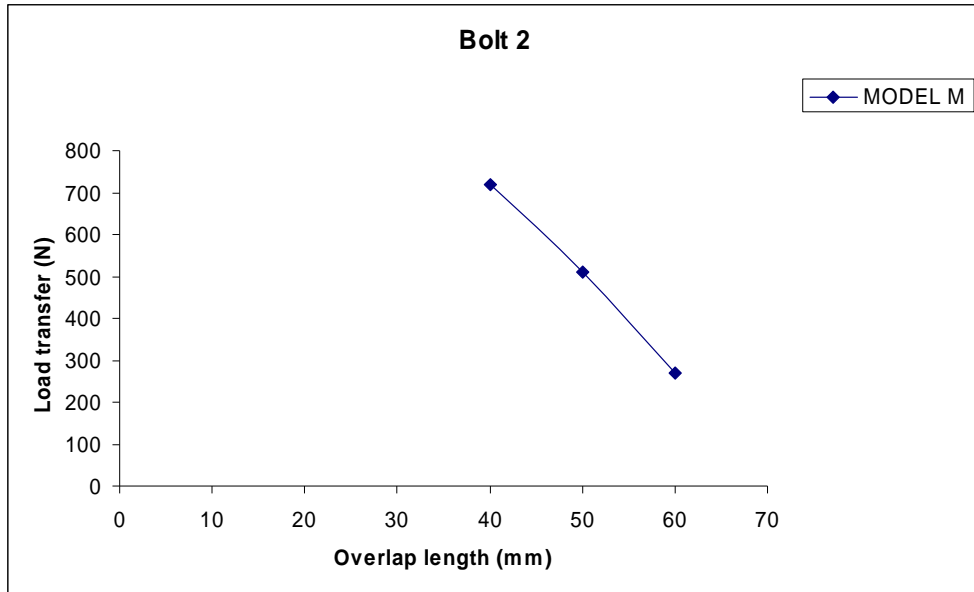


Figure 4.40 Load transfer by bolt 2 for MODEL M

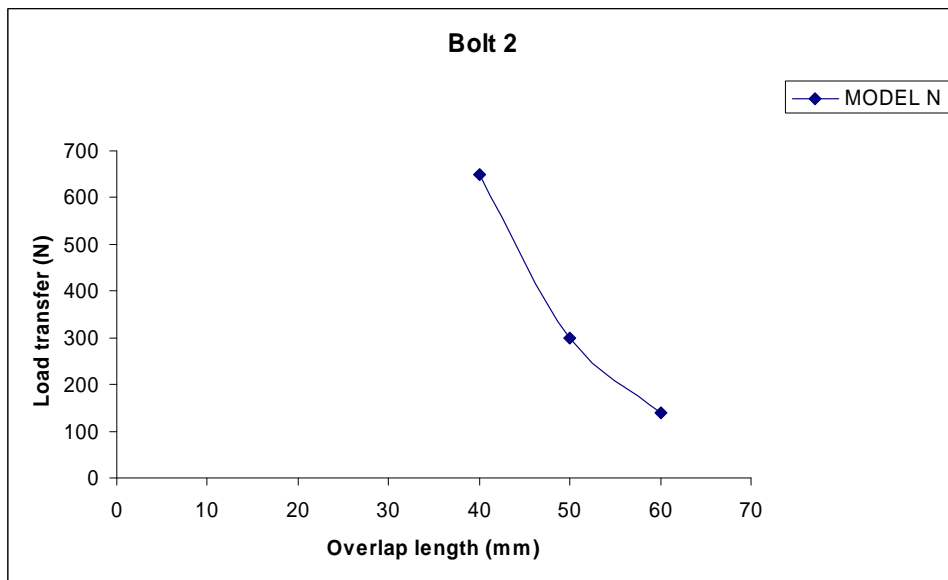


Figure 4.41 Load transfer by bolt 2 for MODEL N

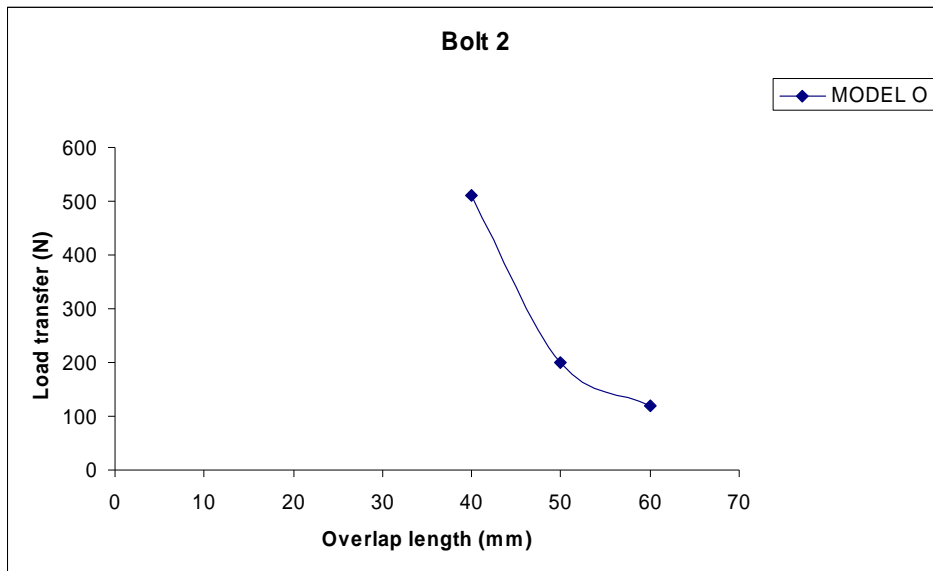


Figure 4.42 Load transfer by bolt 2 for MODEL O

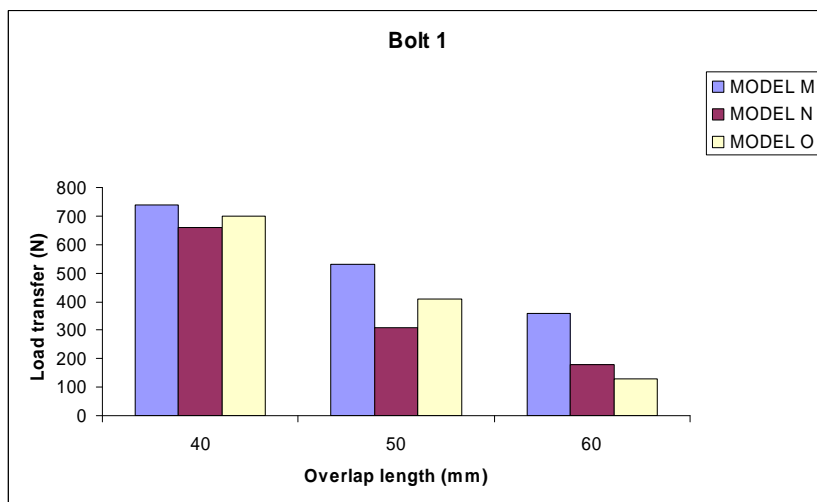


Figure 4.43 Load transfer by bolt 1 for different Overlap lengths.

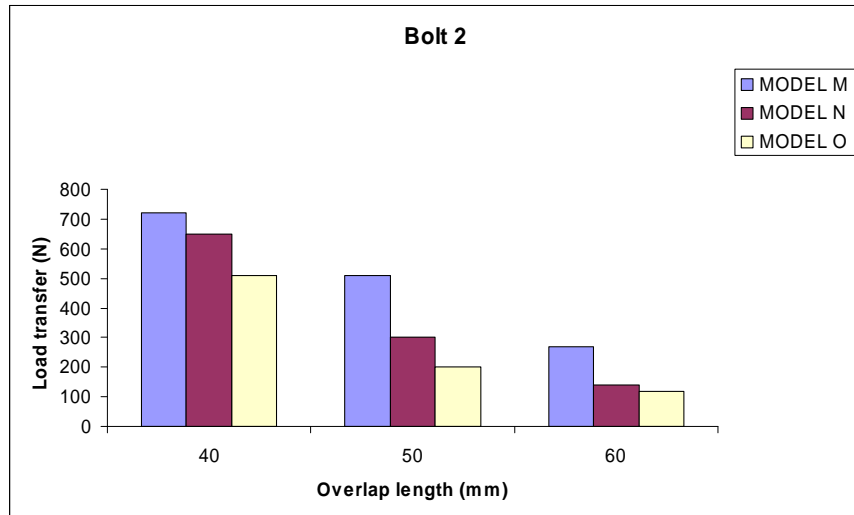


Figure 4.44 Load transfer by bolt 2 for different Overlap lengths.

The load transfer by Bolt 1 decreases by 29% when the Overlap length is increased from 40mm to 50mm as shown in the Figure 4.43. The difference in load transfer by bolt is 34% when the Overlap length of 60mm is used.

The load transfer by Bolt 2 also decreases with the increase of the Overlap length as shown in the Figure 4.44. There is a decrease of 27% when the Overlap length is increased from 40mm to 50mm and the decreases is 36% for the Overlap length of 60mm.

This phenomenon is attributed to the fact that with the increase in the over lap length there is a decrease in the load transfer by bolt.

4.7 Results and Discussions

A difference of 7% load transfer is shown by Bolt 1 when carbon/fiber epoxy is used over HTA/6376 and 16% difference when Laminate (Hexcel composites) is used as shown in the Figure 4.11.

A difference of 6% load transfer is shown by Bolt 2 when carbon/fiber epoxy is used over HTA/6376 and the difference is 12% when Laminate is used as shown in the Figure 4.12.

Observation from plots in Figures 4.11 and 4.12 shows a significant change in load transfer by the bolt along Y-axis with the change of elastic properties of the plates on the X-axis.

Bolt 1 show increase of 48% in load transfer when the Adherend thickness changed from 1.8mm to 3.6mm as shown in the Figure 4.27. The difference in load transfer by bolt is 54% when the Adherend thickness of 5.4mm is used.

The load transfer by bolt 2 also showed increases with the increase of the Adherend thickness as shown in the Figure 4.28. 43% increase in load transfer when the Adherend thickness varied from 1.8mm to 3.6 mm and 47% increase for the Adherend thickness of 5.4mm.

Observed made from the plot that Adherend thickness is directly proportional to the load transfer.

Increase in tensile load from 1000N to 3000N in Bolt 1, load transfer increased by 65% as shown in the Figure 4.19. The difference in load transfer by bolt is 25% when the tensile load of 4000N is used.

Load transfer by bolt 2 also increases with the increase of the tensile load as shown in the Figure 4.20. There is a 60% increase as the tensile load is increased from 1000N to 3000N and 20% increase for tensile load of 4000N.

It can be observed from the plots that as tensile load values along X direction increases load transfer values changes by bolt on the Y axis as seen in the Figures 4.19 and 4.20.

As the bolt diameter increases from 6mm to 7mm, the load transfer by Bolt 1 increases by 24% as shown in the Figure 4.35. The difference in load transfer by bolt is 13% when the bolt diameter of 8mm is used.

Load transfer by bolt 2 also shows that load transfer is directly proportional to bolt diameter as shown in the Figure 4.36. Increase of 22% was observed when the bolt diameter is changed from 6mm to 7mm and an 11% increase for the 8mm bolt diameter.

It can be observed from the plots that there is increase in bolt diameter values along X direction there is change of load transfer values by bolt on the Y axis as seen in the Figures 4.35 and 4.36.

Load transfer decreased by 29% of Bolt 1, when the Overlap length is changed from 40mm to 50mm as shown in the Figure 4.43. The difference in load transfer by bolt is 34% when the Overlap length of 60mm is used.

The load transfer by bolt 2 also decreases with the increase of the Overlap length as shown in the Figure 4.44. There is a decrease of 27% when the Overlap length is increased from 40mm to 50mm and the decreases is 36% for the Overlap length of 60mm.

This phenomenon is attributed to the fact that with the increase in the overlap length there is a decrease in the load transfer by bolt.

CHAPTER FIVE

CONCLUSIONS AND FUTURE WORK

5.1 Conclusions

The main aim of this thesis is to predict the load transfer in the hybrid single lap joint. A 3D finite element model was developed to investigate effects of different parameters such as material properties, tensile load, adherend thickness, bolt diameter and overlap length on the load transfer by bolt. The bolt load results obtained from the finite element analysis for single bolted single lap hybrid (bonded/bolted) joint have been validated by using an experimental solution for single bolted single lap hybrid (bonded/bolted) joint. Load transfer values predicted by the experimental models and the one with finite element method were compared and they are observed to have a good agreement.

The conclusions of the investigation in this thesis are

- (a) The elastic properties of the plate materials have significant effect on the load distribution by the bolt.
- (b) With the increase of the applied tensile load, increase of load transfer by bolt has been observed.
- (c) Increase in the Adherend thickness increases the load transfer by bolt.
- (d) Bolt diameter seems to have an impact on the load transfer by bolt, as diameter increases, transfer of load by bolt increase.
- (e) The load transfer developed is affected by the overlap length, as the overlap length increases there is a decrease in the load transfer values.

5.2 Future Work

A parametric study is done to investigate the effects of various parameters such as material properties, tensile load, adherend thickness, bolt diameter and overlap length on load transfer by bolt in a single lap hybrid joint by using ABAQUS 6.4 version. In addition to this there is a need to study of;

- (a) Load transfer in multi fastened single and double lap hybrid (bonded/bolted) shear and tensile joints.
- (b) Stress distribution around the hole in multi fastened single and double lap hybrid (bonded/bolted) shear and tensile joints.

REFERENCES

LIST OF REFERENCES

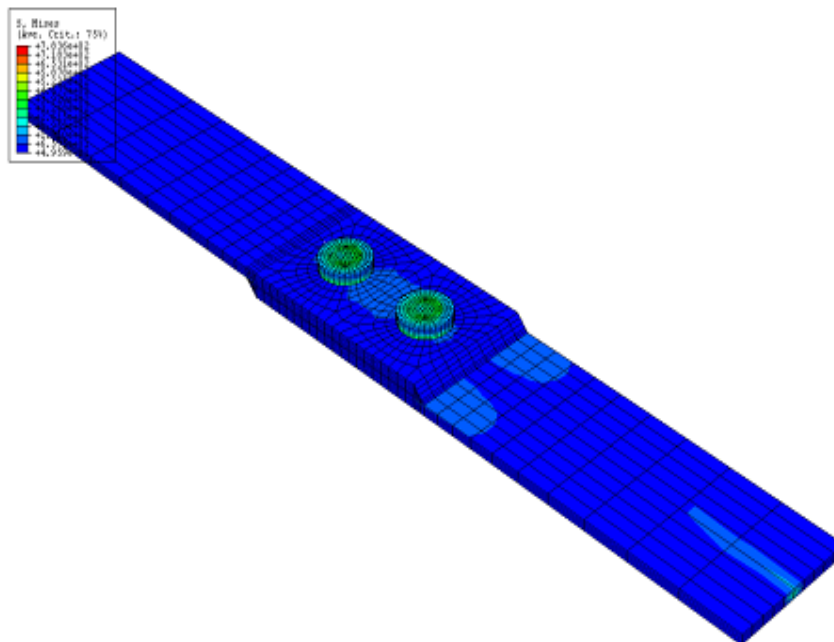
- [1] ABAQUS/Standard Users Manual, Version 6.4, 2006.
- [2] Cope, D.A., and Lacy, T.E., “Stress Intensity Determination in Lap Joints with Mechanical Fasteners,” 41st AIAA/ASME/ASCEIAHS/ASC Structures, Structural Dynamics, and Material conference and Exhibit, pp. 1-10, 2000.
- [3] Drabek, T., and Bohm, H.J., “Micromechanical Finite Element Analysis of Metal Matrix Composites using Nonlocal Ductile Failure Models,” *Computational Materials Science*, Vol. 37, pp. 29-36, 2006.
- [4] Fukuoka, T., and Takaki, T., “Mechanical Behavior of Bolted Joint in Various clamping Configurations,” *Journal of Pressure Vessel Technology*, Vol. 120, 1998, pp226-231.
- [5] Katepalli, N.B., “Parametric study of Stress Concentration in Bolted lap joints between Particulate metal matrix Composite materials”. Masters Thesis, Wichita State University, 2006.
- [6] Lehnhoff, T.F., and Wistehuff, W.E., “Nonlinear Effects on the Stresses and Deformations of Bolted Joints,” *Journal of Pressure Vessel Technology*, Vol. 118, pp. 54-58, 1996.
- [7] Menzemer, C.C., Fei, L., and Srivatsan, T.S., “Design Criteria for Bolted Connection Elements in Aluminum Alloy 6601,” *Journal of Mechanical Design*, Vol. 121, pp. 348-358, 1999.
- [8] Riccio, A., and Marciano, L., “Effects of Geometrical and Material Features on Damage Onset and Propagation in Single-lap Bolted Composite Joint sunder Tensile Load: Part I– Experimental Studies,” *Journal of Composite Materials*, Vol. 39, PP 2071, 2005.
- [9] Kelly, G., Load transfer in hybrid (bonded/bolted) composite single-lap joints. *Composite Structures*, Volume 69, Issue 1, Pages 35-43, available online 2 June 2004.
- [10] Ananthram K.S., “Finite element and Analytical Models for Load transfer calculations in Mechanically Fastened Aluminum/Composite Hybrid joints” Masters Thesis, Wichita State University, 2005.
- [11] Lehnhoff, T.F., and Bunyard, B.A., “Effect of bolt threads on the Stiffness of Bolted Joints,” *Journal of Pressure Vessel Technology*, Vol. 381, pp. 141-146, 1998.
- [12] Eric, P., Marc, S., Jacques, H., Frédéric, L., “Analytical two-dimensional model of a hybrid (bolted/bonded) single-lap joint,” *Journal of Aircraft*, v 44, n 2, p 573-582, March/April 2007.

- [13] Joint Design, www.ellsworth.com, cited 2006.
- [14] Rodriguez, D., Carlin, J., and Rey, R., “Stress Concentration Study in Bolted joints by Finite Element Modeling: Experimental and Analytical Approach,” *European Conference of Spacecraft Structures, Materials and Mechanical Testing*, pp. 2-6, 2005.
- [15] Meka, U.S., “Finite Element and Analytical Models for Load transfer Calculations in Structures utilizing Metal and Composites with Large CTE differences” Master’s Thesis, Wichita State University, 2007.
- [16] Weeton, J.W., Peters, D.M., and Thomas, K.L., “Engineers *Guide To Composite Materials*,” American Society for Metals, 1987.
- [17] Hibbitt, H.B., Nagtegaal, J.C., “Computer Process for Prescribing an Assembly Load to Provide Pre-tensioning Simulation in the Design Analysis of Load Bearing Structures”. January 1997.
- [18] Snyder, B.D., Burns, J.G., and Venkayya, V.B., “Composite Bolted Joints Analysis Programs,” Proceedings of the AIAA/ASME/ ASCE/AHS/ASC 29th Structures, *Structural Dynamics and Materials Conference*, AIAA, Washington, D. C., April 2005.
- [19] Technical Information, Bolted joints, handbook, 2000.
- [20] Gerbert, G., and Bastedt, H., “Centrically Loaded Bolted Joints” *Journal of Mechanical Design*, Vol. 115, pp 701-705, 1993.
- [21] Bickford, J.H., “An Introduction to the Design and Behavior of Bolted Joints”, Third Edition, Revised and Expanded, 2003.

APPENDIX A

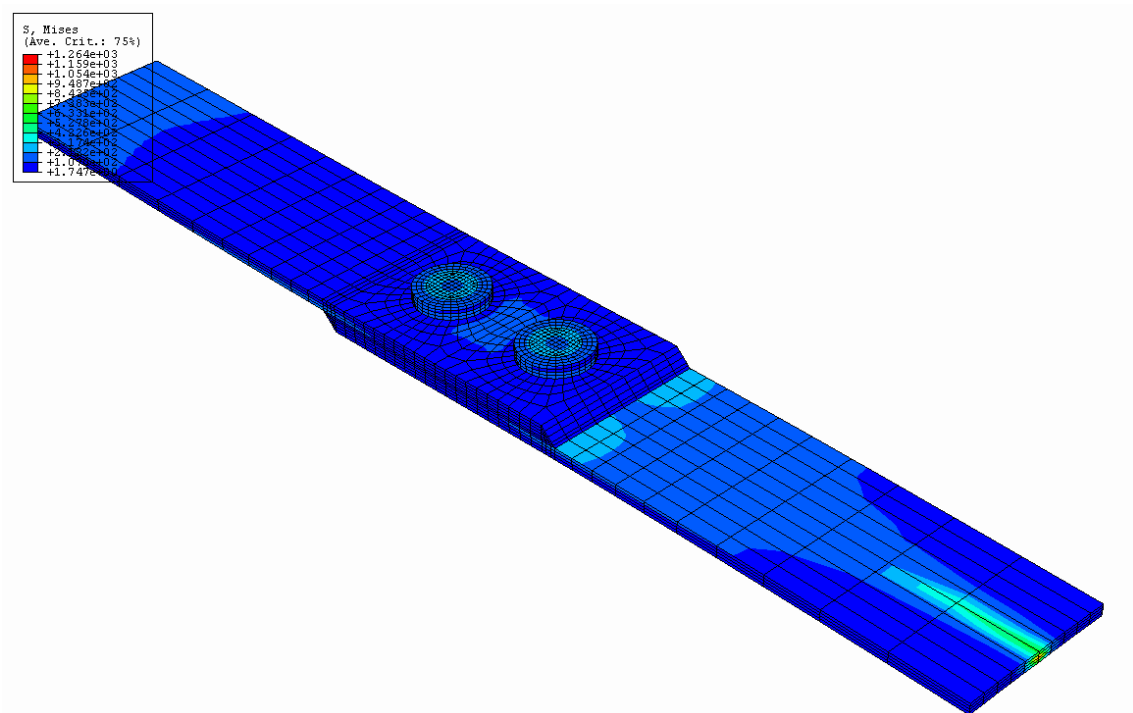
MODEL A Description and Results

Model	Model A
Adherend Thickness	1.8 mm
Bolt Diameter	6mm
Tensile Load	1000 N
Overlap Length	40 mm
Material	Carbon/fiber epoxy
Load transfer by bolt1	164 N
Load transfer by bolt2	160 N



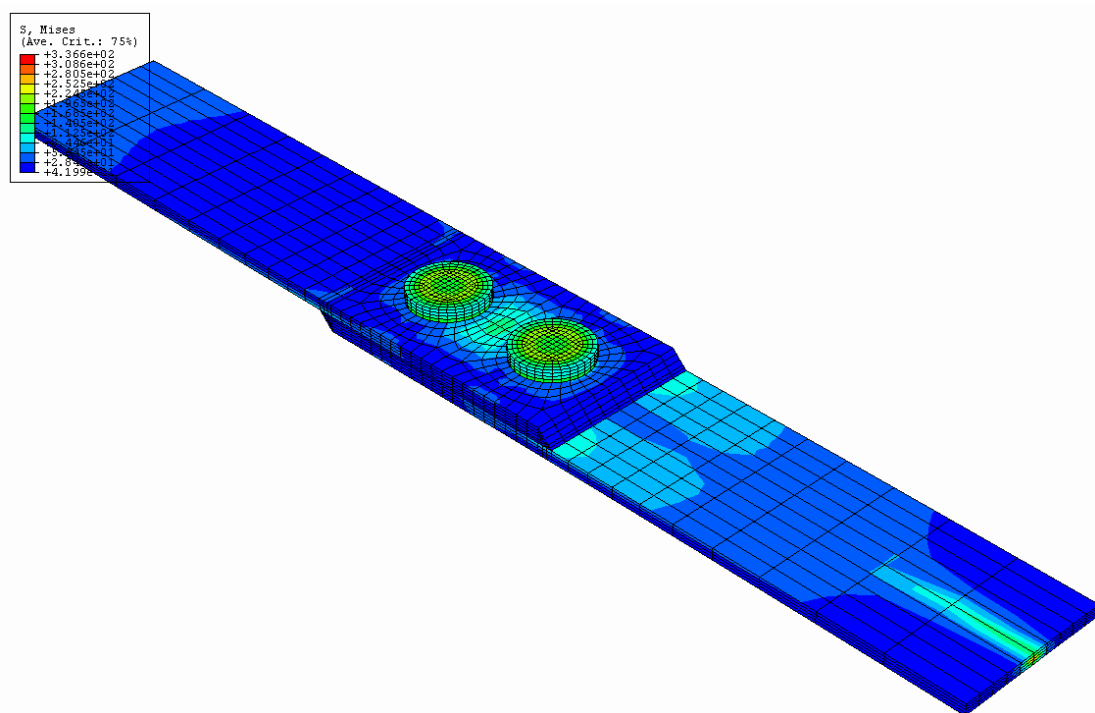
MODEL B Description and Results

Model	Model B
Adherend Thickness	1.8 mm
Bolt Diameter	7mm
Tensile Load	1000 N
Overlap Length	40 mm
Material	HTA/6376
Load transfer by bolt1	180 N
Load transfer by bolt2	160 N



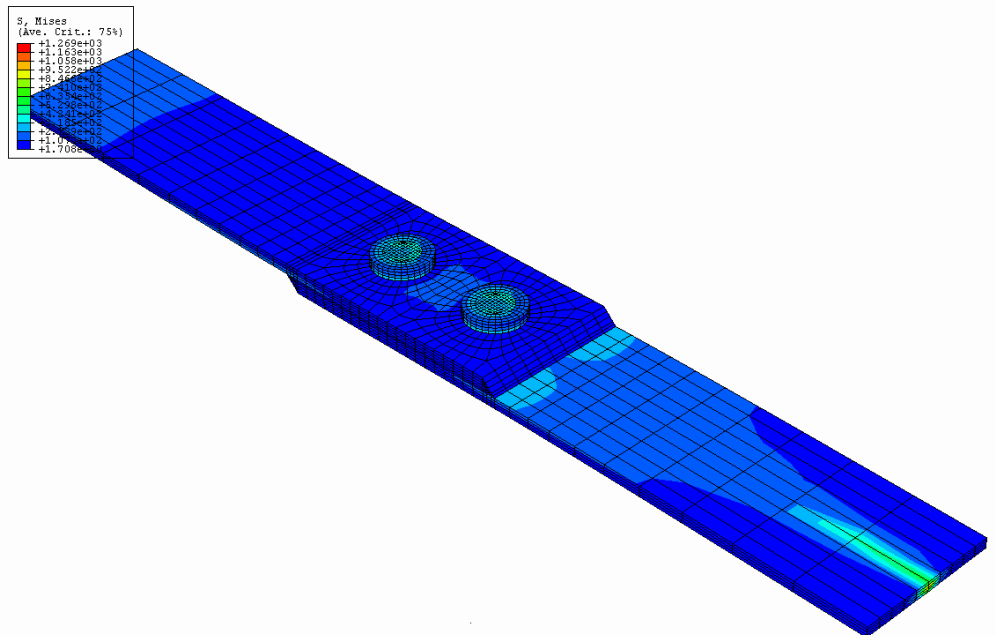
MODEL C Description and Results

Model	Model C
Adherend Thickness	1.8 mm
Bolt Diameter	8mm
Tensile Load	1000 N
Overlap Length	40 mm
Material	Laminate (Hexcel composites)
Load transfer by bolt1	190 N
Load transfer by bolt2	180 N



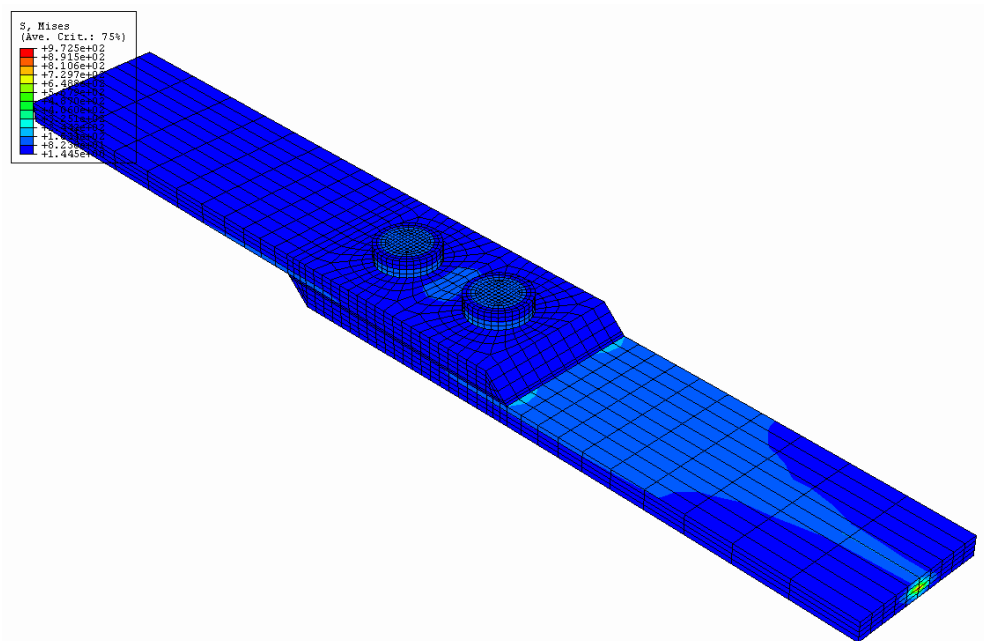
MODEL D Description and Results

Model	Model D
Adherend Thickness	1.8 mm
Bolt Diameter	6mm
Tensile Load	1000 N
Overlap Length	40 mm
Material	Carbon/fiber epoxy
Load transfer by bolt1	164 N
Load transfer by bolt2	160 N



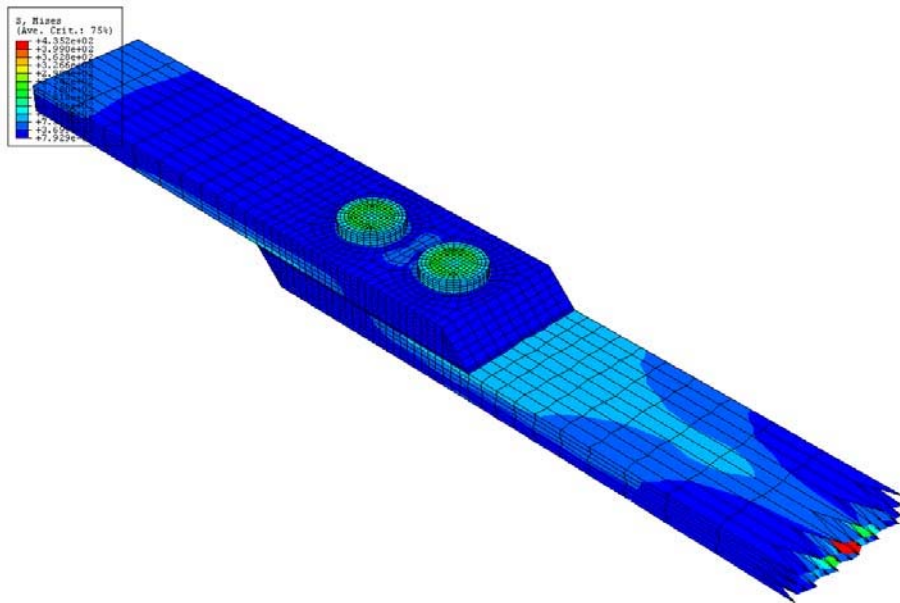
MODEL E Description and Results

Model	Model E
Adherend Thickness	3.6 mm
Bolt Diameter	7mm
Tensile Load	1000 N
Overlap Length	40 mm
Material	Carbon/fiber epoxy
Load transfer by bolt1	270 N
Load transfer by bolt2	250 N



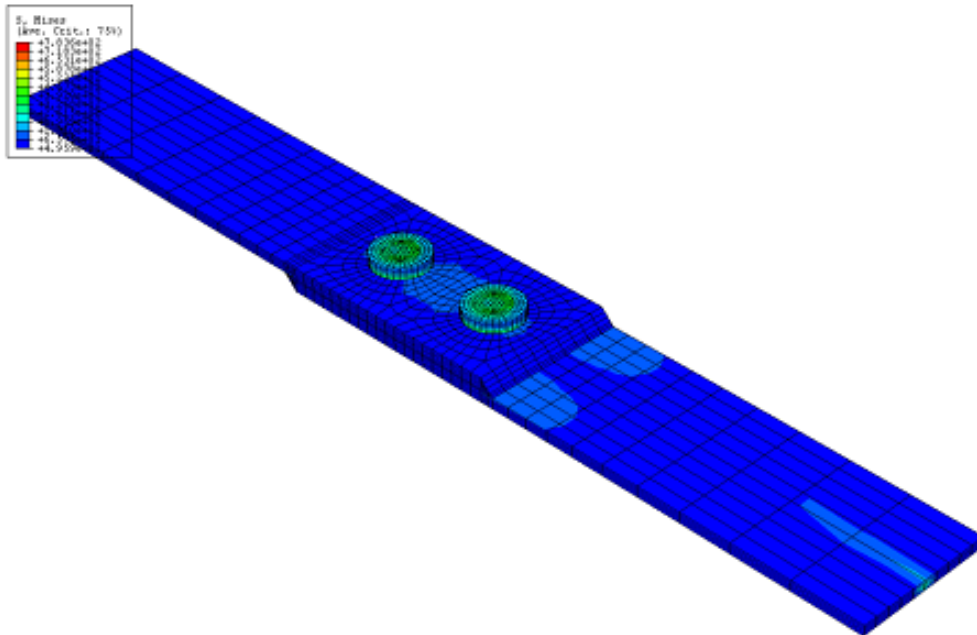
MODEL F Description and Results

Model	Model F
Adherend Thickness	5.4 mm
Bolt Diameter	8mm
Tensile Load	1000 N
Overlap Length	40 mm
Material	Carbon/fiber epoxy
Load transfer by bolt1	320 N
Load transfer by bolt2	310 N



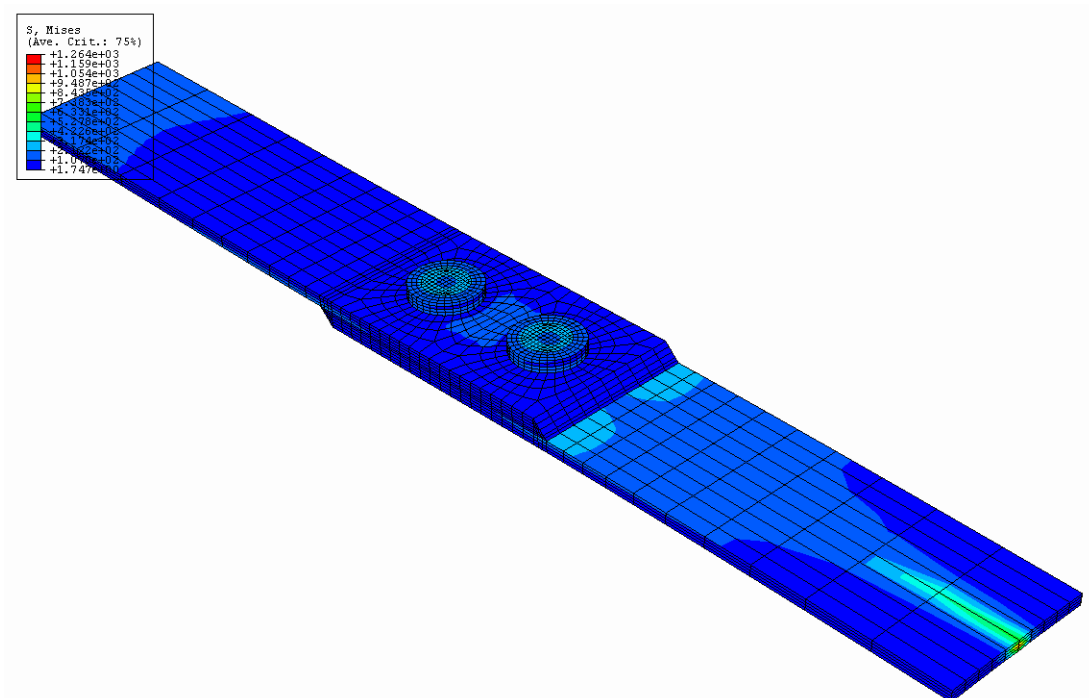
MODEL G Description and Results

Model	Model G
Adherend Thickness	1.8 mm
Bolt Diameter	6mm
Tensile Load	1000 N
Overlap Length	40 mm
Material	Carbon/fiber epoxy
Load transfer by bolt1	164 N
Load transfer by bolt2	160 N



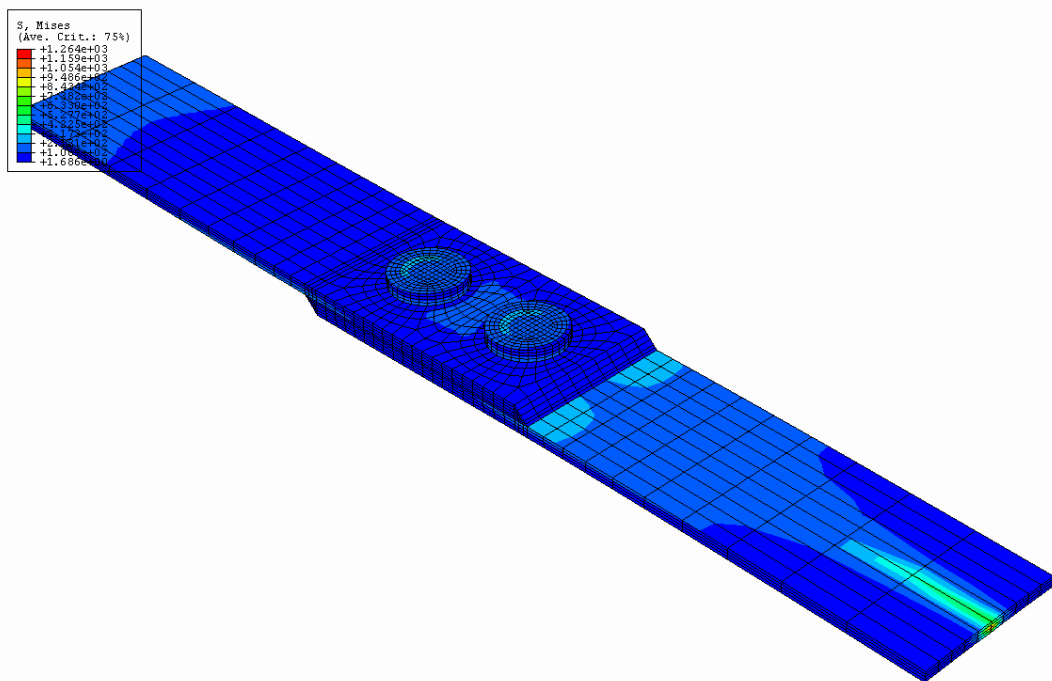
MODEL H Description and Results

Model	Model H
Adherend Thickness	1.8 mm
Bolt Diameter	7mm
Tensile Load	3000 N
Overlap Length	40 mm
Material	Carbon/fiber epoxy
Load transfer by bolt1	500 N
Load transfer by bolt2	480 N



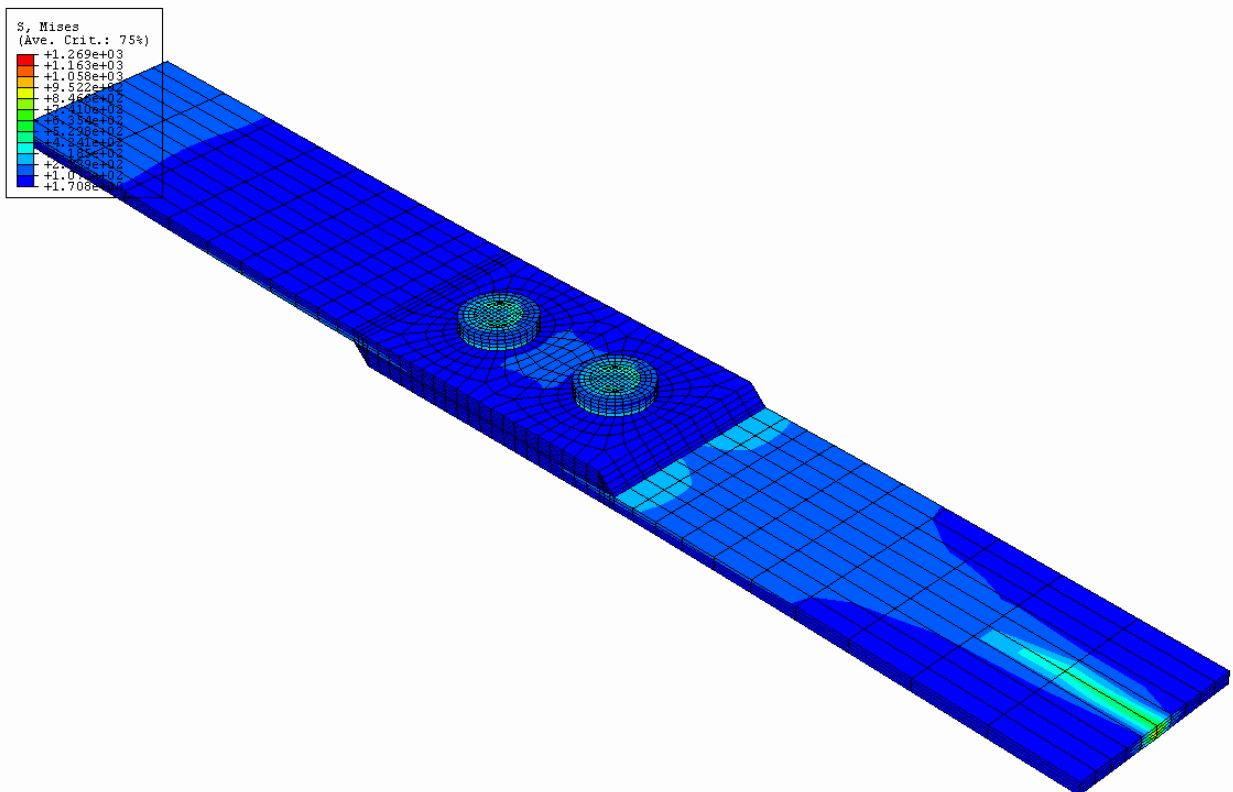
MODEL I Description and Results

Model	Model I
Adherend Thickness	1.8 mm
Bolt Diameter	8mm
Tensile Load	4000 N
Overlap Length	40 mm
Material	Carbon/fiber epoxy
Load transfer by bolt1	700 N
Load transfer by bolt2	680 N



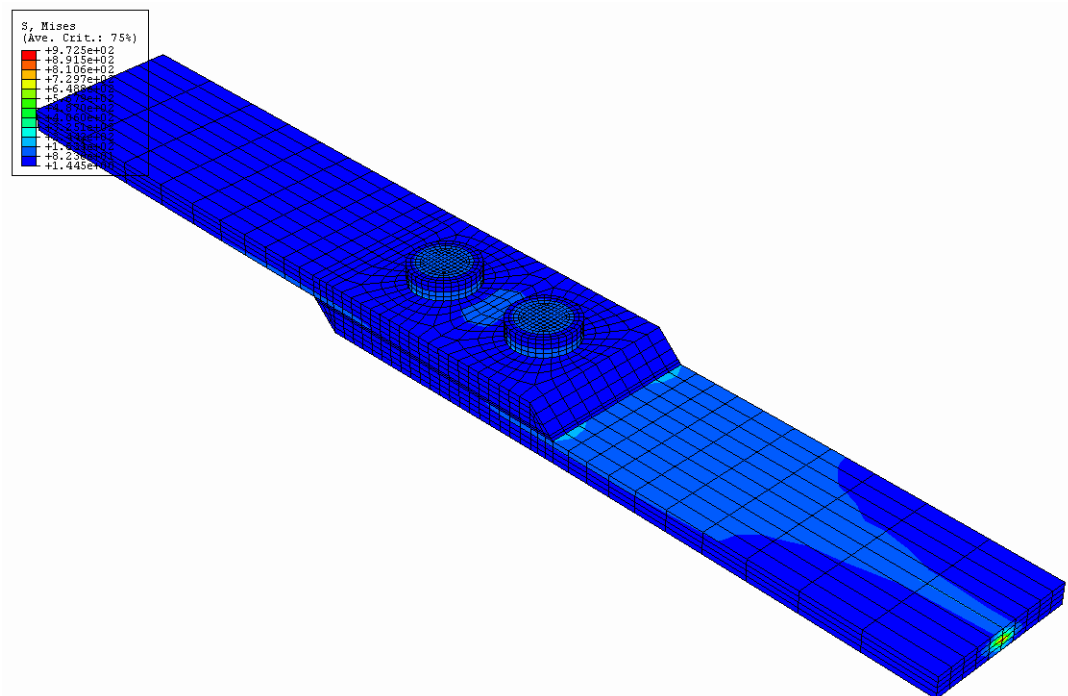
MODEL J Description and Results

Model	Model J
Adherend Thickness	1.8 mm
Bolt Diameter	6mm
Tensile Load	1000 N
Overlap Length	40 mm
Material	Carbon/fiber epoxy
Load transfer by bolt1	164 N
Load transfer by bolt2	160 N



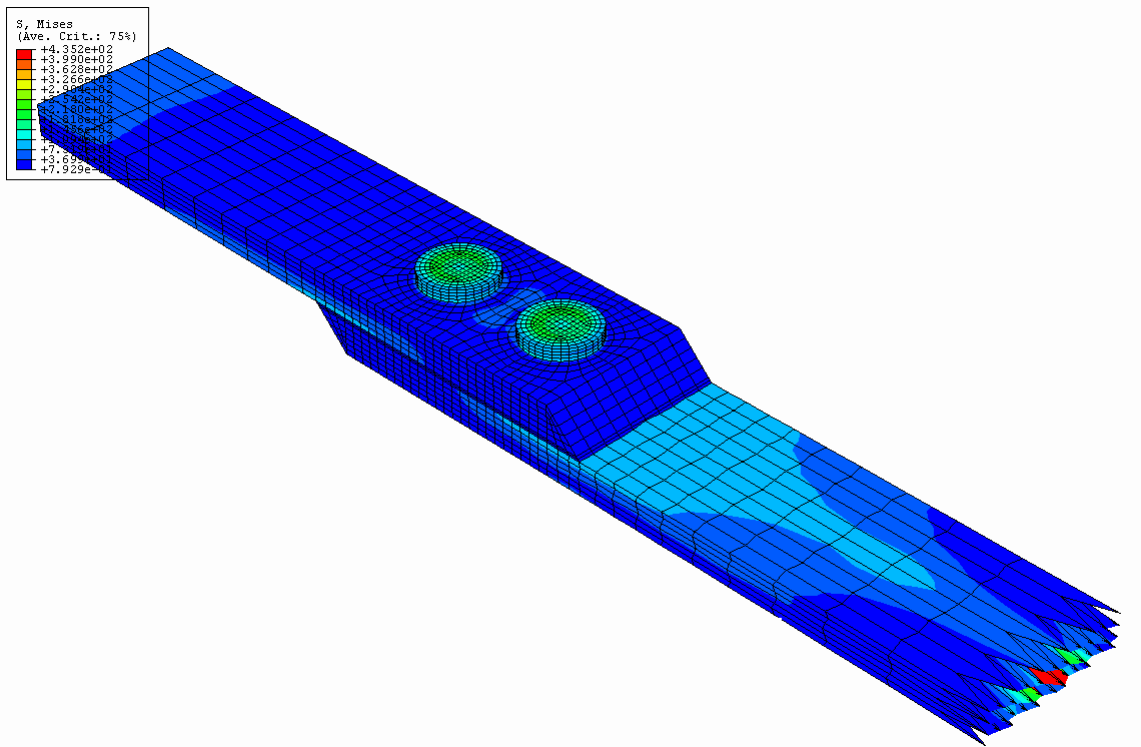
MODEL K Description and Results

Model	Model K
Adherend Thickness	3.6 mm
Bolt Diameter	7mm
Tensile Load	1000 N
Overlap Length	40 mm
Material	Carbon/fiber epoxy
Load transfer by bolt1	270 N
Load transfer by bolt2	250 N



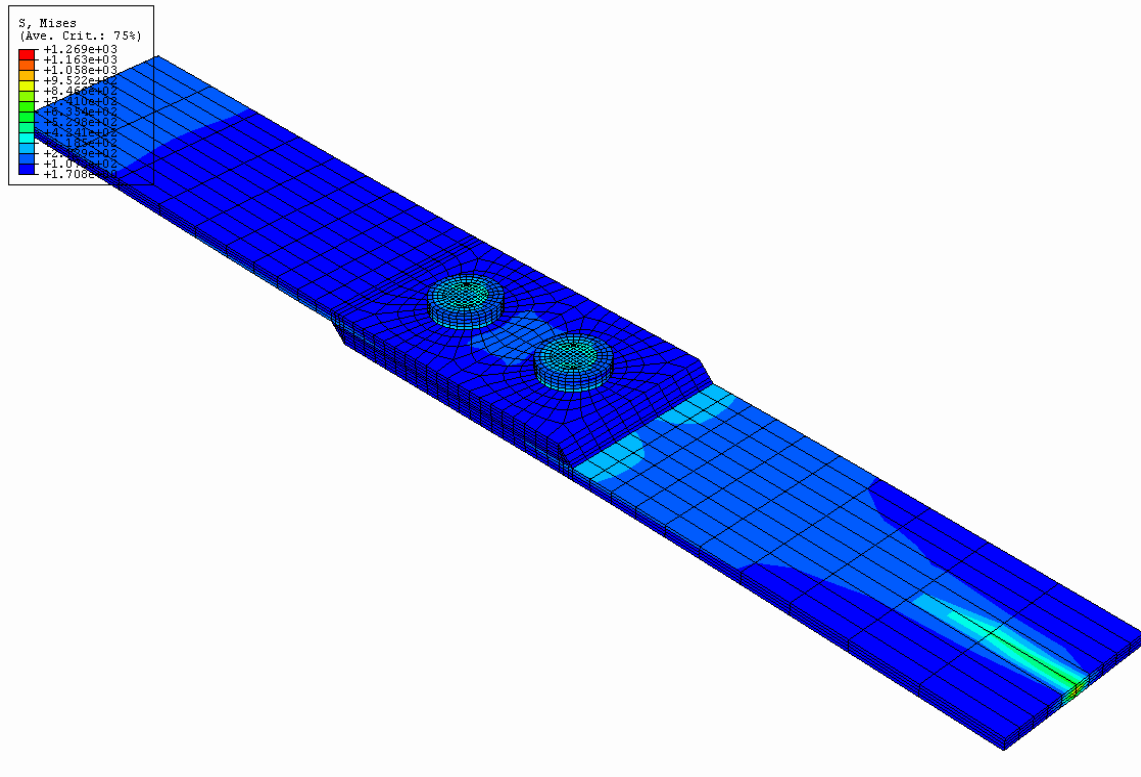
MODEL L Description and Results

Model	Model L
Adherend Thickness	5.4 mm
Bolt Diameter	8mm
Tensile Load	1000 N
Overlap Length	40 mm
Material	Carbon/fiber epoxy
Load transfer by bolt1	720 N
Load transfer by bolt2	700 N



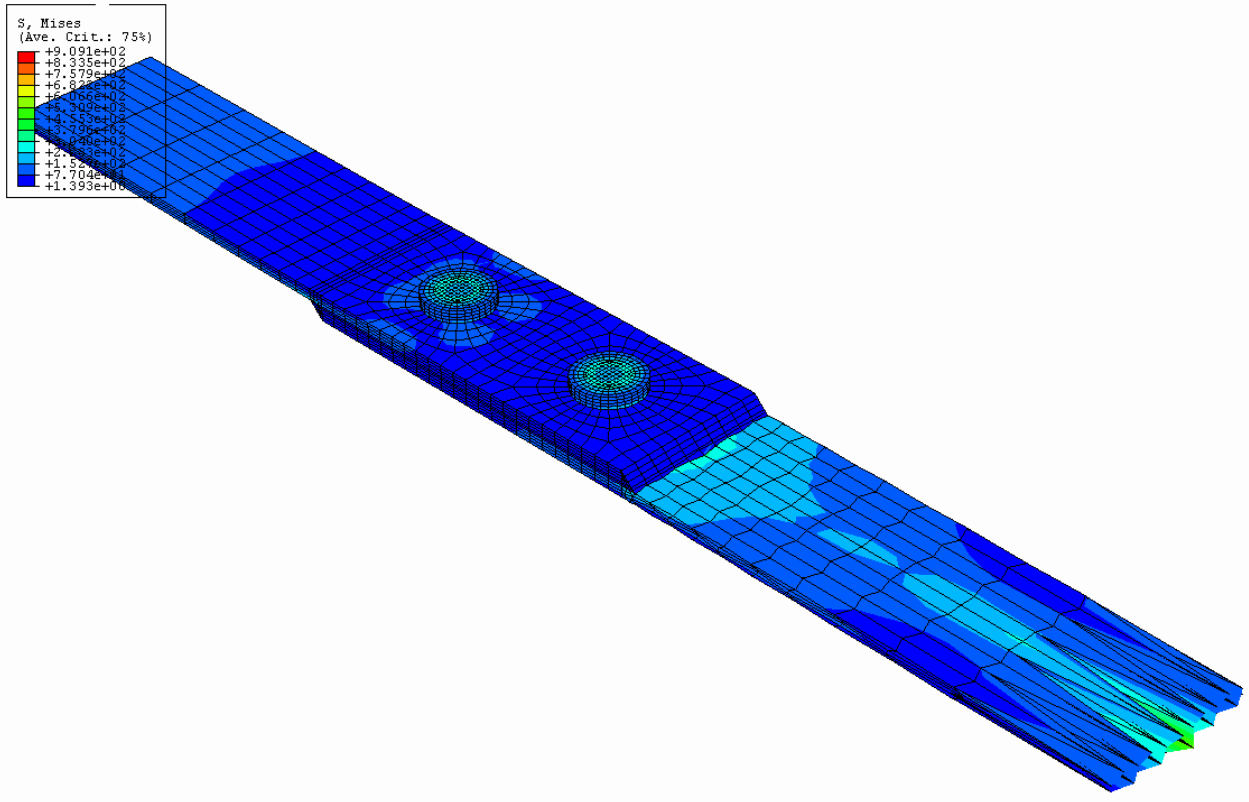
MODEL M Description and Results

Model	Model M
Adherend Thickness	1.8 mm
Bolt Diameter	6mm
Tensile Load	4000 N
Overlap Length	40 mm
Material	Carbon/fiber epoxy
Load transfer by bolt1	320 N
Load transfer by bolt2	310 N



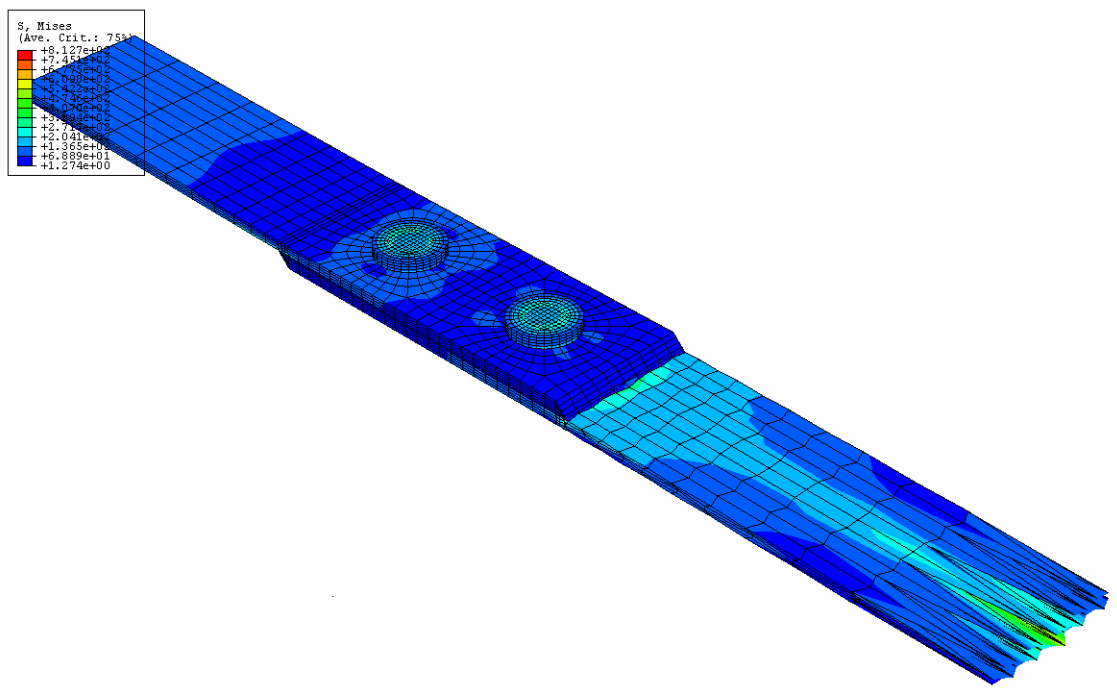
MODEL N Description and Results

Model	Model N
Adherend Thickness	1.8 mm
Bolt Diameter	7mm
Tensile Load	4000 N
Overlap Length	50 mm
Material	Carbon/fiber epoxy
Load transfer by bolt1	520 N
Load transfer by bolt2	500 N



MODEL O Description and Results

Model	Model O
Adherend Thickness	1.8 mm
Bolt Diameter	8mm
Tensile Load	4000 N
Overlap Length	60 mm
Material	Carbon/fiber epoxy
Load transfer by bolt1	340 N
Load transfer by bolt2	320 N



APPENDIX B

Heading

Job name: bd81 Model name: bd814

Preprint, echo=NO, model=NO, history=NO, contact=NO

*

PARTS

*

Part, name=BOLT-1

End Part

Part, name=BOLT-2

End Part

Part, name=PLATE1-1

End Part

*

ASSEMBLY

*

Assembly, name=Assembly

*

Instance, name=PLATE1-1, part=PLATE1-1

Node

1,	100.,	0.,	0.
2,	100.,	1.8,	0.
3,	110.,	1.8,	0.
4,	110.,	0.,	0.
5,	100.,	0.,	6.5

.

.

.

.

*Element, type=C3D8I

1,	1481,	1482,	4809,	4802,	155,	156,	1461,	1460
2,	1482,	1483,	4810,	4809,	156,	157,	1462,	1461
3,	1483,	1484,	4811,	4810,	157,	158,	1463,	1462
4,	1484,	162,	1472,	4811,	158,	1,	159,	1463
5,	4802,	4809,	4799,	4798,	1460,	1461,	1465,	1464

.

.

.

.

*Elset, elset=_I1, internal

1, 2, 3, 4, 5, 6, 7, 8, 9, 10, 11, 12, 13, 14, 15, 16

17, 18, 19, 20, 21, 22, 23, 24, 25, 26, 27, 28, 29, 30, 31, 32
33, 34, 35, 36, 37, 38, 39, 40, 41, 42, 43, 44, 45, 46, 47, 48
49, 50, 51, 52, 53, 54, 55, 56, 57, 58, 59, 60, 61, 62, 63, 64

*Elset, elset=_I2, internal

265, 266, 267, 268, 269, 270, 271, 272, 273, 274, 275, 276, 277, 278, 279, 280
281, 282, 283, 284, 285, 286, 287, 288, 289, 290, 291, 292, 293, 294, 295, 296
297, 298, 299, 300, 301, 302, 303, 304, 305, 306, 307, 308, 309, 310, 311, 312

.

.

.

.

*Elset, elset=_I3, internal

1321, 1322, 1323, 1324, 1325, 1326, 1327, 1328, 1329, 1330, 1331, 1332, 1333, 1334,
1335, 1336
1337, 1338, 1339, 1340, 1341, 1342, 1343, 1344, 1345, 1346, 1347, 1348, 1349, 1350,
1351, 1352
1353, 1354, 1355, 1356, 1357, 1358, 1359, 1360, 1361, 1362, 1363, 1364, 1365, 1366,
1367, 1368

.

.

.

.

*Orientation, name=Ori-1

1., 0., 0., 0., 1., 0.
1, 0.

Region: (Section-2-_I2:_I2), (Controls:Default)

Section: Section-2-_I2

*Solid Section, elset=_I2, material=ADHESIVE

1.,

*Orientation, name=Ori-2

1., 0., 0., 0., 1., 0.
1, 0.

Region: (Section-3-_I3:_I3), (Controls:EC-1), (Material Orientation:_I3)

Section: Section-3-_I3

Solid Section, elset=_I3, orientation=Ori-2, controls=EC-1, material=ADHEREND

1.,

Region: (Section-4-_I4:_I4), (Controls:EC-1)

Section: Section-4-_I4

Solid Section, elset=_I4, controls=EC-1, material=ADHESIVE

1.,

End Instance

*

*Instance, name=BOLT-1, part=BOLT-1

*Node

1,	104.,	-0.3,	12.5
2,	100.,	-0.3,	12.5
3,	100.,	-2.4,	12.5
4,	104.,	-2.4,	12.5
5,	100.,	-0.3,	8.5

.

.

.

.

Elset, elset=_I1, internal, generate

1, 1536, 1

Elset, elset=_I2, internal, generate

1537, 2304, 1

Section: Section-6-_I2

Solid Section, elset=_I2, controls=EC-1, material=BOLT

1.,

End Instance

*

Instance, name=BOLT-2, part=BOLT-2

Node

1,	84.,	-0.3,	12.5
2,	80.,	-0.3,	12.5
3,	80.,	-2.4,	12.5
4,	84.,	-2.4,	12.5
5,	80.,	-0.3,	8.5

.

.

.

.

.

Elset, elset=PT1, instance=BOLT-1

2, 4, 6, 8, 9, 10, 11, 12, 17, 18, 19, 20, 25, 26, 27, 28

33, 34, 35, 36, 81, 82, 83, 84, 97, 98, 99, 100, 105, 106, 107, 108

113, 114, 115, 116, 121, 122, 123, 124, 130, 132, 134, 136, 177, 178, 179, 180

1009, 1011, 1013, 1015, 1018, 1020, 1022, 1024, 1026, 1028, 1030, 1032, 1034, 1036,

1038, 1040

1042, 1044, 1046, 1048, 1049, 1050, 1051, 1052, 1105, 1107, 1109, 1111, 1114, 1116,

1118, 1120

1122, 1124, 1126, 1128, 1130, 1132, 1134, 1136, 1138, 1140, 1142, 1144, 1145, 1146,

1147, 1148

Elset, elset=PT2, instance=BOLT-2

2, 4, 6, 8, 9, 10, 11, 12, 17, 18, 19, 20, 25, 26, 27, 28

33, 34, 35, 36, 81, 82, 83, 84, 97, 98, 99, 100, 105, 106, 107, 108

113, 114, 115, 116, 121, 122, 123, 124, 130, 132, 134, 136, 177, 178, 179, 180
 1009, 1011, 1013, 1015, 1018, 1020, 1022, 1024, 1026, 1028, 1030, 1032, 1034, 1036,
 1038, 1040
 1042, 1044, 1046, 1048, 1049, 1050, 1051, 1052, 1105, 1107, 1109, 1111, 1114, 1116,
 1118, 1120
 1122, 1124, 1126, 1128, 1130, 1132, 1134, 1136, 1138, 1140, 1142, 1144, 1145, 1146,
 1147, 1148
 *Elset, elset=_PT1_S2, internal, instance=BOLT-1
 81, 82, 83, 84, 177, 178, 179, 180, 1049, 1050, 1051, 1052, 1145, 1146, 1147,
 1148
 *Elset, elset=_PT2_S2, internal, instance=BOLT-2
 81, 82, 83, 84, 177, 178, 179, 180, 1049, 1050, 1051, 1052, 1145, 1146, 1147,
 1148
 *Elset, elset=_BOLT1DOWN_S4, internal, instance=BOLT-1
 73, 74, 75, 76, 77, 78, 79, 80, 137, 138, 139, 140, 141, 142, 143, 144
 961, 962, 963, 964, 965, 966, 967, 968, 1009, 1010, 1011, 1012, 1013, 1014, 1015,
 1016
 1049, 1050, 1051, 1052, 1053, 1054, 1055, 1056, 1057, 1058, 1059, 1060, 1061, 1062,
 1063, 1064
 1105, 1106, 1107, 1108, 1109, 1110, 1111, 1112, 1145, 1146, 1147, 1148, 1149, 1150,
 1151, 1152
 *Elset, elset=_BOLT1DOWN_S3, internal, instance=BOLT-1
 1, 2, 3, 4, 5, 6, 7, 8, 81, 82, 83, 84, 85, 86, 87, 88
 129, 130, 131, 132, 133, 134, 135, 136, 177, 178, 179, 180, 181, 182, 183, 184
 185, 186, 187, 188, 189, 190, 191, 192, 1001, 1002, 1003, 1004, 1005, 1006, 1007,
 1008
 1097, 1098, 1099, 1100, 1101, 1102, 1103, 1104
 *Elset, elset=_BOLT1DOWN_S2, internal, instance=BOLT-1
 89, 90, 91, 92, 93, 94, 95, 96, 1537, 1538, 1539, 1540, 1541, 1542, 1543, 1544
 1545, 1546, 1547, 1548, 1549, 1550, 1551, 1552, 1553, 1554, 1555, 1556, 1557, 1558,
 1559, 1560
 *Elset, elset=_BOLT1DOWN_S1, internal, instance=BOLT-1
 1705, 1706, 1707, 1708, 1709, 1710, 1711, 1712, 1713, 1714, 1715, 1716, 1717, 1718,
 1719, 1720
 1721, 1722, 1723, 1724, 1725, 1726, 1727, 1728, 2185, 2186, 2187, 2188, 2189, 2190,
 2191, 2192
 2193, 2194, 2195, 2196, 2197, 2198, 2199, 2200, 2201, 2202, 2203, 2204, 2205, 2206,
 2207, 2208
 2281, 2282, 2283, 2284, 2285, 2286, 2287, 2288, 2289, 2290, 2291, 2292, 2293, 2294,
 2295, 2296
 2297, 2298, 2299, 2300, 2301, 2302, 2303, 2304
 *Elset, elset=_BOLT1TOP_S3, internal, instance=BOLT-1
 321, 322, 323, 324, 325, 326, 327, 328, 369, 370, 371, 372, 373, 374, 375, 376
 377, 378, 379, 380, 381, 382, 383, 384, 1153, 1154, 1155, 1156, 1157, 1158, 1159,
 1160

1281, 1282, 1283, 1284, 1285, 1286, 1287, 1288, 1297, 1298, 1299, 1300, 1301, 1302, 1303, 1304
1337, 1338, 1339, 1340, 1341, 1342, 1343, 1344
*Elset, elset=_BOLT1TOP_S4, internal, instance=BOLT-1
329, 330, 331, 332, 333, 334, 335, 336, 1161, 1162, 1163, 1164, 1165, 1166, 1167, 1168
1289, 1290, 1291, 1292, 1293, 1294, 1295, 1296
*Elset, elset=_BOLT1TOP_S2, internal, instance=BOLT-1
193, 194, 195, 196, 197, 198, 199, 200, 201, 202, 203, 204, 205, 206, 207, 208
209, 210, 211, 212, 213, 214, 215, 216, 217, 218, 219, 220, 221, 222, 223, 224
1201, 1202, 1203, 1204, 1205, 1206, 1207, 1208, 1209, 1210, 1211, 1212, 1213, 1214, 1215, 1216
*Elset, elset=_BOLT1TOP_S1, internal, instance=BOLT-1
1801, 1802, 1803, 1804, 1805, 1806, 1807, 1808, 1809, 1810, 1811, 1812, 1813, 1814, 1815, 1816
1817, 1818, 1819, 1820, 1821, 1822, 1823, 1824, 1897, 1898, 1899, 1900, 1901, 1902, 1903, 1904
1905, 1906, 1907, 1908, 1909, 1910, 1911, 1912, 1913, 1914, 1915, 1916, 1917, 1918, 1919, 1920
1993, 1994, 1995, 1996, 1997, 1998, 1999, 2000, 2001, 2002, 2003, 2004, 2005, 2006, 2007, 2008
2009, 2010, 2011, 2012, 2013, 2014, 2015, 2016, 2089, 2090, 2091, 2092, 2093, 2094, 2095, 2096
2097, 2098, 2099, 2100, 2101, 2102, 2103, 2104, 2105, 2106, 2107, 2108, 2109, 2110, 2111, 2112
*Elset, elset=_BOLT2DOWN_S4, internal, instance=BOLT-2
73, 74, 75, 76, 77, 78, 79, 80, 137, 138, 139, 140, 141, 142, 143, 144
961, 962, 963, 964, 965, 966, 967, 968, 1009, 1010, 1011, 1012, 1013, 1014, 1015, 1016
1049, 1050, 1051, 1052, 1053, 1054, 1055, 1056, 1057, 1058, 1059, 1060, 1061, 1062, 1063, 1064
1105, 1106, 1107, 1108, 1109, 1110, 1111, 1112, 1145, 1146, 1147, 1148, 1149, 1150, 1151, 1152
*Elset, elset=_BOLT2DOWN_S3, internal, instance=BOLT-2
1, 2, 3, 4, 5, 6, 7, 8, 81, 82, 83, 84, 85, 86, 87, 88
129, 130, 131, 132, 133, 134, 135, 136, 177, 178, 179, 180, 181, 182, 183, 184
185, 186, 187, 188, 189, 190, 191, 192, 1001, 1002, 1003, 1004, 1005, 1006, 1007, 1008
1097, 1098, 1099, 1100, 1101, 1102, 1103, 1104
*Elset, elset=_BOLT2DOWN_S2, internal, instance=BOLT-2
89, 90, 91, 92, 93, 94, 95, 96, 1537, 1538, 1539, 1540, 1541, 1542, 1543, 1544
1545, 1546, 1547, 1548, 1549, 1550, 1551, 1552, 1553, 1554, 1555, 1556, 1557, 1558, 1559, 1560
*Elset, elset=_BOLT2DOWN_S1, internal, instance=BOLT-2
1705, 1706, 1707, 1708, 1709, 1710, 1711, 1712, 1713, 1714, 1715, 1716, 1717, 1718, 1719, 1720

1721, 1722, 1723, 1724, 1725, 1726, 1727, 1728, 2185, 2186, 2187, 2188, 2189, 2190,
 2191, 2192
 2193, 2194, 2195, 2196, 2197, 2198, 2199, 2200, 2201, 2202, 2203, 2204, 2205, 2206,
 2207, 2208
 2281, 2282, 2283, 2284, 2285, 2286, 2287, 2288, 2289, 2290, 2291, 2292, 2293, 2294,
 2295, 2296
 2297, 2298, 2299, 2300, 2301, 2302, 2303, 2304
 *Elset, elset=_BOLT2TOP_S3, internal, instance=BOLT-2
 321, 322, 323, 324, 325, 326, 327, 328, 369, 370, 371, 372, 373, 374, 375, 376
 377, 378, 379, 380, 381, 382, 383, 384, 1153, 1154, 1155, 1156, 1157, 1158, 1159,
 1160
 1281, 1282, 1283, 1284, 1285, 1286, 1287, 1288, 1297, 1298, 1299, 1300, 1301, 1302,
 1303, 1304
 1337, 1338, 1339, 1340, 1341, 1342, 1343, 1344
 *Elset, elset=_BOLT2TOP_S4, internal, instance=BOLT-2
 329, 330, 331, 332, 333, 334, 335, 336, 1161, 1162, 1163, 1164, 1165, 1166, 1167,
 1168
 1289, 1290, 1291, 1292, 1293, 1294, 1295, 1296
 *Elset, elset=_BOLT2TOP_S2, internal, instance=BOLT-2
 193, 194, 195, 196, 197, 198, 199, 200, 201, 202, 203, 204, 205, 206, 207, 208
 209, 210, 211, 212, 213, 214, 215, 216, 217, 218, 219, 220, 221, 222, 223, 224
 1201, 1202, 1203, 1204, 1205, 1206, 1207, 1208, 1209, 1210, 1211, 1212, 1213, 1214,
 1215, 1216
 *Elset, elset=_BOLT2TOP_S1, internal, instance=BOLT-2
 1801, 1802, 1803, 1804, 1805, 1806, 1807, 1808, 1809, 1810, 1811, 1812, 1813, 1814,
 1815, 1816
 1817, 1818, 1819, 1820, 1821, 1822, 1823, 1824, 1897, 1898, 1899, 1900, 1901, 1902,
 1903, 1904
 1905, 1906, 1907, 1908, 1909, 1910, 1911, 1912, 1913, 1914, 1915, 1916, 1917, 1918,
 1919, 1920
 1993, 1994, 1995, 1996, 1997, 1998, 1999, 2000, 2001, 2002, 2003, 2004, 2005, 2006,
 2007, 2008
 2009, 2010, 2011, 2012, 2013, 2014, 2015, 2016, 2089, 2090, 2091, 2092, 2093, 2094,
 2095, 2096
 2097, 2098, 2099, 2100, 2101, 2102, 2103, 2104, 2105, 2106, 2107, 2108, 2109, 2110,
 2111, 2112
 *Elset, elset=_HOLE1DOWN_S6, internal, instance=PLATE1-1
 4499, 4502, 4505, 4508, 4511, 4514, 4517, 4520, 4523, 4526, 4529, 4532, 4535, 4538,
 4541, 4544
 4547, 4550, 4553, 4556, 4559, 4562, 4565, 4568, 4571, 4574, 4577, 4580, 4583, 4586,
 4589, 4592
 4889, 4893, 4897, 4901, 4905, 4909, 4913, 4917, 4921, 4925, 4929, 4933, 4937, 4941,
 4945, 4949
 4953, 4957, 4961, 4965, 4969, 4973, 4977, 4981, 4985, 4989, 4993, 4997, 5001, 5005,
 5009, 5013

5017, 5021, 5025, 5029, 5033, 5037, 5041, 5045, 5049, 5053, 5057, 5061, 5065, 5069, 5073, 5077

*Elset, elset=_HOLE1DOWN_S2, internal, instance=PLATE1-1
4403, 4404, 4405, 4406, 4407, 4408, 4409, 4410, 4411, 4412, 4413, 4414, 4415, 4416, 4417, 4418
4419, 4420, 4421, 4422, 4423, 4424, 4425, 4426, 4427, 4428, 4429, 4430, 4431, 4432, 4433, 4434
4889, 4890, 4891, 4892, 4893, 4894, 4895, 4896, 4897, 4898, 4899, 4900, 4901, 4902, 4903, 4904
4905, 4906, 4907, 4908, 4909, 4910, 4911, 4912, 4913, 4914, 4915, 4916, 4917, 4918, 4919, 4920

*Elset, elset=_HOLE1DOWN_S4, internal, instance=PLATE1-1, generate
4406, 4498, 4

*Elset, elset=_HOLE1DOWN_S1, internal, instance=PLATE1-1, generate
4571, 4594, 1

*Elset, elset=_HOLE1DOWN_S5, internal, instance=PLATE1-1
4993, 4994, 4995, 4996, 5005, 5006, 5007, 5008, 5017, 5018, 5019, 5020, 5029, 5030, 5031, 5032
5041, 5042, 5043, 5044, 5053, 5054, 5055, 5056, 5065, 5066, 5067, 5068, 5077, 5078, 5079, 5080

*Elset, elset=_HOLE1TOP_S6, internal, instance=PLATE1-1, generate
3901, 3994, 3

*Elset, elset=_HOLE1TOP_S2, internal, instance=PLATE1-1
3901, 3902, 3903, 3904, 3905, 3906, 3907, 3908, 3909, 3910, 3911, 3912, 3913, 3914, 3915, 3916
3917, 3918, 3919, 3920, 3921, 3922, 3923, 3924, 4211, 4212, 4213, 4214, 4215, 4216, 4217, 4218
4219, 4220, 4221, 4222, 4223, 4224, 4225, 4226, 4227, 4228, 4229, 4230, 4231, 4232, 4233, 4234

*Elset, elset=_HOLE1TOP_S4, internal, instance=PLATE1-1
3808, 3812, 3816, 3820, 3824, 3828, 3832, 3836, 3840, 3844, 3848, 3852, 3856, 3860, 3864, 3868
3872, 3876, 3880, 3884, 3888, 3892, 3896, 3900, 4118, 4122, 4126, 4130, 4134, 4138, 4142, 4146
4150, 4154, 4158, 4162, 4166, 4170, 4174, 4178, 4182, 4186, 4190, 4194, 4198, 4202, 4206, 4210
4213, 4216, 4219, 4222, 4225, 4228, 4231, 4234, 4237, 4240, 4243, 4246, 4249, 4252, 4255, 4258
4261, 4264, 4267, 4270, 4273, 4276, 4279, 4282, 4285, 4288, 4291, 4294, 4297, 4300, 4303, 4306

*Elset, elset=_HOLE1TOP_S5, internal, instance=PLATE1-1
3813, 3814, 3815, 3816, 3825, 3826, 3827, 3828, 3837, 3838, 3839, 3840, 3849, 3850, 3851, 3852
3861, 3862, 3863, 3864, 3873, 3874, 3875, 3876, 3885, 3886, 3887, 3888, 3897, 3898, 3899, 3900

4123, 4124, 4125, 4126, 4135, 4136, 4137, 4138, 4147, 4148, 4149, 4150, 4159, 4160,
 4161, 4162
 4171, 4172, 4173, 4174, 4183, 4184, 4185, 4186, 4195, 4196, 4197, 4198, 4207, 4208,
 4209, 4210
 *Elset, elset=_HOLE2TOP_S1, internal, instance=PLATE1-1
 3429, 3430, 3431, 3432, 3433, 3434, 3435, 3436, 3437, 3438, 3439, 3440, 3441, 3442,
 3443, 3444
 3445, 3446, 3447, 3448, 3449, 3450, 3451, 3452, 4667, 4668, 4669, 4670, 4671, 4672,
 4673, 4674
 4675, 4676, 4677, 4678, 4679, 4680, 4681, 4682, 4683, 4684, 4685, 4686, 4687, 4688,
 4689, 4690
 *Elset, elset=_HOLE2TOP_S6, internal, instance=PLATE1-1
 3453, 3457, 3461, 3465, 3469, 3473, 3477, 3481, 3485, 3489, 3493, 3497, 3501, 3505,
 3509, 3513
 3517, 3521, 3525, 3529, 3533, 3537, 3541, 3545, 3549, 3553, 3557, 3561, 3565, 3569,
 3573, 3577
 3581, 3585, 3589, 3593, 3597, 3601, 3605, 3609, 3613, 3617, 3621, 3625, 3629, 3633,
 3637, 3641
 4595, 4598, 4601, 4604, 4607, 4610, 4613, 4616, 4619, 4622, 4625, 4628, 4631, 4634,
 4637, 4640
 4643, 4646, 4649, 4652, 4655, 4658, 4661, 4664, 4667, 4670, 4673, 4676, 4679, 4682,
 4685, 4688
 *Elset, elset=_HOLE2TOP_S4, internal, instance=PLATE1-1, generate
 3359, 3452, 3
 *Elset, elset=_HOLE2TOP_S5, internal, instance=PLATE1-1
 3461, 3462, 3463, 3464, 3473, 3474, 3475, 3476, 3485, 3486, 3487, 3488, 3497, 3498,
 3499, 3500
 3509, 3510, 3511, 3512, 3521, 3522, 3523, 3524, 3533, 3534, 3535, 3536, 3545, 3546,
 3547, 3548
 3557, 3558, 3559, 3560, 3569, 3570, 3571, 3572, 3581, 3582, 3583, 3584, 3593, 3594,
 3595, 3596
 3605, 3606, 3607, 3608, 3617, 3618, 3619, 3620, 3629, 3630, 3631, 3632, 3641, 3642,
 3643, 3644
 *Elset, elset=_HOLE2DOWN_S6, internal, instance=PLATE1-1
 2895, 2899, 2903, 2907, 2911, 2915, 2919, 2923, 2927, 2931, 2935, 2939, 2943, 2947,
 2951, 2955
 2959, 2963, 2967, 2971, 2975, 2979, 2983, 2987, 2991, 2994, 2997, 3000, 3003, 3006,
 3009, 3012
 3015, 3018, 3021, 3024, 3027, 3030, 3033, 3036, 3039, 3042, 3045, 3048, 3051, 3054,
 3057, 3060
 3063, 3066, 3069, 3072, 3075, 3078, 3081, 3084, 3135, 3139, 3143, 3147, 3151, 3155,
 3159, 3163
 3167, 3171, 3175, 3179, 3183, 3187, 3191, 3195, 3199, 3203, 3207, 3211, 3215, 3219,
 3223, 3227
 *Elset, elset=_HOLE2DOWN_S4, internal, instance=PLATE1-1, generate
 2643, 2736, 3

*Elset, elset=_HOLE2DOWN_S1, internal, instance=PLATE1-1
2713, 2714, 2715, 2716, 2717, 2718, 2719, 2720, 2721, 2722, 2723, 2724, 2725, 2726,
2727, 2728
2729, 2730, 2731, 2732, 2733, 2734, 2735, 2736, 3063, 3064, 3065, 3066, 3067, 3068,
3069, 3070
3071, 3072, 3073, 3074, 3075, 3076, 3077, 3078, 3079, 3080, 3081, 3082, 3083, 3084,
3085, 3086

*Elset, elset=_HOLE2DOWN_S5, internal, instance=PLATE1-1
2903, 2904, 2905, 2906, 2915, 2916, 2917, 2918, 2927, 2928, 2929, 2930, 2939, 2940,
2941, 2942
2951, 2952, 2953, 2954, 2963, 2964, 2965, 2966, 2975, 2976, 2977, 2978, 2987, 2988,
2989, 2990
3143, 3144, 3145, 3146, 3155, 3156, 3157, 3158, 3167, 3168, 3169, 3170, 3179, 3180,
3181, 3182
3191, 3192, 3193, 3194, 3203, 3204, 3205, 3206, 3215, 3216, 3217, 3218, 3227, 3228,
3229, 3230

*Elset, elset=_PT1_S3, internal, instance=BOLT-1
9, 10, 11, 12, 17, 18, 19, 20, 25, 26, 27, 28, 33, 34, 35, 36
97, 98, 99, 100, 105, 106, 107, 108, 113, 114, 115, 116, 121, 122, 123, 124
1009, 1011, 1013, 1015, 1105, 1107, 1109, 1111

*Elset, elset=_PT2_S3, internal, instance=BOLT-2
9, 10, 11, 12, 17, 18, 19, 20, 25, 26, 27, 28, 33, 34, 35, 36
97, 98, 99, 100, 105, 106, 107, 108, 113, 114, 115, 116, 121, 122, 123, 124
1009, 1011, 1013, 1015, 1105, 1107, 1109, 1111

*Nset, nset=_PickedSet94, internal, instance=PLATE1-1
143, 144, 145, 146, 147, 148, 1311, 1312, 1313, 1314, 1333, 1334, 1335, 1336, 1346,
1347
1348, 1349, 1350, 1351, 1352, 1353, 1354, 1355, 1365, 1366, 1367, 1368, 1378, 1379,
1380, 4426
4427, 4428, 4429, 4430, 4431, 4432, 4433, 4434, 4435, 4436, 4437, 4510, 4511, 4512,
4513, 4514
4515, 4516, 4517, 4518, 4519, 4520, 4521

*Nset, nset=_PickedSet95, internal, instance=PLATE1-1
1350,

*Nset, nset=_PickedSet96, internal, instance=PLATE1-1
1426, 1458

*Nset, nset=_PickedSet97, internal, instance=PLATE1-1
1429,

*Elset, elset=_BOLT1DOWN_S4, internal, instance=BOLT-1
73, 74, 75, 76, 77, 78, 79, 80, 137, 138, 139, 140, 141, 142, 143, 144
961, 962, 963, 964, 965, 966, 967, 968, 1009, 1010, 1011, 1012, 1013, 1014, 1015,
1016
1049, 1050, 1051, 1052, 1053, 1054, 1055, 1056, 1057, 1058, 1059, 1060, 1061, 1062,
1063, 1064
1105, 1106, 1107, 1108, 1109, 1110, 1111, 1112, 1145, 1146, 1147, 1148, 1149, 1150,
1151, 1152

*Elset, elset=_BOLT1DOWN_S3, internal, instance=BOLT-1
 1, 2, 3, 4, 5, 6, 7, 8, 81, 82, 83, 84, 85, 86, 87, 88
 129, 130, 131, 132, 133, 134, 135, 136, 177, 178, 179, 180, 181, 182, 183, 184
 185, 186, 187, 188, 189, 190, 191, 192, 1001, 1002, 1003, 1004, 1005, 1006, 1007,
 1008
 1097, 1098, 1099, 1100, 1101, 1102, 1103, 1104

*Elset, elset=_BOLT1DOWN_S2, internal, instance=BOLT-1
 89, 90, 91, 92, 93, 94, 95, 96, 1537, 1538, 1539, 1540, 1541, 1542, 1543, 1544
 1545, 1546, 1547, 1548, 1549, 1550, 1551, 1552, 1553, 1554, 1555, 1556, 1557, 1558,
 1559, 1560

*Elset, elset=_BOLT1DOWN_S1, internal, instance=BOLT-1
 1705, 1706, 1707, 1708, 1709, 1710, 1711, 1712, 1713, 1714, 1715, 1716, 1717, 1718,
 1719, 1720
 1721, 1722, 1723, 1724, 1725, 1726, 1727, 1728, 2185, 2186, 2187, 2188, 2189, 2190,
 2191, 2192
 2193, 2194, 2195, 2196, 2197, 2198, 2199, 2200, 2201, 2202, 2203, 2204, 2205, 2206,
 2207, 2208
 2281, 2282, 2283, 2284, 2285, 2286, 2287, 2288, 2289, 2290, 2291, 2292, 2293, 2294,
 2295, 2296
 2297, 2298, 2299, 2300, 2301, 2302, 2303, 2304

*Surface, type=ELEMENT, name=BOLT1DOWN
 _BOLT1DOWN_S4, S4
 _BOLT1DOWN_S3, S3
 _BOLT1DOWN_S2, S2
 _BOLT1DOWN_S1, S1

*Elset, elset=_BOLT1TOP_S3, internal, instance=BOLT-1
 321, 322, 323, 324, 325, 326, 327, 328, 369, 370, 371, 372, 373, 374, 375, 376
 377, 378, 379, 380, 381, 382, 383, 384, 1153, 1154, 1155, 1156, 1157, 1158, 1159,
 1160
 1281, 1282, 1283, 1284, 1285, 1286, 1287, 1288, 1297, 1298, 1299, 1300, 1301, 1302,
 1303, 1304
 1337, 1338, 1339, 1340, 1341, 1342, 1343, 1344

*Elset, elset=_BOLT1TOP_S4, internal, instance=BOLT-1
 329, 330, 331, 332, 333, 334, 335, 336, 1161, 1162, 1163, 1164, 1165, 1166, 1167,
 1168
 1289, 1290, 1291, 1292, 1293, 1294, 1295, 1296

*Elset, elset=_BOLT1TOP_S2, internal, instance=BOLT-1
 193, 194, 195, 196, 197, 198, 199, 200, 201, 202, 203, 204, 205, 206, 207, 208
 209, 210, 211, 212, 213, 214, 215, 216, 217, 218, 219, 220, 221, 222, 223, 224
 1201, 1202, 1203, 1204, 1205, 1206, 1207, 1208, 1209, 1210, 1211, 1212, 1213, 1214,
 1215, 1216

*Elset, elset=_BOLT1TOP_S1, internal, instance=BOLT-1
 1801, 1802, 1803, 1804, 1805, 1806, 1807, 1808, 1809, 1810, 1811, 1812, 1813, 1814,
 1815, 1816
 1817, 1818, 1819, 1820, 1821, 1822, 1823, 1824, 1897, 1898, 1899, 1900, 1901, 1902,
 1903, 1904

1905, 1906, 1907, 1908, 1909, 1910, 1911, 1912, 1913, 1914, 1915, 1916, 1917, 1918,
1919, 1920
1993, 1994, 1995, 1996, 1997, 1998, 1999, 2000, 2001, 2002, 2003, 2004, 2005, 2006,
2007, 2008
2009, 2010, 2011, 2012, 2013, 2014, 2015, 2016, 2089, 2090, 2091, 2092, 2093, 2094,
2095, 2096
2097, 2098, 2099, 2100, 2101, 2102, 2103, 2104, 2105, 2106, 2107, 2108, 2109, 2110,
2111, 2112

*Surface, type=ELEMENT, name=BOLT1TOP

_BOLT1TOP_S3, S3

_BOLT1TOP_S4, S4

_BOLT1TOP_S2, S2

_BOLT1TOP_S1, S1

*Elset, elset=_BOLT2DOWN_S4, internal, instance=BOLT-2

73, 74, 75, 76, 77, 78, 79, 80, 137, 138, 139, 140, 141, 142, 143, 144

961, 962, 963, 964, 965, 966, 967, 968, 1009, 1010, 1011, 1012, 1013, 1014, 1015,
1016

1049, 1050, 1051, 1052, 1053, 1054, 1055, 1056, 1057, 1058, 1059, 1060, 1061, 1062,
1063, 1064

1105, 1106, 1107, 1108, 1109, 1110, 1111, 1112, 1145, 1146, 1147, 1148, 1149, 1150,
1151, 1152

*Elset, elset=_BOLT2DOWN_S3, internal, instance=BOLT-2

1, 2, 3, 4, 5, 6, 7, 8, 81, 82, 83, 84, 85, 86, 87, 88

129, 130, 131, 132, 133, 134, 135, 136, 177, 178, 179, 180, 181, 182, 183, 184
185, 186, 187, 188, 189, 190, 191, 192, 1001, 1002, 1003, 1004, 1005, 1006, 1007,
1008

1097, 1098, 1099, 1100, 1101, 1102, 1103, 1104

*Elset, elset=_BOLT2DOWN_S2, internal, instance=BOLT-2

89, 90, 91, 92, 93, 94, 95, 96, 1537, 1538, 1539, 1540, 1541, 1542, 1543, 1544
1545, 1546, 1547, 1548, 1549, 1550, 1551, 1552, 1553, 1554, 1555, 1556, 1557, 1558,
1559, 1560

*Elset, elset=_BOLT2DOWN_S1, internal, instance=BOLT-2

1705, 1706, 1707, 1708, 1709, 1710, 1711, 1712, 1713, 1714, 1715, 1716, 1717, 1718,
1719, 1720

1721, 1722, 1723, 1724, 1725, 1726, 1727, 1728, 2185, 2186, 2187, 2188, 2189, 2190,
2191, 2192

2193, 2194, 2195, 2196, 2197, 2198, 2199, 2200, 2201, 2202, 2203, 2204, 2205, 2206,
2207, 2208

2281, 2282, 2283, 2284, 2285, 2286, 2287, 2288, 2289, 2290, 2291, 2292, 2293, 2294,
2295, 2296

2297, 2298, 2299, 2300, 2301, 2302, 2303, 2304

*Surface, type=ELEMENT, name=BOLT2DOWN

_BOLT2DOWN_S4, S4

_BOLT2DOWN_S3, S3

_BOLT2DOWN_S2, S2

_BOLT2DOWN_S1, S1

*Elset, elset=_BOLT2TOP_S3, internal, instance=BOLT-2
 321, 322, 323, 324, 325, 326, 327, 328, 369, 370, 371, 372, 373, 374, 375, 376
 377, 378, 379, 380, 381, 382, 383, 384, 1153, 1154, 1155, 1156, 1157, 1158, 1159,
 1160
 1281, 1282, 1283, 1284, 1285, 1286, 1287, 1288, 1297, 1298, 1299, 1300, 1301, 1302,
 1303, 1304
 1337, 1338, 1339, 1340, 1341, 1342, 1343, 1344

*Elset, elset=_BOLT2TOP_S4, internal, instance=BOLT-2
 329, 330, 331, 332, 333, 334, 335, 336, 1161, 1162, 1163, 1164, 1165, 1166, 1167,
 1168
 1289, 1290, 1291, 1292, 1293, 1294, 1295, 1296

*Elset, elset=_BOLT2TOP_S2, internal, instance=BOLT-2
 193, 194, 195, 196, 197, 198, 199, 200, 201, 202, 203, 204, 205, 206, 207, 208
 209, 210, 211, 212, 213, 214, 215, 216, 217, 218, 219, 220, 221, 222, 223, 224
 1201, 1202, 1203, 1204, 1205, 1206, 1207, 1208, 1209, 1210, 1211, 1212, 1213, 1214,
 1215, 1216

*Elset, elset=_BOLT2TOP_S1, internal, instance=BOLT-2
 1801, 1802, 1803, 1804, 1805, 1806, 1807, 1808, 1809, 1810, 1811, 1812, 1813, 1814,
 1815, 1816
 1817, 1818, 1819, 1820, 1821, 1822, 1823, 1824, 1897, 1898, 1899, 1900, 1901, 1902,
 1903, 1904
 1905, 1906, 1907, 1908, 1909, 1910, 1911, 1912, 1913, 1914, 1915, 1916, 1917, 1918,
 1919, 1920
 1993, 1994, 1995, 1996, 1997, 1998, 1999, 2000, 2001, 2002, 2003, 2004, 2005, 2006,
 2007, 2008
 2009, 2010, 2011, 2012, 2013, 2014, 2015, 2016, 2089, 2090, 2091, 2092, 2093, 2094,
 2095, 2096
 2097, 2098, 2099, 2100, 2101, 2102, 2103, 2104, 2105, 2106, 2107, 2108, 2109, 2110,
 2111, 2112

*Surface, type=ELEMENT, name=BOLT2TOP
 _BOLT2TOP_S3, S3
 _BOLT2TOP_S4, S4
 _BOLT2TOP_S2, S2
 _BOLT2TOP_S1, S1

*Elset, elset=_HOLE1DOWN_S6, internal, instance=PLATE1-1
 4499, 4502, 4505, 4508, 4511, 4514, 4517, 4520, 4523, 4526, 4529, 4532, 4535, 4538,
 4541, 4544
 4547, 4550, 4553, 4556, 4559, 4562, 4565, 4568, 4571, 4574, 4577, 4580, 4583, 4586,
 4589, 4592
 4889, 4893, 4897, 4901, 4905, 4909, 4913, 4917, 4921, 4925, 4929, 4933, 4937, 4941,
 4945, 4949
 4953, 4957, 4961, 4965, 4969, 4973, 4977, 4981, 4985, 4989, 4993, 4997, 5001, 5005,
 5009, 5013
 5017, 5021, 5025, 5029, 5033, 5037, 5041, 5045, 5049, 5053, 5057, 5061, 5065, 5069,
 5073, 5077

*Elset, elset=_HOLE1DOWN_S2, internal, instance=PLATE1-1

4403, 4404, 4405, 4406, 4407, 4408, 4409, 4410, 4411, 4412, 4413, 4414, 4415, 4416,
 4417, 4418
 4419, 4420, 4421, 4422, 4423, 4424, 4425, 4426, 4427, 4428, 4429, 4430, 4431, 4432,
 4433, 4434
 4889, 4890, 4891, 4892, 4893, 4894, 4895, 4896, 4897, 4898, 4899, 4900, 4901, 4902,
 4903, 4904
 4905, 4906, 4907, 4908, 4909, 4910, 4911, 4912, 4913, 4914, 4915, 4916, 4917, 4918,
 4919, 4920
 *Elset, elset=_HOLE1DOWN_S4, internal, instance=PLATE1-1, generate
 4406, 4498, 4
 *Elset, elset=_HOLE1DOWN_S1, internal, instance=PLATE1-1, generate
 4571, 4594, 1
 *Elset, elset=_HOLE1DOWN_S5, internal, instance=PLATE1-1
 4993, 4994, 4995, 4996, 5005, 5006, 5007, 5008, 5017, 5018, 5019, 5020, 5029, 5030,
 5031, 5032
 5041, 5042, 5043, 5044, 5053, 5054, 5055, 5056, 5065, 5066, 5067, 5068, 5077, 5078,
 5079, 5080
 *Surface, type=ELEMENT, name=HOLE1DOWN
 _HOLE1DOWN_S6, S6
 _HOLE1DOWN_S2, S2
 _HOLE1DOWN_S4, S4
 _HOLE1DOWN_S1, S1
 _HOLE1DOWN_S5, S5
 *Elset, elset=_HOLE1TOP_S6, internal, instance=PLATE1-1, generate
 3901, 3994, 3
 *Elset, elset=_HOLE1TOP_S2, internal, instance=PLATE1-1
 3901, 3902, 3903, 3904, 3905, 3906, 3907, 3908, 3909, 3910, 3911, 3912, 3913, 3914,
 3915, 3916
 3917, 3918, 3919, 3920, 3921, 3922, 3923, 3924, 4211, 4212, 4213, 4214, 4215, 4216,
 4217, 4218
 4219, 4220, 4221, 4222, 4223, 4224, 4225, 4226, 4227, 4228, 4229, 4230, 4231, 4232,
 4233, 4234
 *Elset, elset=_HOLE1TOP_S4, internal, instance=PLATE1-1
 3808, 3812, 3816, 3820, 3824, 3828, 3832, 3836, 3840, 3844, 3848, 3852, 3856, 3860,
 3864, 3868
 3872, 3876, 3880, 3884, 3888, 3892, 3896, 3900, 4118, 4122, 4126, 4130, 4134, 4138,
 4142, 4146
 4150, 4154, 4158, 4162, 4166, 4170, 4174, 4178, 4182, 4186, 4190, 4194, 4198, 4202,
 4206, 4210
 4213, 4216, 4219, 4222, 4225, 4228, 4231, 4234, 4237, 4240, 4243, 4246, 4249, 4252,
 4255, 4258
 4261, 4264, 4267, 4270, 4273, 4276, 4279, 4282, 4285, 4288, 4291, 4294, 4297, 4300,
 4303, 4306
 *Elset, elset=_HOLE1TOP_S5, internal, instance=PLATE1-1
 3813, 3814, 3815, 3816, 3825, 3826, 3827, 3828, 3837, 3838, 3839, 3840, 3849, 3850,
 3851, 3852

3861, 3862, 3863, 3864, 3873, 3874, 3875, 3876, 3885, 3886, 3887, 3888, 3897, 3898,
 3899, 3900
 4123, 4124, 4125, 4126, 4135, 4136, 4137, 4138, 4147, 4148, 4149, 4150, 4159, 4160,
 4161, 4162
 4171, 4172, 4173, 4174, 4183, 4184, 4185, 4186, 4195, 4196, 4197, 4198, 4207, 4208,
 4209, 4210
 *Surface, type=ELEMENT, name=HOLE1TOP
 _HOLE1TOP_S6, S6
 _HOLE1TOP_S2, S2
 _HOLE1TOP_S4, S4
 _HOLE1TOP_S5, S5
 *Elset, elset=_HOLE2TOP_S1, internal, instance=PLATE1-1
 3429, 3430, 3431, 3432, 3433, 3434, 3435, 3436, 3437, 3438, 3439, 3440, 3441, 3442,
 3443, 3444
 3445, 3446, 3447, 3448, 3449, 3450, 3451, 3452, 4667, 4668, 4669, 4670, 4671, 4672,
 4673, 4674
 4675, 4676, 4677, 4678, 4679, 4680, 4681, 4682, 4683, 4684, 4685, 4686, 4687, 4688,
 4689, 4690
 *Elset, elset=_HOLE2TOP_S6, internal, instance=PLATE1-1
 3453, 3457, 3461, 3465, 3469, 3473, 3477, 3481, 3485, 3489, 3493, 3497, 3501, 3505,
 3509, 3513
 3517, 3521, 3525, 3529, 3533, 3537, 3541, 3545, 3549, 3553, 3557, 3561, 3565, 3569,
 3573, 3577
 3581, 3585, 3589, 3593, 3597, 3601, 3605, 3609, 3613, 3617, 3621, 3625, 3629, 3633,
 3637, 3641
 4595, 4598, 4601, 4604, 4607, 4610, 4613, 4616, 4619, 4622, 4625, 4628, 4631, 4634,
 4637, 4640
 4643, 4646, 4649, 4652, 4655, 4658, 4661, 4664, 4667, 4670, 4673, 4676, 4679, 4682,
 4685, 4688
 *Elset, elset=_HOLE2TOP_S4, internal, instance=PLATE1-1, generate
 3359, 3452, 3
 *Elset, elset=_HOLE2TOP_S5, internal, instance=PLATE1-1
 3461, 3462, 3463, 3464, 3473, 3474, 3475, 3476, 3485, 3486, 3487, 3488, 3497, 3498,
 3499, 3500
 3509, 3510, 3511, 3512, 3521, 3522, 3523, 3524, 3533, 3534, 3535, 3536, 3545, 3546,
 3547, 3548
 3557, 3558, 3559, 3560, 3569, 3570, 3571, 3572, 3581, 3582, 3583, 3584, 3593, 3594,
 3595, 3596
 3605, 3606, 3607, 3608, 3617, 3618, 3619, 3620, 3629, 3630, 3631, 3632, 3641, 3642,
 3643, 3644
 *Surface, type=ELEMENT, name=HOLE2TOP
 _HOLE2TOP_S1, S1
 _HOLE2TOP_S6, S6
 _HOLE2TOP_S4, S4
 _HOLE2TOP_S5, S5
 *Elset, elset=_HOLE2DOWN_S6, internal, instance=PLATE1-1

2895, 2899, 2903, 2907, 2911, 2915, 2919, 2923, 2927, 2931, 2935, 2939, 2943, 2947,
 2951, 2955
 2959, 2963, 2967, 2971, 2975, 2979, 2983, 2987, 2991, 2994, 2997, 3000, 3003, 3006,
 3009, 3012
 3015, 3018, 3021, 3024, 3027, 3030, 3033, 3036, 3039, 3042, 3045, 3048, 3051, 3054,
 3057, 3060
 3063, 3066, 3069, 3072, 3075, 3078, 3081, 3084, 3135, 3139, 3143, 3147, 3151, 3155,
 3159, 3163
 3167, 3171, 3175, 3179, 3183, 3187, 3191, 3195, 3199, 3203, 3207, 3211, 3215, 3219,
 3223, 3227
 *Elset, elset=_HOLE2DOWN_S4, internal, instance=PLATE1-1, generate
 2643, 2736, 3
 *Elset, elset=_HOLE2DOWN_S1, internal, instance=PLATE1-1
 2713, 2714, 2715, 2716, 2717, 2718, 2719, 2720, 2721, 2722, 2723, 2724, 2725, 2726,
 2727, 2728
 2729, 2730, 2731, 2732, 2733, 2734, 2735, 2736, 3063, 3064, 3065, 3066, 3067, 3068,
 3069, 3070
 3071, 3072, 3073, 3074, 3075, 3076, 3077, 3078, 3079, 3080, 3081, 3082, 3083, 3084,
 3085, 3086
 *Elset, elset=_HOLE2DOWN_S5, internal, instance=PLATE1-1
 2903, 2904, 2905, 2906, 2915, 2916, 2917, 2918, 2927, 2928, 2929, 2930, 2939, 2940,
 2941, 2942
 2951, 2952, 2953, 2954, 2963, 2964, 2965, 2966, 2975, 2976, 2977, 2978, 2987, 2988,
 2989, 2990
 3143, 3144, 3145, 3146, 3155, 3156, 3157, 3158, 3167, 3168, 3169, 3170, 3179, 3180,
 3181, 3182
 3191, 3192, 3193, 3194, 3203, 3204, 3205, 3206, 3215, 3216, 3217, 3218, 3227, 3228,
 3229, 3230
 *Surface, type=ELEMENT, name=HOLE2DOWN
 _HOLE2DOWN_S6, S6
 _HOLE2DOWN_S4, S4
 _HOLE2DOWN_S1, S1
 _HOLE2DOWN_S5, S5
 *Elset, elset=_PT1_S4, internal, instance=BOLT-1
 2, 4, 6, 8, 130, 132, 134, 136, 1018, 1020, 1022, 1024, 1026, 1028, 1030, 1032
 1034, 1036, 1038, 1040, 1042, 1044, 1046, 1048, 1114, 1116, 1118, 1120, 1122, 1124,
 1126, 1128
 1130, 1132, 1134, 1136, 1138, 1140, 1142, 1144
 *Surface, type=ELEMENT, name=PT1
 _PT1_S4, S4
 _PT1_S3, S3
 _PT1_S2, S2
 *Elset, elset=_PT2_S4, internal, instance=BOLT-2
 2, 4, 6, 8, 130, 132, 134, 136, 1018, 1020, 1022, 1024, 1026, 1028, 1030, 1032
 1034, 1036, 1038, 1040, 1042, 1044, 1046, 1048, 1114, 1116, 1118, 1120, 1122, 1124,
 1126, 1128

```

1130, 1132, 1134, 1136, 1138, 1140, 1142, 1144
*Surface, type=ELEMENT, name=PT2
_PT2_S4, S4
_PT2_S3, S3
_PT2_S2, S2
*NODE
100001, 100, -0.3, -10
*NODE
100002, 80, -0.3, -10
*PRE-TENSION SECTION,SURFACE=PT1,NODE=100001
*PRE-TENSION SECTION,SURFACE=PT2,NODE=100002
*End Assembly
**
** ELEMENT CONTROLS
**
*Section Controls, name=EC-1, hourglass=RELAX STIFFNESS
1., 1., 1.
**
** MATERIALS
**
*Material, name=ADHEREND
*Elastic, type=ENGINEERING CONSTANTS
140000.,10000.,11000., 0.3, 0.3, 0.5, 5200., 5200.
----
```